RGB-thermal Based Denosing Methods: A Review of Deep Learning Based Image Denosing Algorithm and Application

IEEE Publication Technology, *Staff, IEEE,*

***Abstract*—Recently, vision-based detection techonology has been developed fast and general pupose object detection algorithm has been applied in various scene. VD can be categorized into two major categories, single-modal, single RGB or single thermal, and bimodal, according to the modal type used. Generally, the first stage of image processing in VD is denoising, removing the redundancy information and promising the post processing task. Thus, this paper will give a review on RGB-thermal deep learning based image denoising methods, investigating the RGB-thermal based denoising procedure, methods, benchmark and performance. After the introduction of denoising models, main results on public RGB and thermal datasets are presented and analyzed, and conclusion of objective comparison in practical effect will be proposed. This review can serve as a reference for researchers in RGB-infrared denoising, image restoration, and related fields.**

***Index Terms*—Image denoising, RGB-thermal based, Single modal, Bi-modal, Deep learning based methods.**

I. INTRODUCTION

VISION-BASED, Detection (VD) is a relative new technology that supporting task such as rescue in fire scene through intelligent analysis of video and image using advanced analytical algorithms [1].

The primary motivation of VD is to realize early detection which is initially RGB based. However, when solving general purpose object detection problem, due to the limitation of the imaging mechanism of visible images, detection algorithms based on visible images may fail as they maybe unreliable in certain circumstances [1]. For example, considering the firefighting situation with heavy smoke, RGB based detection is not powerful enough since the camera is not able to get clear image [2]. On the contrary, the infrared images detecting thermal information of objects are insensitive to these factors. They can provide complementary information to visible images. Thus, in recent years, researchers begin exploring performing object detection with infrared images. However, the infrared images typically have low resolutions and poor textures, and are also unreliable in certain conditions such as environment with little temperature difference [2]. Therefore, more researchers begin to investigate object detection method based on the fusion of visible and infrared images to overcome the inherent shortcomings of the methods based on single-modal images.

This paper was produced by the IEEE Publication Technology Group. They are in Piscataway, NJ.

Manuscript received April 19, 2021; revised August 16, 2021.

VD can be categorized into two major categories, single-modal, single RGB or single thermal, and bimodal, according to the modal type used [3]. And there are two sub categories in bimodal detection including infrared-assisted RGB detection and RGB-assisted infrared detection which depends on primary modality utilized during detection [3].

Generally, the first stage of VD is data pre-processing. Since the images are easily corrupted due to various noises which occur in nature and poor performance of electronic devices, denoising is unavoidable before practical processing [3]. Considering the development trend of VD, this paper will focus on deep learning based denoising technology in RGB-thermal image processing and its application.

Although other important research has been conducted in the field of image denoising in recent years, none of them is comprehensive enough for summary. Firstly, most of them either only concerns traditional denoising methods in some specific aspects or they only select some representative algorithms for conclusion. For example, "Survey of Image Denoising Techniques" [2] only covers the traditional denoising techniques, while "Deep learning on image denoising: An overview" [3] only refers to some deep learning denoising algorithms. Secondly, the summary content for each method is not complete enough that many significant details are ignored. For example, they will only briefly introduce concepts or formula of methods but the merits or drawbacks, experiment results, relative research papers will not always be covered. Thirdly, the relationship of methods are not clearly summarized. They either do not pay attention to the historical timeline development of different methods or focus on the comparison of idea or performance among methods. Fourthly, none of the summary reviews the techniques from the perspective of application, the real effect in dealing with practical problems. Finally, most of denoising review only focus on RGB denoising and few of them concerns about thermal denoising which is also very roughly. There is no review covers both of the single modals or multiple modals source denoising. This overview covers more than 700 papers for deep learning based image denoising in recent years. Specially, this overview covers almost all of papers related to deep learning based image denoising methods and application in rencent 5 years. The main contributions in this paper can be summarized as follows:

- To the best of our knowledge, this is the first review on deep learning based denoising methods in RGB-thermal based image processing for both single modal and bi-

modal. There are only review for RGB based denoising, this paper tries to fulfill this gap.
- This review divide these deep learning based approaches into five categories: MLP, CNN, ResNet, GAN, GNN. Section 3 starts by the brief discussion of the history development of the RGB and thermal deep learning based image denoising methods and followed by introduction of concrete state-of-the-art deep learning-based algorithm. Each category is introduced and summarized according to core idea and representative methods. For each method, concepts and theories, pros and cons, performance evaluation and corresponding practical applications are introduced. Specially, the performance evaluation of each method in section 3 is cited from other papers and demonstrated on public (RGB) data set.
- This overview pay special attention to the performance of different denoising methods on thermal image. Since most of the denoising methods are tested based on the RGB datasets, this overview also evaluates these denoising methods with the thermal datasets for comparison and supplementation. In the last experiment section, main results on thermal datasets are presented and analyzed providing an objective comparison in practical effect.

Section 2 gives background information on RGB-thermal based image pre-processing technology including its history and development, and general procedure. Section 3 demonstrates deep learning based denoising methods in details. A comparison among methods will be made for reference and suggestion on models selection under different processing situation will be given. Section 4 specially illustrates the experiment performance of different models on both RGB and thermal benchmark datasets respectively. Sections 5 concludes the paper.

II. Background of Image Denoising

Image noise is random variation of information such as brightness or color in images, and is usually produced during the signal generation and transportation process, by the interference from equipment and transmission channel [2].

For general digital images, in addition to the noise caused by external environmental such as lighting conditions, the noise will also be produced in the collection and transmission process because of the digital equipment [2]. On the one hand, during the process of signal generation, various noise will be introduced due to the sensor material, electronic components and circuit structure. On the other hand, during the process of signal transmission, the digital image will also be contaminated by multiple noises due to the imperfection of the transmission medium and the recording equipment [2].

According to the principle of infrared photography, the external environmental noise of the special infrared image is different from the digital image, which is mainly derived from the thermal radiation of the scenery, the atmosphere and other backgrounds [2]. Compared to the visible light images, apart from the external conditions as detection environment, the quality of infrared images is also more easily affected by various equipment factors such as the detector component and the photoelectric conversion circuit during the acquisition and transmission process. Moreover, the cause of electrical elements based noise during the collection and transmission of infrared images is more diverse and complex than the visible light images, which includes the inherent pattern noise caused by the inconsistent response of the detector, the thermal noise caused by the electronic thermal vibration in the device, and the scattering noise caused by the uneven electron emission [2].

Whether in digital or infrared images. additional noise will seriously affect the quality of collected image. The presence of mixed random noise fills the image with a wide variety of noise points, reducing the clarity and covering the details of the image, which seriously affects the extraction of effective information. The existence of noise reduces the effective value of image signal and brings serious effects not only on the direct extraction of the image information, but also the subsequent processing such as image enhancement and target detection and tracking.

Therefore, execution of denoising is very necessary for image improvement. Mostly denoising is implemented for acquisition of high quality image. The essence of denoising is separating the noise from the observed image, removing the mixed useless noise information from the real signal, while retaining useful features and keeping the integrity of the original image information as far as possible.

As the basis and premise of image processing, suppressing the noise can significantly weaken the spotted point on the image, effectively improving the subjective visual perception of image and extraction of useful information in image. Meanwhile, image denoising will promise completeness of original signal and remove redundancy contributing to success in post processing. Denoising can provide a guarantee for subsequent works such as image enhancement and target detection. Since inhibition of noise in images is an inevitable technical problem in image processing, denoising has already become an important research direction in the field of image processing.

A. Basic Principle of Noise Model

A noisy image can be modeled as follows:

$$g(x, y) = f(x, y) + \eta(x, y) \tag{1}$$

Where $f(x, y)$ is the original image pixel, $\eta(x, y)$ is the noise term and $g(x, y)$ is the resulting noisy pixel.

The image noise can be divided into different types according to relationship between noise and signal, the causes of the noise, statistical characteristics of noise and the probability distribution of noise respectively [3].

1) -Relationship:: According to the relationship between noise and signal, noise can be divided into two categories: additive noise and multiplicative noise. Additive noise indicates that its relationship with an image signal is additive. Additive noise is inherent whether the image signal is in presence or absence.

Multiplicative noise indicates the multiplication relationship with the image signal. In contrast to the case of additive noise, it is dependent on the image signal. The multiplicative noise will disappear when the multiplicative signal disappears.

2) -Cause:: According to the causes of the noise, the image noise can be divided into external noise and internal noise. External noise refers to the noise caused by external environment interference, and internal noise refers to the noise caused by the internal equipment interference.

3) -Statistic:: According to the statistical characteristics of the noise, the image noise can be divided into stationary noise and non-stationary noise. Stationary noise refers to noise with time-invariant statistic property while non-stationary noise is time-variant.

4) -Distribution:: According to the probability distribution of the noise, common noise mainly includes Gaussian noise, Rayleigh noise, exponent noise, gamma noise, uniform noise, and pretzel noise.

B. Types of Noise

1) -Gaussian noise:: Gaussian noise is a class of random noise that obeys the Gaussian distribution, which is a common continuous probability distribution.

Generally, Gaussian noise is additive, independent at each pixel and independent of the signal intensity, reducing the clarity of image edges and blur texture detail [3]. For digital images, the standard model of amplifier noise is primarily caused by Johnson Nyquist noise which is often taken as a major part of the "read noise" of an image sensor. The main reasons of producing Gaussian noise in digital imaging can be: incorrect collection of the image sensor because of the dark or uneven light, over high temperature in image sensor caused by long time working, the mutual interference in the circuit or the superposition among existed electric noise. For the infrared images, the noise caused by the photon fluctuations of the infrared background radiation, the infrared detector photoelectric conversion, and the signal readout and processing circuit are randomly distributed both in time and space. The produced random noise distributes independently from each other, and can be simply modeled as Gaussian noise. Grayscale value data obeying normal distribution with same size as image matrix can be directly superimposed to the original image to generate a thermal image contaminated with Gaussian noise [3].

2) -Salt-and-pepper noise:: Pretzel noise, also called as pulse noise, is a more common noise in daily life. It is characterized by a discrete distribution, mainly consisting of irregular burr noise with large amplitude and short duration [3].

The pretzel noise in the digital images is mainly due to the analog-to-digital converter failure caused by strong and transient interference during the image acquisition process or bit errors in transmission. It is specifically manifested as the randomly distributed white spots or black spots on the image. The containing of pretzel noise can be indicated by black pixels in brighter areas, or bright pixels in dark areas, mostly presenting in smooth areas. For infrared image, when the gaze imaging device producing infrared image, the device directly causes the photoelectric reaction on sensors of the focal plane. Blind elements will appear at some pixels, and the distribution of bright-dark point noise on the image is similar to pretzel noise [3].

3) -Rayleigh noise:: The Rayleigh noise is noise that obeys the Rayleigh distribution, characterized by independent components with roughly the same Gaussian distribution [3].

In contrast to the Gaussian distribution, the probability density curve of the Rayleigh distribution shifts globally to the right, approximated by the crooked histogram. The Rayleigh distribution is often used to describe the time-varying properties of flat fading signal and its independent sub-components.

4) -Gamma noise:: Gamma noise, also known as Irish noise, follows the distribution of the gamma curve [3].

5) -Exponential noise:: Exponential noise refers to noise whose probability density function follows an exponential distribution [3].

6) -Uniform noise:: Uniform noise refers to noise whose probability density function follows uniform distribution [3].

7) -Anisotropic noise:: Some noise sources show up with a significant orientation in images such as row noise or column noise. Anisotropic noise textures are interesting for many visualization and graphics applications. The spot samples can be used as input for texture generation especially suitable for the visualization of tensor fields that can be used to define a metric for the anisotropic density field [3]. In infrared imaging, stripe noise is another common noise, which is mostly presented in the infrared images produced by scanning devices. The focal plane of the scanning imaging device presents a one-dimensional linear distribution. When imaging, only one row of data can be collected simultaneously, and then the focal plane is moved according to some certain frequency to produce multiple sets of data for creation of the complete image. If some blind elements are presented in the scanning imaging device, a bright dark line along the sweep surface will be generated in the image, which is the stripe noise.

III. Classification of Deep Learning Based Denoising Algorithms

Although most of the traditional methods have achieved relatively good performance in image denoising, they suffered from several unavoidable drawbacks including undesirable effect in the case of multiple noise, wrecking of details image, image clarity and quality reduction. Therefore, seeking a better denoising scheme has become the center of research for many technological researchers.

The original deep learning technologies were first used in image processing in [4]. After applied to image processing from the very beginning, deep learning was quickly extended to the image denoising direction. Authors in [5] and [6] firstly used the neural network with both the known shift-invariant blur function and additive noise to recover the latent clean image. After that, the neural network with weighting factors was used to remove more complex noise [5], rather than Gaussian. In 1989, Tamura propose a feedforward network to make a tradeoff between denoising efficiency and performance reducing the high computational costs. The feedforward network can smooth the given corrupted image by Kuwahara filters, which were similar to convolutions. In addition, this research proved that the mean squared error (MSE) acted as a loss function which was not unique to neural networks [7], [8]. Subsequently, for the purpose of acceleration of the convergence of the trained network and promotion of the denoising performance, more optimization algorithms were used in [3], [9], [10]. The combination of maximum entropy and primal–dual Lagrangian multipliers to enhance the expressive ability of neural networks proved to be a good tool for image denoising in [11]. Greedy algorithms and asynchronous algorithms were applied in neural networks in [12], to further make a trade off between fast execution and denoising performance. Cellular neural networks (CENNs) mainly used nodes with templates to obtain the averaging function and effectively suppress the noise in [13], [14]. Alternatively, as for eliminating the noise, designing a novel network architecture either increasing the depth or changing activation function proved to be very competitive in [14]. Although good denoising results can be obtained through these methods, parameters of the templates are always required to be set manually. The gradient descent was developed in [15], [16] to resolve this problem.

These deep techniques indeed can improve denoising performance to some extent. However, the addition of new plug-in units were not possible in these networks, which limited their applications in the real world in [4]. Considering the limitation in flexibility, convolutional neural networks (CNNs) were proposed in [17], [18]. Deep networks were first applied in image denoising in 2015 in [19], [20]. The proposed network need not manually set parameters for removing the noise. After then, deep networks were widely applied in speech [21], video [22], and image restoration [23], [24]. Authors in [25] used multiple convolutions and deconvolutions to suppress the noise and recover the high-resolution image. For addressing multiple low-level tasks via a model, a denoising CNN (DnCNN) [26], batch normalization (BN) [27], rectified linear unit (ReLU) [28] and residual learning (RL) [29] was proposed to deal with image denoising, super-resolution, and JPEG image deblocking. Taking into account the trade off between denoising performance and speed, a color non-local network (CNLNet) [30], combined non-local self-similarity (NLSS) and CNN to efficiently remove color-image noise. In terms of blind denoising, a fast and flexible denoising CNN (FFDNet) [31], presented different noise levels and the noisy image patch as the input of a denoising network to improve denoising speed and process blind denoising. For handling unpaired noisy images, a generative adversarial network (GAN) CNN blind denoiser (GCBD) [32], resolved this problem by first generating the ground truth, then inputting the obtained ground truth into the GAN to train the denoiser. Alternatively, a convolutional blind denoising network (CBD-Net) [33], removed the noise from the given real noisy image by two sub-networks, one in charge of estimating the noise of the real noisy image, and the other for obtaining the latent clean image. For more complex corrupted images, a deep plug-and-play super-resolution (DPSR) method [34], was developed to estimate blur kernel and noise, and recover a high-resolution image.

A. Structure of Deep Learning Networks

Neural networks are the basis of machine learning methods, which in turn are the basis of deep learning techniques [35]. A neural network is essentially a nonlinear function that maps the vectorized inputs through several hidden layers to a vectortized output. Most neural networks consist of neurons, input X, activation function f , weights $W = [W_0, W_1, ..., W_{n-1}]$ and biases $b = [b_0, b_1, ..., b_n]$. And activation functions such as sigmoid [36], [37], and tanh [38], [39], can convert the linear input into non-linearity through W and b.

The part in the middle of the MP neuron model is the activation function, which can be understood as a perceptron. Since the output follows the step function curve, the output value jumps between 0 and 1 when the weighted input changes around the threshold, and small changes in the input will not be reflected in the output. Therefore, the activation function is introduced to modify the perceptron model. The activation function converts the linear input into non-linear factors which will be activated in the following layers contributing to strong flexibility for non-linear cases.

Note that if the neural network has multiple layers, it is regarded as multilayer perceptron (MLP) [40]. In addition, the middle layers are treated as hidden layers besides the input and output layers. This process can be expressed as:

$$\begin{aligned} f(X;W;b) = f(W^n f(W^{n-1} ... \\ f(W^0 X + b^0) ... b^{n-1}) + b^n) \end{aligned} \tag{2}$$

where n is the final layer of the neural network.

In the multilayer perceptron, how to correct the weights of the middle layer is a problem and the Back Propagation (BP) reverse network, a feed-forward network is always used to correct the weight values.

The main principle of the BP network is the backward propagation algorithm which is also known as error back propagation. The input information of the neural network model spreads forward from left to right. The final weighted output is produced with backward propagation layer by layer of the neuronal activation function. For individual neurons, forward propagation refers to the process of the input x to the output, $h_{w,b}(x)$. But after multiple layers of transmission, there must exist gap between the $h_{w,b}(x)$ and the ideal output y. The cost function is as following:

$$J(\theta) = j(x, b; x, y) = \frac{1}{2} ||h_{w,b}(x) - y||^2 \tag{3}$$

A fixed sample set, $\{(x^{(1)}, y^{(1)}), ..., (x^{(m)}, y^{(m)})\}$ containing m samples. The gradient descent can be used to train the weight values. The cost function of the entire sample is:

$$J(w, b) = [\frac{1}{m} \sum_{i}^{m} j(\theta)] + \frac{\lambda}{2} \sum_{l=1}^{n_l-1} \sum_{i=1}^{s_l} \sum_{j=1}^{s_l+1} (w_{ji}^{(l)})^2 \tag{4}$$

According to the formula, the first term is the mean variance, and the second term is the regularization term, which is mainly used to prevent overfitting in the training of the neural network model, also called as the weight attenuation term. Overfitting is prevented by reducing the magnitude of the weights.

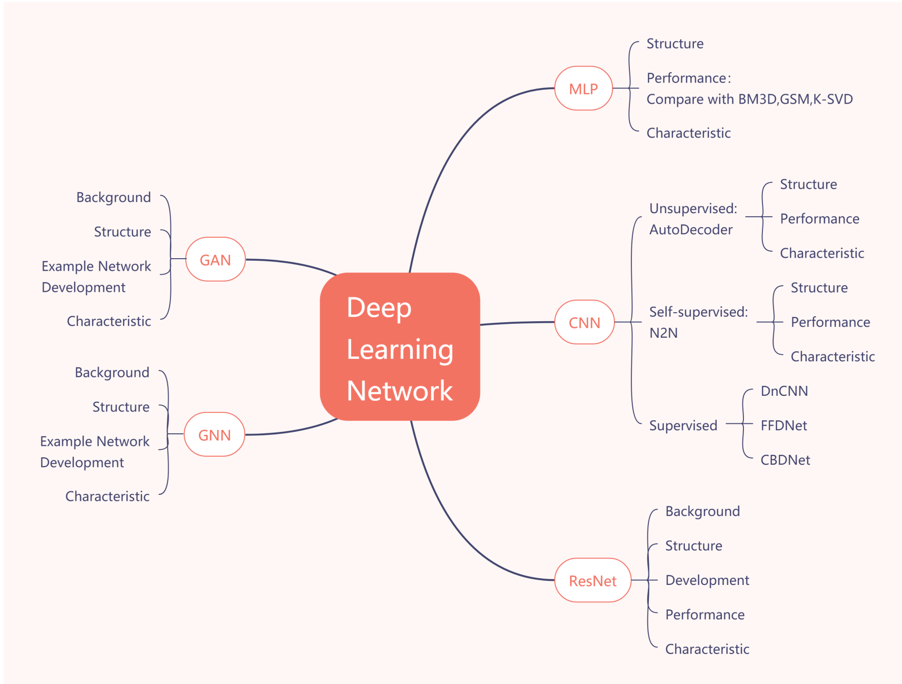

Fig. 1. Framework of the deep learning based denoising methods.

B. Framework of Deep Learning Methods

According to the model structure used in the training, the categories of deep learning-based denoising methods are shown in the following Fig.1. And a summary of deep learning based denoising methods is shown in Table I as following.

C. Multi-layer perceptron network: MLP

MLP is an early image denoising method, which was designed to train the dennoising model for image processing task by constructing a perceptron network with four hidden layers. The mapping relationship between noisy image and clean image was learned through MLP, and finally a nonlinear function was generated to achieve image denoising purpose.

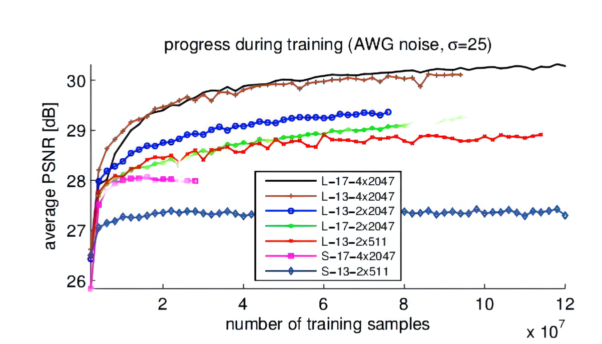

Fig. 2. Improving average PSNR on the images "Barbara" and "Lena" while training with $\sigma = 25$.

As shown in the experiments, in the Fig.2 and Fig.3 the performance of the MLP network has reached the standard of BM3D algorithm in denoising, surpassing the GSM and K-SVD algorithms, which officially declared the transcendence

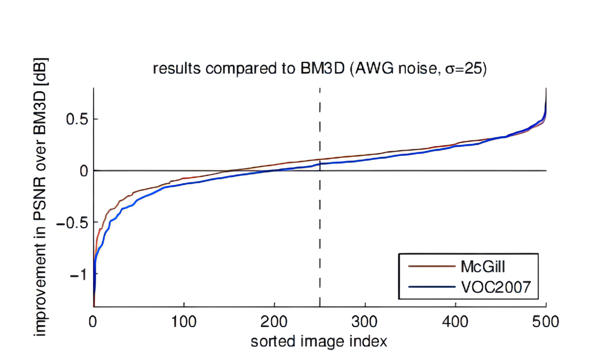

Fig. 3. Performance profile of MLP on two datasets of 500 test images compared to BM3D.

of the neural network denoising algorithm to the traditional algorithm. Neural networks can achieve higher denoising performance with corresponding deeper training network and training set with sufficient high-quality net-noise image pairs.

ANN based image restoration approach was presented in [41] to provide a new approach for image identification using multilayer perceptron. By investigating the distribution invariance of the natural image patches with respect to linear transforms, authors showed in [42] how to make a single existing MLP well across all levels of Gaussian noise. Authors concentrated on comparing and combining two of main neural network, models MLPs and CNNs for image denoising in [43]. MLP was implemented in [44] to recover higher-dimensional signals from lower dimensional, noisy, and blurry measurements. MLP were used in [45] to map the features from noisy images into FR-IQA scores, which showed that the use of a priori known noise variance significantly im-

TABLE I
SUMMARY OF DEEP LEARNING BASED DENOISING METHODS

Basic Network	Methods	Advantages	Limitations	Noise	Situation
CNN	DnCNN	Supervised learning	Low usage efficiency	Real Noise	Normal Light
	DnCNN-S	Easy to extract features	in shallow features	Synthesis Noise	Normal Light
	DnCNN-B	Better expression ability	Easy to lose texture	Synthesis Noise	Normal Light
	FFDNet	Optimizable Structure	Hard for dense noise	Real Noise	Low Light
	CBDNet	Expandable Stucture	Hard to balance	Real Noise	Low Light
	GCBDNet		noise-target balance	Real Noise	Normal Light
	PRIDNet		Unclear denoising/oversmooth	Synthesis Noise	Normal Light
CNN	N2N	Self-supervised learning	Easily to be influenced	Real Noise	Normal Light
	N2V	No need of training set	by neighbor pixel	Synthesis Noise	Normal Light
	N2S	Simple structure	Exist gap between real	Synthesis Noise	Normal Light
	S2S	Stable training process	and prediction value	Real Noise	Low Light
	NAC	Few parameters	Weak ability to	Real Noise	Low Light
	VDN	Little storage demand	express complex feature	Real Noise	Normal Light
	FOCNet			Synthesis Noise	Normal Light
ResNet	FC-AIDE	Solve gradient disappear Solve gradient explosion	Hard to design network structure	Real Noise	Normal Light
	CycleISP	Fast convergence rate Maximum info. flow	Hard to optimize target function Dense connection leads	Real Noise	Normal Light
	PADNet	Long distance correlation relationship computation	to overfitting phenomenon Inconsistency between objective	Real Noise	Normal Light
	GRDN	Increase high frequency info. usage	index and subjective feeling	Real Noise	Normal Light
GAN	GCBD	Help to generate noise image	Unstable of training network Slow convergence speed	Real Noise	Normal Light
	ADGAN	Expand the noise dataset Solve the problem of	Uncontroable model Unable to display	Real Noise	Normal Light
	MPIDACNN	ground truth insufficient	distribution of generative model	Real Noise	Normal Light
GNN	GCDN	Help to deal with unstructured data	Uncontrollable graph size Complex graph topology	Real Noise	Normal Light
	DeepGLR	Help with noise regression	Non-fixed node for reference	Real Noise	Normal Light
	OverNet	with graph topology	Daynamic graph topology decrease the feature expression ability	Real Noise	Normal Light

proved prediction accuracy. The author showed in [46] how a complex-valued neural network, the multilayer neural network with multi-valued neurons (MLMVN), could be efficiently used for impulse noise filtering. MLP was used in [47] with multi-valued neurons (MLMVN) as an intelligent tool for speckle noise filtering. A novel reconstruction algorithm was presented in [48] to address the noise artifacts of path tracing, where Stein's unbiased risk estimator (SURE) was adopted to estimate the noise level per pixel that guides adaptive sampling process and modified MLPs network was used to predict the optimal reconstruction parameters. The problem of prediction of denoising efficiency of images in a blind manner under additive white Gaussian noise condition was considered in [49]. The denoising efficiency prediction employed MLP to create a regression model. The proposed technique did not require a priori knowledge of a noise variance and used a moderate amount of image data for analysis.

MLP has also been used for multi-modal image denoising application. Compared to conventional denoising algorithms, MLP applied in [50] could restore images without blurring them, making it attractive for use in medical imaging where the preservation of anatomical details was critical. It was showed that denoising could be efficiently done using a nonlinear filter, which operated along patch neighborhoods and multiple copies of the original image. The use of patches enabled the algorithm to account for spatial correlations in the random field whereas the multiple copies were used to recognize the noise statistics. The non-linear filter, which was implemented by a hierarchical multistage system of MLP, outperformed state-of-the-art denoising algorithms such as those based on collaborative filtering and total variation.

Although MLP had excellent denoising performance and could learn the nonlinear model well, limitations still existed. A series of hyperparameters are required to be adjusted to fit the noise function, resulting in unadaptive function. On the other hand, since MLP needs to learn the noise map of a specific noise level when training, the denoising effect will be greatly reduced if the training set contains images without the noise level.

D. Convolutional Neural Network: CNN

In addition to multilayer perceptron, image denoising can also be implemented based on the CNN. Currently, CNN-based image denoising methods mainly include unsupervised learning, self-supervised learning, and supervised learning.

Unsupervised learning methods use given training samples to find patterns rather than label matching and finish specific tasks, such as unpairing real low-resolution images. Supervised learning methods use the given label to put the obtained features closer to the target for learning parameters and training the denoising model. Semi-supervised learning methods apply a model from a given data distribution to build a learner for labeling unlabeled samples.

1) Unsupervised:: At present, the denoising performance of the unsupervised learning autoencoder is also outstanding. This is done by first corrupting the initial input x into $\hat{x}$ by means of a stochastic mapping $\hat{x} \sim q_D(\hat{x}|x)$. Corrupted input $\hat{x}$ is then mapped, as with the basic autoencoder, to a hidden representation $y = f_\theta(\hat{x}) = s(W\hat{x} + b)$ from which we reconstruct a $z = g_\theta(y)$. Parameters θ and θ' are trained to minimize the average reconstruction error over a training set, that is, to have z as close as possible to the uncorrupted input x.

The key difference is that z is now a deterministic function of $\hat{x}$ rather than x. As previously, the considered reconstruction error is either the cross-entropy loss $L_H(x, z) = IH(B(x))||B(z))$, with an affine+sigmoid decoder, or the squared error loss $L_2(x, z) = ||x-z||^2$, with an affine decoder. Parameters are initialized at random and then optimized by stochastic gradient descent. Note that each time a training example x is presented, a different corrupted version $\hat{x}$ of it is generated according to $q_D(\hat{x}|x)$.

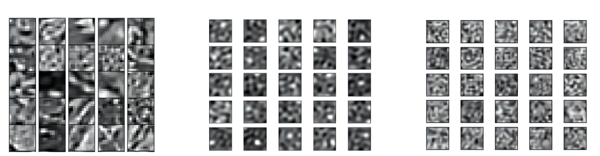

Fig. 4. Regular autoencoder trained on natural image patches. Left: some of the 12 × 12 image patches used for training. Middle: filters learnt by a regular under-complete autoencoder (50 hidden units) using tied weights and L_2 reconstruction error. Right: filters learnt by a regular over-complete autoencoder (200 hidden units).

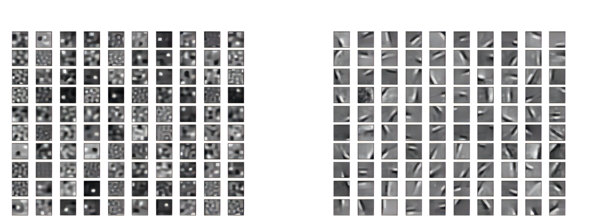

Fig. 5. Weight decay vs. Gaussian noise. Typical filters learnt from natural image patches in the over-complete case (200 hidden units). Left: regular autoencoder with weight decay.

200 hidden units over-complete noiseless autoencoders was trained regularized with L_2 weight decay, as well as 200 hidden units denoising autoencoders with isotropic Gaussian noise (but no weight decay). Resulting filters are shown in Fig.4 and Fig.5. Note that a denoising autoencoder with a noise level of zero is identical to a regular autoencoder. So, naturally, filters learnt by a denoising autoencoder at small noise levels look like those obtained with a regular autoencoder. With a sufficiently large noise level however ($\sigma = 0.5$), the denoising autoencoder learns Gabor-like local oriented edge detectors. The L_2 regularized autoencoder on the other hand learnt nothing interesting beyond restoring some of the local blob detectors found in the under-complete case. From this experiment, it is clear that training with sufficiently large noise yields a qualitatively very different outcome than training with a weight decay regularization.

There have been many researchers explored the denoising auto-encoder, enriching its structure. An unsupervised image feature extraction method was presented in [51], which was a stacked multi-granularity convolution denoising auto-encoder (SMGCDAE) based on CNN with a multi-granularity kernel. A convolutional self-encoding network (DeCS-Net) was designed in [52], which integrated the superiority of CNN and AE to learn multi-scale features. Image super-resolution architecture, coupled deep convolutional auto-encoder (CDCA), was proposed in [53], which simultaneously calculated the convolutional features of low-resolution (LR) and high-resolution (HR) image patches and learns the non-linear function that maps these convolutional features of LR image patches to their corresponding HR image patches convolutional features. An elastic stacked denoising auto-encoder model, was propsed in [54], which was an upgraded model of a stacked autoencoder algorithm based on the principle of annealing (ElasticSDAE), a novel method of adaptively obtaining the noise level. Statistical features of restored image residuals produced by DAE was studied in [55] and an improved training loss function was proposed based on method noise and entropy maximization principle, with residual statistics as constraint conditions. Skip connections from initial layers of encoder to the final layers of decoder was used in [56] to improve the performance of AE. A GAN based auto-encoder network was introduced in [57] to denoise the CT images. The network first maped CT images to low dimensional manifolds and then restored the images from its corresponding manifold representations. The reconstruction algorithm separately calculated perceptual similarity, learned the latent feature maps, and achieved more accurate and visually pleasing reconstructions. Inspired by the idea of deep learning, the autoencoder was combined with, deconvolution network, and shortcut connections in [58] into the residual encoder–decoder convolutional neural network (RED-CNN) for low-dose CT imaging. Recurrent residual U-net (R2U-Net) based autoencoder model was applied in [59] for digital pathology, dermoscopy, MRI and CT images denoising. The stacked non-local auto-encoder was developed in [60], which exploited self-similar information in natural images for stability. A robust auto-encoder called correntropy-based contractive auto-encoder (CCAE) was investigated in [61] to learn robust features from data with non-Gaussian noises and outliers. Since remnant radial streaking noise remained under physiologic imaging Conditions, a spatio-temporal denoising auto-encoder (ST-DAE) was employed in [62] to further remove these streaking noise.

These auto-encoders also have been applied to different scenario in image denoising. Authors focused on the design of auto-encoder (AE) and stacked auto-encoder (SAE) based approaches for denoising of certain military aircrafts in [63]. Framework proposed in [64] was combination of AE and CNN for denoising the fibrous dysplasia image. DAE technique was applied in [65] on 2-DGE images motivated by its ability to learn a robust representation to partially corrupted input. A lightweight convolutional AE was implemented in [66] to mimic a recent state-of-the-art method in OCT image denoising. A novel old film speckle noise removal AE was proposed in [67], which included speckle noise detection and an inpainting based speckle noise reduction procedures. A preprocessing AE for the enhancement of ancient and degraded document images was presented in [68]. AE was used in [69] to reduce the speckle noise in SAR image. A ton of sonar images were trained in AE for denoising, and the results were achievedby injecting the original sonar images [70]. DAE module was applied in [71] for denoising in brain tumors detection. A new EIT image reconstruction algorithm was proposed in [72] based on the CDAE deep learning algorithm. An averagely deep encoder-decoder neural network was used in [73] to minimize the typical motion blurring noise introduced in the input image captured by the camera setup on the production lines. DAE module was investigated for noise detection and removal in [74] in the task of robust facial alignment. The framework proposed in [75] rigorously denoised a face with dynamic expressions in a progressive way, which termed as stacked face denoising auto-encoders (SFDAE).

Some other kinds of unsupervised CNN for denoising was also proposed in some paper. For example, an HSI denoising method called Stein's unbiased risk estimateconvolutional neural network (SURE-CNN) was presented in [76], which was based on an unsupervised CNN and SURE. Since SURE was an unbiased estimate of the mean squared error (MSE) of an estimator, training a CNN using the SURE loss could yield similar results as using the MSE with ground truth in supervised learning. Also, a subspace version of SURE-CNN was proposed to reduce the running time. A novel unsupervised randomnoise-suppression method that could train a network directly on noisy target data without noise-free labels was proposed in [77], which was inspired by the simple denoising idea of averaging multiple noisy observations. An end-to-end CNN was constructed in [78] to solve the denoising task. Adjacent traces of seismic data, which contained similar seismic phases and interface features, were used as the inputs and labels of the training set. A novel approach was presented in [79] to attenuate seismic random noise based on deep CNN in an unsupervised learning manner. Experimental tests on synthetic and real data demonstrated the effectiveness and superiority of the proposed method compared with state-of-the-art denoising methods.

Representing features of images through learning hidden layer units, the input and output of autoencoder can be easily obtained. In this case, picture size changes does not require too much consideration, and good data features can be learned. However, dropout is always necessary in this model leading to incompleteness of learning information. And because unsupervised learning features are mainly used in this algorithm and the model is pretrained layer by layer, rather than directly for denoising, the improvement of denoising effect is limited.

2) Self-supervised:: Unlike the unsupervised autodecoder, self-supervised models such as Noise2Noise (N2N), Noise2Void (N2V), Noise2Self (N2S), Self2Self (S2S) takes advantage of the independence between the pixels to find the mapping relationship between the target pixels.

Noise2Noise: N2N

Authors figured out in [80] that it was possible to learn to restore images by only looking at corrupted examples, at performance at and sometimes exceeding training using clean data, without explicit image priors or likelihood models of the corruption. The denoising effect of corrupted targets was firstly studied using synthetic additive Gaussian noise. As the noise has zero mean, the L_2 loss was used for training to recover the mean. Other types of synthetic noise were then experimented.

There have been many research in N2N model. For example, an analysis of the N2N learning strategy was done in [81] using real noise and synthetic datasets. Demonstration using diverse network architectures and loss functions, that the duplicity of information in the noisy pairs was exploited to reach increased denoising performance of N2N. And the N2N method presented in [82] requiring only a single noisy realization of each training example and a statistical model of the noise distribution, and is applicable to a wide variety of noise models, including spatially structured noise. The work was built most directly upon the approaches of N2N, N2V and N2S. Like N2V and N2S, the requirement of paired noisy training data was removed which was needed in N2N. The improved N2N allowed spatially correlated noise models, which were problematic for N2V and N2S. On the other hand, the ability to sample from the noise distribution was also required, which the three aforementioned methods did not.

N2N has also found success in denoising application. An iterative DECT reconstruction algorithm with a N2N prior was proposed in [83]. The algorithm directly estimated material images from projection data and thus significantly reduced possible bias. A collaborative technique was introduced in [84] to train multiple N2N generators simultaneously and learned the image representation from LDCT images. Inspired by the previous work of N2N training, a similar neural network was trained in [85] by pairing one noise realization to an ensemble of noise realizations. A block random sampler was proposed in [86] that could generate training pairs using raw seismic data, which satisfied the training assumption of N2N that the training pair had a similar signal. N2N paradigm was explored in [87] to reconstruct the SMLM images, which was applied to synthetic data and to real 2-D SMLM data of actin filaments. A novel end-to-end self-supervised SAR denoising model, enhanced N2N (EN2N), which could be trained without a noise-free image was proposed in [88].

Noise2Void: N2V

Inspired by the idea in N2N that independent pairs of noisy images could be used, a training scheme N2V was introduced in [89]. Despite advantages of N2N training, there were at least two shortcomings to this approach: (i).N2N training required the availability of pairs of noisy images, and (ii).the acquisition of such pairs with (quasi) constant s was only possible for (quasi) static scenes. Thus, N2V, a novel training scheme was presented to overcome both limitations.

Two simple statistical assumptions were made: (i).the signal s is not pixel-wise independent, (ii).the noise n is conditionally pixel-wise independent given the signals. On the one hand, a blind-spot network was trained using only individual noisy training images, which allowed N2V to extract the input patch and target value from the same noisy training image. It could be trained by minimizing the empirical risk. On the other hand, a masking scheme was used to avoid this problem: the value in the center of each input patch was replaced with a randomly selected value form the surrounding area. This effectively erased the pixel's information and prevented the network from learning the identity.

Some paper developed the N2V structure. Probabilistic Noise2Void (PN2V), which trained CNNs for prediction of per-pixel intensity distributions was presented in [90]. After that, PN2V improved by introducing parametric noise models based on Gaussian mixture models (GMM) was introduced in [91] requiring an additional noise model for which calibration data needed to be acquired. Improved N2V was also proposed in [92], where a flow-based generative model was firstly used to learn a prior from clean images and then a denoising network without the need for any clean targets was trained. To overcome the limitation of pixel-wise independent noise assumption, structured Noise2Void (STRUCTN2V) was introduced in [93], which was a generalization of blind spot networks that enabled removal of structured noise without requiring an explicit noise model or ground truth data. Specifically, an extended blind mask rather than a single pixel/blind spot was used, whose shape was adapted to the structure of the noise.

N2V has also found success in denoising tasks. For example, a denoising technique for PET based on the Noise2Void paradigm was presented in [94], which required only a single noisy image for training thus ensuring wider applicability and adoptability. N2V network was used in [95] to improve cell/nuclei segmentation in microscopy data, when only limited training data for noisy micro-graphs were available.

Other Models

The self-supervision image denoising framework have become a popular topic. A Noise2Self (N2S) structure was proposed in [96] generalizing recent work on training neural nets from noisy images and on cross-validation for matrix factorization. A Self2Self (S2S) network was presented in [97], which was trained with dropout on the pairs of Bernoulli-sampled instances of the input image, and the result was estimated by averaging the predictions generated from multiple instances of the trained model with dropout. A novel image denoising scheme, interdependent self-cooperative learning (ISCL), that leveraged unpaired learning by combining cyclic adversarial learning with self-supervised residual learning was proposed in [98]. A very simple yet effective method was presented in [99], named Neighbor2Neighbor to train an effective image denoising model with only noisy images. Noise2Inverse (N2I), a deep CNN based denoising method was applied in [100] for linear image reconstruction algorithms that did not require any additional clean or noisy data. Since the networks learned from external images inherently suffered from a domain gap problem that the image priors and noise statistics were very different between the training and test images, a novel NoisyasClean (NAC) strategy was proposed in [101]. Since the ratio of visual signal to noise on small objects was very low, making it difficult to extract rich features for detection, a self-supervised feature enhancement network (FEN) was trained in [102]. To free image prior learning from the image collection burden, a novel self-supervised learning method for Gaussian mixture model (SS-GMM) was proposed in [103]. The blindspot model for self-supervised denoising was extended in [104] to handle Poisson-Gaussian noise. And an improved training scheme that avoided hyperparameters and adapted the denoiser to the test data was introduced. Inspired by recent works on blind-spot denoising networks, a self-supervised Bayesian despeckling method Speckle2Void was trained in [105]. A class of self-supervised structured denoisers that could be decomposed as the sum of a non-linear image-dependent mapping, a linear noise-dependent term and a small residual term was presented in [106].

Application

Additionally, different types of CNN based self-supervised networks have found success in various applications. As for medical image, in order to alleviate the performance limitation brought by the lack of pixel-level annotation in COVID-19 pneumonia lesion segmentation task, a denoising self-supervised framework was constructed in [107], where the semantic features from massive unlabelled data were learned. A self-supervised deep learning neural network for low lose CT reconstruction in the sense of penalized weighted least-squares (PWLS) was applied in [108]. As for seismic noise, a self-supervised two step approach to attenuate ground-roll noise in seismic prestack images was implemented in [109]. Similarly, a novel self-supervised learning framework was used in [110] to reconstruct and perform blind denoising of seismic data images. As for depth maps, a fully self-supervised convolutional deep auto-encoder that learned to denoise depth maps was used in [111], surpassing the lack of ground truth data. Similarly a deep neural network was learned in [112] to denoise the lower-quality depth using the matched higher-quality data as a source of supervision signal. As for video, self supervised model was utilized in [113] to reconstruct videos and the auto-encoder was learned both spatial and temporal relations of video frames to process the downstream task easily. Similarly, a self-supervised approach for training multi-frame video denoising networks that predicted each frame from a stack of frames around it was realized in [114].

However, the self-supervision methods ignore the dependency between the spatial information, and the ability of extracted features for noise expression is insufficient. Meanwhile, the adjustment mode of the network training parameters lacks flexibility, which cannot well represent the complex mapping relationship between the noise-containing images and the clear images.

3) Supervised:: Supervised learning-based image denoising methods such as denoising convolutional neural network (DnCNN), a fast and flexible denoising network (FFDNet) and GAN-basedconvolutional blind denoising network (GCBD-Net) use Gaussian hybrid models to train on multiple sample images of different noise levels and verify the denoising effect of the above methods on real noise images.

Denoising Convolutional Neural Network: DnCNN

In 2017, one of the best current deep learning-based denoising algorithms, DnCNN was proposed [26]. DnCNN borrows the residual learning methods, but DnCNN does not add connection and activation at every two layers of convolution. It changes the output of the network to a clean image and a residual image of the reconstructed image. According to the ResNet theory, when the residue is 0, the stacking layers are equivalent to the constant map, which is very easy to train and optimize. Thus, the residual image as the output of the network is suitable for image reconstruction. Batch normalization is also used in DnCNN, which is added to mitigate the shift of internal covariates before the activation function, promising faster training, better performance, and lessing the network impact on the initialization variables.

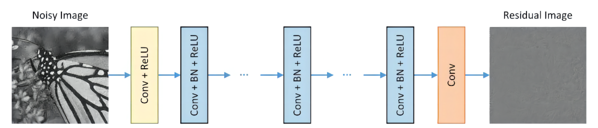

Fig. 6. The architecture of the proposed DnCNN network.

The input of DnCNN is a noisy observation $y = x + v$. Discriminative denoising models such as MLP [40] and CSF [115] aims to learn a mapping function $F(y) = x$ to predict the latent clean image. For DnCNN, we adopt the residual learning formulation to train a residual mapping $R(y) \approx v$, and then we have $x = y - R(y)$. Formally, the averaged mean squared error between the desired residual images and estimated ones from noisy input

$$l(\theta) = \frac{1}{2N} \sum_{i=1}^{N} ||R(y_i; \theta) - (y_i - x_i)||_F^2 \quad (5)$$

can be adopted as the loss function to learn the trainable parameters θ in DnCNN. Here $(y_i, x_i)_{l=1}^{N}$ represents N noisy-clean training image (patch) pairs. Fig.6 illustrates the architecture of the proposed DnCNN for learning.

Investigating the construction of feed-forward DnCNNs, DnCNN embraces the progress in very deep architecture, learning algorithm, and regularization method into image denoising. Specifically, residual learning and batch normalization are utilized to speed up the training process as well as boost the denoising performance. Different from the other existing discriminative denoising models which usually train a specific model for additive white Gaussian noise at a certain noise level, the DnCNN model is able to handle Gaussian denoising with unknown noise level (i.e., blind Gaussian denoising). With the residual learning strategy, DnCNN implicitly removes the latent clean image in the hidden layers. This property motivates training of the single DnCNN model to tackle with several general image denoising tasks, such as Gaussian denoising, single image super-resolution, and JPEG image deblocking.

Comparing the proposed DnCNN method with several state-of-the-art denoising methods, two non-local similarity based methods are included (i.e.,BM3D [116] and WNNM [117]), one generative method (i.e.,EPLL [118]), three discrimina-tive training based methods (i.e., MLP [40], CSF [115] and TNRD [119]). Note that CSF and TNRD are highly efficient by GPU implementation while offering good image quality.

The average PSNR results of different methods on the BSD68 dataset are shown in Table II. Both DnCNN-S and DnCNN-B can achieve the best PSNR results than the competing methods. Compared to the benchmark BM3D, the methods MLP and TNRD have anotable PSNR gain of about 0.35dB. There are few methods can outperform BM3D by more than 0.3dB on average. In contrast, DnCNN-S model outperforms BM3D by 0.6dB on all the three noise levels. Particularly, even with a single model without known noise level, DnCNN-B can still outperform the competing methods which is trained for the known specific noise level. It should be noted that both DnCNN-S and DnCNN-B outperform BM3D by about 0.6dB when $\sigma = 50$, which is very close to the estimated PSNR bound over BM3D (0.7dB).

Fig.7 and Fig.8 illustrate the visual results of different methods. It can be seen that BM3D, WNNM, EPLL and MLP tend to produce over-smooth edges and textures. While preserving sharp edges and fine details, TNRD is likely to generate artifacts in the smooth region. In contrast, DnCNN-S and DnCNN-B can not only recover sharp edges and fine details but also yield visually pleasant results in the smooth region.

The DnCNN has been developed further in many papers. A blind DnCNN model for random-valued impulse noise (RVIN) denoising was invented in [120] with a flexible noise ratio predictor (NRP) as an indicator. A combining deep convolutional generative adversarial networks (DCGAN) and denoising convolutional neural network ring strucutred light (DnCNN-RSL) was adopted in [121] to denoise. A fast and flexible convolutional neural network (FFCNN) based on DnCNN was used in [122] for denoising. DnCNN was aoptimized in [123] for additive white Gaussian noise (AWGN) to obtain the hardware-friendly Light-DnCNN and an energy-efficient denoising accelerator was designed based on Light-DnCNN. A discriminative denoised algorithm DnCNN whose loss function was changed was used for denoising in [124] with additive image quality assessment (IQA) part. Residual learning and batch normalization were utilized in [26] to speed up the training process of DnCNN as well as boost the denoising performance. In order to further process non-differentiated high-dimensional data including documents, images, the noise reduction model based on DnCNN and adaptive Butterworth filtering was proposed in [125]. Incorporating recent advances in architectural building blocks and network architecture search and building upon the success of the DnCNN architectures, an efficient convolutional blind image denoising network was introduced in [126]. DnCNN that grasped the advancement in profound engineering, learning calculation and regularization technique was used in [127] for denoising. The Nadam optimization algorithm that was different from the common gradient descent algorithm was used in DnCNN-N model in [128] to solve the Gaussian denoising task. Two techniques, were incorporated in [129] for denoising

TABLE II
THE AVERAGE PSNR(DB) RESULTS OF DIFFERENT METHODS ON THE BSD68 DATASET. THE BEST RESULTS ARE HIGHLIGHTED IN BOLD.

Mehotds	BM3D	WNNM	EPLL	MLP	CSF	TNRD	DnCNN-S	DnCNN-B	FFDNet
$\sigma = 15$	31.07	31.37	31.21	-	31.24	31.42	31.73	31.61	31.63
$\sigma = 25$	28.57	28.83	28.68	28.96	28.74	28.92	29.23	29.16	29.19
$\sigma = 50$	25.62	25.87	25.67	26.03	-	25.97	26.23	26.23	26.29

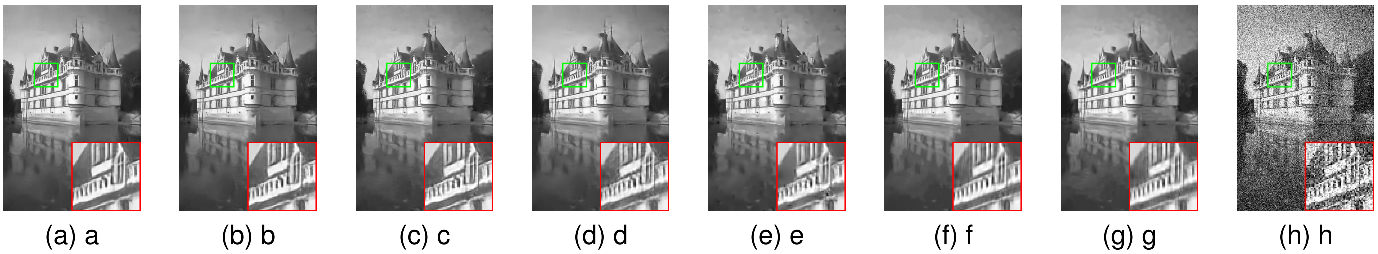

Fig. 7. Denoising results of one image from BSD68 with noise level 50. (a) Noisy/14.76dB. (b) BM3D/26.21dB. (c) WNNM/26.51dB. (d) EPLL/26.36dB. (e) MLP/26.54dB. (f) TNRD/26.59dB. (g) DnCNN-S/26.90dB. (h) DnCNN-B/26.92dB.

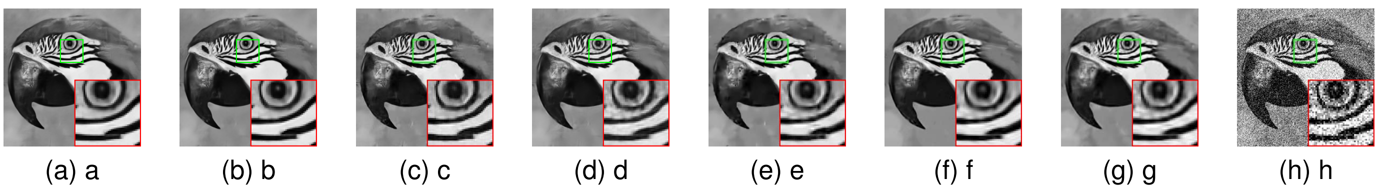

Fig. 8. Denoising results of the image “parrot” with noise level 50. (a) Noisy/15.00dB. (b) BM3D/25.90dB. (c) WNNM/26.14dB. (d) EPLL/25.95dB. (e) MLP/26.12dB. (f) TNRD/26.16dB. (g) DnCNN-S/26.48dB. (h) DnCNN-B/26.48dB.

namely, the grey wolf optimizer (GWO) and DnCNN, within a framework developed based on the quaternion discrete cosine transform (QDCT). Based on DnCNN an improved denoising algorithm was proposed in [130], where leakly ReLU function was used instead of ReLU activation function for training to extract and learn the features of the input image.

DnCNN has also been utilized in different denoising scenario. For example, denoising method that combined the total variation (TV) regularization method with a DnCNN was implemented in [131] for surveillance camera images. To solve the problem of underwater sonar images such as gray distortion, blurred edge, various shapes, and missing dataset, DnCNN for image denoising was proposed in [132], which integrated the receptive field block and attention search function. A training DnCNN was used in [133] for laser speckle contrast imaging LSCI denoising in a log-transformed domain. As for SAR imaging, the interferometric phase denoising convolutional neural network (IPDnCNN) was introduced in [134] to estimate the phase noise in radar image. DnCNN was modified in [135] to estimate the phase noise in normal pixels and remove it from the interferogram. An adaptive processing flow that combines noise reduction and image contrast enhancement, was developed in [136], which could effectively improve the interpretability and applicability of images with strong coherent speckle noise in SAR images. The single channel SAR images was used in [137] to train the DnCNN model. As for medical imaging, A network combining bidirectional convolutional long short-term memory (ConvLSTM) with 3D DnCNN to generate clearer images was applied in [138] to denoise CEUS Image. A medical image denoising pipeline based on the content-noise complementary learning (CNCL) strategy was presented in [139], and was implemented as a generative adversarial network, where various representative network DnCNN was investigated as the predictors. In order to obtain reconstructed inverse problem of electrical impedance tomography (EIT) images with good edge preservation, a DnCNN was proposed in [140]. An iterative positron emission tomography (PET) reconstruction using a CNN prior was presented in [141]. DnCNN was utilized in [142] and was trained by using full-dose images as the ground truth where low dose images were reconstructed from downsampled data by Poisson thinning as input. As for seismic imaging, a novel method alternating direction method of multipliers-based denoising convolutional neural network (ADMM-CNN) by combining low-rank decomposition with feed-forward DnCNN was presented in [143]. A novel multiscale DnCNN (MSDCNN) was developed in [144] as an attempt for random seismic noise suppression. Unlike conventional DnCNN, MSDCNN had a hierarchical structure capable of extracting features at different scales and capturing informative and discriminatory features through effective information integration. A deep convolutional neural network denoising model based on noise estimation (MCD-DCNN) was presented in [145], which was primarily composed of two modules, the noise estimation module and the denoising module. An improved feed-forward DnCNN was proposed in [146] to suppress random noise in desert seismic data. An end to end 3-D-DnCNN was designed in [147] that took raw 3-D cubes as input in order to better extract the features of the 3-D spatial structure of poststack seismic data. Also, there is some other special application. A novel denoising convolutional neural networks based dust accumulation status evaluation of photovoltaic panel was proposed in [148]. For example, according to the comparison among the different combinations of DnCNN and VGG-16, AlexNet, ResNet models, the serial connection of DnCNN and ResNet-50 model could achieve real-time monitoring and quantitative evaluation tasks of dust accumulation status with a higher accuracy and better time-consuming performance.

Fast and Flexible Denoising Convolutional Neural Network: FFDNet

The second year after DnCNN was published, Zhang et al., proposed FFDnet, providing a fast denoising solution [31]. The proposal of FFDNet is to achieve the following three objectives:

- Fast speed: The denoiser is expected to be highly efficient without sacrificing denoising performance.
- Flexibility: The denoiser is able to handle images with different noise levels and even spatially variant noise.
- Robustness: The denoiser should introduce no visual artifacts in controlling the trade-off between noise reduction and detail preservation.

To overcome the drawbacks of existing CNN based denoising methods, FFDNet was introduced. Specifically, FFDNet is formulated as $x = F(y, M; \theta)$, where M is a noise level map. In the DnCNN model $x = F(y; \theta_\sigma)$, the parameters σ vary with the change of noise level σ, while in the FFDNet model, the noise level map is modeled as an input and the model parameters are invariant to noise level. Thus, FFDNet provides a flexible way to handle different noise levels with a single network.

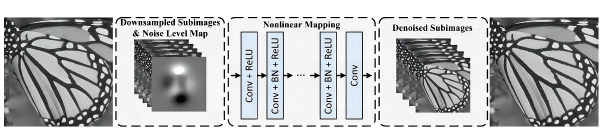

Fig. 9. The architecture of the proposed FFDNet for image denoising. The input image is reshaped to four sub-images, which are then input to the CNN together with a noise level map. The final output is reconstructed by the four denoised sub-images.

Fig.9 illustrates the architecture of FFDNet. The first layer is a reversible downsampling operator which reshapes a noisy image y into four downsampled sub-images. A tunable noise level map M is furthere concatednated with the downsampled sub-images to form a tensor y of size $\frac{W}{2} \times \frac{H}{2} \times (4C + 1)$ as the inputs to CNN. For spatially invariant AWGN with noise level σ, M is a uniform map with all elements being σ. With the tensor y as input, the following CNN consists of a series of 3×3 convolution layers. Each layer is composed of a specific combination of three types of operations: convolution (Conv), rectified linear units (ReLU), and batch normalization (BN). More specifically, $Conv + ReLU$ is adopted for the first convolution layer, $Conv + BN + ReLU$ for the middle layers, and $Conv$ for the last convolution layer. Zero-padding is employed to keep the size of feature maps unchanged after each convolution. After the last convolution layer, an upscaling operation is applied as the reverse operator of the downsampling operator applied in the input stage to produce the estimated clean image x of size $W \times H \times C$.

It can be concluded from the experiment that FFDNet surpasses BM3D by a large margin and outperforms WNNM, MLP and TNRD by about 0.2dB for a wide range of noise levels on BSD68. And, FFDNet is slightly inferior to DnCNN when the noise level is low (e.g., $\sigma \leq 25$), but gradually outperforms DnCNN with the increase of noise level (e.g., $\sigma > 25$). This phenomenon maybe resulted from the trade-off between receptive field size and modeling capacity. FFDNet has a larger receptive field than DnCNN, thus favoring for removing strong noise, while DnCNN has better modeling capacity which is beneficial for denoising images with lower noise level.

There was plenty of effort for development of FFDnet. An improved combination of nonlocally centralized sparse representation (NCSR) with a FFDNet using a spatial local fusion strategy (ICID) was shown in [149]. FFDNet with a tunable noise level map was implemented as the input in [31] for denoising. The proposed FFDNet worked on downsampled sub-images, achieving a good trade-off between inference speed and denoising performance. In contrast to the existing discriminative denoisers, the implemented FFDNet enjoyed several desirable properties, including: 1).the ability to handle a wide range of noise levels effectively with a single network; 2).the ability to remove spatially variant noise by specifying a non-uniform noise level map; and 3).faster speed than benchmark BM3D even on CPU without sacrificing denoising performance.

FFDnet was also applied in many different denoising scenario. A FFDNet-based deep learning image change detection framework was presented in [150], which achieved a good trade off between inference speed and denoising performance. A hybrid regularization model from deep prior and low-rank prior was used in [151]. The local deep prior was explored by a FFDNet. The final model, combined by the local deep and low-rank priors, was solved by the alternating directional method of multipliers under the plug-and-play framework. A different approach for LAPAN-A3 satellite imagery denoising, namely BM3D, FastNLM, and FFDNet was applied in [152]. This method tried to compare in terms of denoising performance, with three different cases of AWGN, model, and mixed noise. A method that incorporated a weighted FFDNet and a 2-DTV or 3-DTV denoiser together into the plug-andplay framework for snapshot compressive imaging (SCI) denoising was realized in [153].

GAN-based Convolutional Blind Denoising Neural Network: GCBDNet

These approaches mentioned above needs to train a deep denoising network with paired training datasets and learn the underlying noise model implicitly, which obtains remarkable results. For the denoising problem of known noise like

Gaussian noise, it is possible to form paired training data and leverage these methods to achieve state-of-the-art performance. Particularly, CNNs based approaches don't have to depend on human knowledge of image priors. They could fully exploit the great capability of the network architecture to learn from data, which breaks through the limitations of prior based methods and further improves the performance. In general, on the premise that the paired training dataset is available, this kind of approaches outperforms the previous methods.

However, such a paired training dataset would be unavailable or hard to derive in reality. Generally, only noisy images with the noise information unknown can be collected. In addition, real noises are more complex so that using the existing models, which were trained for denoising known noises (e.g. Gaussian noise), to address realistic problems couldn't achieve good results. As such, lacking paired training datasets, these approaches might not be exploited to deal with the blind denoising problems directly.

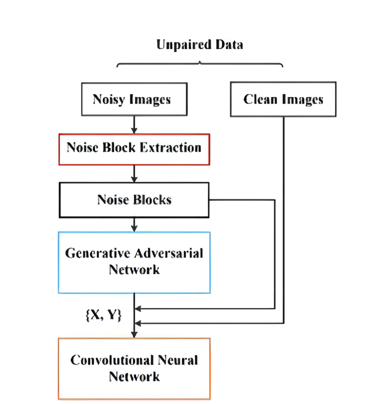

Fig. 10. An overview of the proposed GCBD framework. Given unpaired data, approximate noise blocks extracted from noisy images are exploited to train a Generative Adversarial Network (GAN)for noise modeling and sampling. A large number of noise blocks are sampled from the trained GAN model. Then, both extracted and generated noise blocks are combined with clean images to obtain paired training data which is used to train a deep Convolutional Neural Network (CNN) for denoising the input noisy images.

Thus, a GAN-CNN based framework was proposed to address the problem of image blind denoising, which achieves impressive results. An overview of the proposed CBDNet frame work is illustrated in Fig.10. Given unpaired data, approximate noise blocks extracted from noisy images are exploited to train a GAN for noise modeling and sampling. A large number of noise blocks are sampled from the trained GAN model. Then, both extracted and generated noise blocks are combined with clean images to obtain paired training data which is used to train a deep CNN for denoising the input noisy images.

TABLE III
THE PSNR (DB) RESULTS OF ALL THE COMPARED METHODS ON BSD68 IN SYNTHETIC NOISE DENOISING TASKS

Guassian Noise						
Mode	Non-Blind				Blind	
Method	BM3D	EPLL	NCSR	WNNM	DnCNN-B	GCBD
$\sigma = 15$	31.07	31.21	31.19	31.37	31.61	31.59
$\sigma = 25$	28.57	28.68	28.62	28.83	29.16	29.15
Mixture Noise						
Mode	Non-Blind				Blind	
Method	BM3D	EPLL	NCSR	WNNM	DnCNN-B	GCBD
$s = 15$	41.08	41.06	41.06	41.04	40.75	42.00
$s = 25$	37.85	37.76	37.98	37.63	37.54	39.87

The competing approaches include BM3D [116], EPLL [118], NCSR [154], WNNM [117], DnCNN [26] and the proposed GCBD. Firstly different types of zero-mean synthetic noise data are generated and added to BSD68 to evaluate all the competing methods. It's essential to conduct experiments of blind Gaussian denoising since Gaussian noise is one of the widely-studied noises. Table III above shows different results of all the compared methods. Though no noise information is provided, GCBD still outperforms BM3D, EPLL, WNNM and Multiscale. Particularly, GCBD achieves comparable results with DnCNN-B.

Besides Gaussian noise, the performance of several methods are further evaluated in complex noise denoising tasks. The mixture noise [155] adopted in the experiments consists of 10 percent uniform noise $[-s, s]$, 20 percent Gaussian noise $N(0, 1)$ and 70 percent Gaussian noise $N(0, 0.01)$. Table above also shows the quantitative results. In this task, GCBD also performs much better than BM3D, EPLL, and WNNM, which further shows the superiority of GCBD in blind denoising problems.

It can be concluded that CNN has achieved a great success in image recognition, mainly because the structure of CNN is very suitable for learning image features. Because CNN has the structure of local receptive field, which is very conducive to sensory images like the human eye. Moreover, it has much reduced parameters than multi-layer perceptron network, and it is not easy to fall into overfitting. It is more suitable for training deep network, and has achieved very good results in image denoising. In particular, DnCNN, an image denoising technology based on deep convolution residual learning method, is one of the best in image denoising algorithms.

However, CNN-based image denoising method mainly focuses on extracting feature information and optimizing network structure. CNN has certain limitations, which are mainly reflected in the following two aspects. On the one hand, single convolutional neural network has no memory function, and shallow pixel-level information will be greatly lost during pooling, resulting in residual noise. On the other hand, increasing number of convolutional layers also leads to increasing number of parameters and calculation consumption.

E. Residual Network: ResNet

The development of basic networks in deep learning ranges from ALexNet (5 convolutional layers), VGG (19 convolutional layers) to GoogLeNet (22 convolutional layers), and the network structure is getting deeper. This is because deeper networks can extract more complex feature patterns, so that theoretically deeper networks can yield better results. But as the network depth constantly increases, the following two problems often arise:

Firstly, the network convergence becomes very difficult or even not converging accompanying with long time training. Problem of gradient disappearance/gradient explosion will appear.

- Gradient disappearance means that when the gradient (less than 1.0) is backpropagated to the front layer, the repeated multiplication may make the gradient infinitely small.
- Gradient explosion means that when the gradient (greater than 1.0) is backpropagated to the front layer, repeated multiplication may make the gradient become very large or even infinite, leading to overflow.

Secondly, with the network depth increasing, accuracy gets saturated (which might be unsurprising) and then degrades rapidly. Unexpectedly, such degradation is not caused by overfitting, and adding more layers to a suitably deep model leads to higher training error.

Therefore, on the one hand, the ResNet deep residual network is proposed to solve the defects caused by the increasing network depth promising good performance and efficiency even in the case of deep layers (even at 1000 layers).

The ResNet based denoising approach on the other hand can better compensate the limitations of CNN. In CNN, light networks can acquire pixel-level features, and deep networks acquire more semantic features. Semantic information is important in tasks such as identification, classification, but shallow pixel-level features are more critical for tasks such as denoising, super-resolution. Therefore, many residual network based denoising methods are designed to make full use of the shallow features.

A residual framework can be constructed from a plain network by introducing a deep residual learning framework. Instead of hoping each few stacked layers directly fit a desired underlying mapping, these laryers explicitly fit a residual mapping. Formally, denoting the desired underlying mapping as $H(x)$, let the stacked nonlinear layers fit another mapping of $F(x) := H(x) - x$. The original mapping is recast into $F(x) + x$. It is hypothesized that it is easier to optimize the residual mapping than to optimize the original, unreferenced mapping. To the extreme, if an identity mapping were optimal, it would be easier to push the residual to zero than to fit an identity mapping by a stack of nonlinear layers. Specially, the formulation of $F(x)+x$ can be realized by feedforward neural networks with "shortcut connections". Shortcut connections are those skipping one or more layers.

The residual network has become a popular topic in image denoising field. Over 150 papers in recent years related to residual network and deep learning technology in image denoising are discussed in details in the following.

Some papers focused on developed the residual network for general purpose denoise, including denoising, dehazing, derain, light revising, resolution enhancement and image restoration.

1) Denoising: Most of the denoising framework was based on the combination of CNN and residual network [156]–[174]. For example, One step forward was took in [156] by investigating the construction of feed-forward DnCNNs to embrace the progress in very deep architecture, learning algorithm, and regularization method into image denoising. Specifically, residual learning and batch normalization were utilized to speed up the training process as well as boost the denoising performance. Similarly, enhanced deep convolution neural network (EDCNN), for image denoising was presented in [160], which adopted the residual learning in both global and local manners. Some other module would be added into the network such as the dual path network (DPN) that combined the advantages of residual and densely connected networks used in [159], the non-local algorithm applied with a lightweight residual CNN in [160], the chain of identity mapping modules utilized in [161], the multi-wavelet residual dense convolutional neural network presented in [166], and the robust median filter (MF) forensic method using CNN based multiple residuals learning realized in [171].

Some of the learning structure was developed further utilizing the technique of dilate convolution [175]–[179]. The proposed method in [175] combined dilated convolution with skip connection of residual learning, which is trained by our proposed mixed loss function during back propagation. Dilated convolutions were used in the proposed model in [176] to extract more features by enlarging the receptive field and residual learning was adopted to overcome exploding gradient and vanishing gradient problems. The dilated residual CNN for Gaussian image denoising in [177] the DC-ResBlock, a ResBlock with an extra dilated convolution in [178] and the multi-scale trainable deep residual convolutional neural network (DCMSNet) based on dilated convolution was proposed in [179].

Some of the learning structure was developed with attention blocks [180]–[183] such as the deep boosting denoising net (DBDnet) in [180], the attention residual convolutional neural network (ARCNN) and its extension to blind denoising, flexible attention residual convolutional neural network (FARCNN) in [181], the PID controller guide attention neural network (PAN-Net), taking advantage of both the proportional-integralderivative (PID) controller and attention neural network in [182] and the residual dilated attention Nnetwork (RDAN). composed of a series of tailored residual dilated attention blocks (RDAB) and residual convolution attention blocks (RCAB) in [183].

The residual blocks could also been applied into other networks structure. Taking U-net for example, in [184] a residual dense neural network (RDUNet) was presented for image denoising based on the densely connected hierarchical network. The encoding and decoding layers of the RDUNet consisted of densely connected convolutional layers to reuse the feature maps and local residual learning to avoid the vanishing gradient problem and speed up the learning process. Multi-scale residual dense network (MRDN) and multi-scale residual dense cascaded U-Net with block-connection (MCU-Net) were built upon a newly designed multi-scale residual dense block (MRDB) in [185], and MCU-Net used MRDB to connect the encoder and decoder of the U-Net.

As for GAN, a grouped residual dense network (GRDN) combined with GAN was presented in [186]. Also another novel algorithm was shown in [187] to obtain more image features by adding multi-level convolution of the generative network, and adds multiple residual blocks and global residuals to extract and learn the features of the input noisy image to avoid the loss of features. Apart from the U-net and GAN, a Monte Carlo denoising network was combined with residual aggregation module and dense connections in [188].

2) Dehazing: The residual networks for general denoising could also be applied for dehazing [189]–[206]. The end-to-end dual attention fusion network (DAF-Net) in [189] for dehazing consisted of three residual groups, and each group comprises three residual dual attention fusion modules. Encoder recurrent decoder network (ERDN) in [190] consisted of two key components an encoder and a decoder. The proposed encoder was constructed by a residual efficient spatial pyramid (rESP) module such that it could effectively process hazy images at any resolution to extract relevant features at multiple contextual levels.

3) Derain: Some residual networks for general denoising were be explore to derain [?], [?], [207]–[210]. For example, a robust rain removal method was proposed in [207] with single images using an attentive composite residual network. A single-to-dual encoder-decoder structure was constructed, which consisted of an attentive net that identififies regions containing rain components during encoding, followed by a dual-channel architecture which recovered the background and detail components of the identified regions during decoding.

4) Light Revising: The residual networks for general denoising were also useful in light revising [211]–[215]. On the one hand, the network was required for light enhancement. The deep lowlight residual convolutional network (LRCNN) in [211] was proposed , which utilized the sparse coding feature to get the true signal and adaptively adjusted the image exposure in the low-light state. The residual connections in LRCNN helped to preserve more potential detail information in the original picture and accelerate the training speed of the network. On the other hand, the network was required for burst condition. Inspired by the extension of the gradient descent method that could handle non-smooth functions, namely the proximal gradient descent, and modern deep learning techniques, a residual based convolutional iterative network with a transparent architecture was investigated in [213].

5) Resolution: The ResNet for denoising was also popular in image resolution enhancement [216]–[224]. For example. The edge profile super-resolution (EPSR) method for structural information preservation and texture restoration was presented in [217]. EPSR was achieved by stacking modified fractal residual network (mFRN) structures hierarchically and repeatedly. Each mFRN was composed of many residual edge profile blocks (REPBs) that extract features and preserve the edge, structure, and texture information of the image.

6) Restoration: The ResNet for denoising was also useful in image restoration [225]–[231]. For example, to advance the practicability of restoration algorithms, a novel single-stage blind real image restoration network (R2Net) was realized in [227] by employing a modular architecture. A residual on the residual structure was utilized to ease low-frequency information flow and feature attention was applied to exploit the channel dependencies.

The ResNet has also been widely applied in different image denoising scenario, including the medical image, synthetic aperture radar (SAR) image [232]–[240], hyperspectral image [241]–[243], seismic image [244]–[254], and video [255]–[259]. Specially, as for medical image, the ResNet could be used for computed tomography (CT) [260]–[268], magnetic resonance imaging (MRI) [269], [270], [270]–[272], X ray [273], optical coherence tomography (OCT) [274], [275], positron emission computed tomography (PET) [276]–[279], laser [280], and 3D image denosing [281]–[283]. Meanwhile, the ResNet has also been utilized in some other special practical application [?], [284]–[303].

The ResNet-based image denoising method has relatively good characteristic expression ability for long-distance spatial correlation by maximizing information flow. However, a main problem in such methods is that multiple use of residual connections can easily lead to overfitting of the network.

F. Generative Adversarial Networks: GAN

Most CNN and ResNet-based denoising methods require noise-free clear image and noisy images pairs for supervised learning training samples. But in practice, the acquisition of paired training samples is difficult. Due to the strong learning ability of GAN, realistic noise maps can be obtained through adversarial learning training strategies, which can alleviate the problem of insufficient paired training samples to some extent.

GAN was developed by Ian Goodfellow et al. [304] in the year 2014. GANs consist of two neural networks: one is the Generator and the other is the Discriminator. The goal of the Generator is to learn to generate fake sample distribution to deceive the Discriminator whereas the goal of the Discriminator is to learn to distinguish between real and fake distribution generated by the Generator.

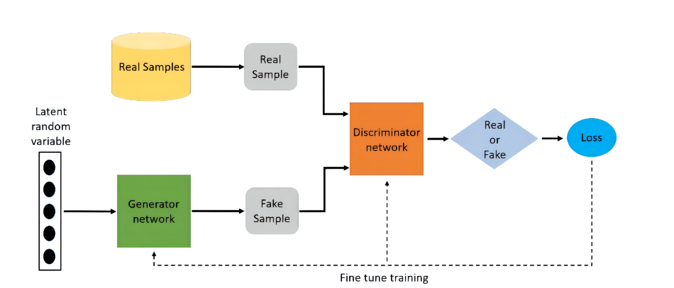

Fig. 11. Basic GAN architecture.

The general architecture of GAN which is comprised of the Generator and the Discriminator is shown in Figure 11. The Generator (G) takes in as input some random noise vector Z and then tries to generate an image using this noise vector indicated as $G(z)$. The generated image is then passed to the Discriminator and based on the output of the Discriminator the parameters of the Generator are updated. The Discriminator (D) is a binary classifier which simultaneously takes a look at both real and fake samples generated by the Generator and tries to decide which ones are real and which ones are fake. Given a sample image X, the Discriminator models the probability of the image being fake or real. The probabilities are then passed back to the Generator as feedback.

Over time each of the Generator and the Discriminator model tries to one up each other by competing against each other this is where the term "adversarial" of Generative Adversarial Networks comes from, and the optimization is based on the minimax game problem. During training both the Generator's and Discriminator's parameters are updated using back propagation with the ultimate goal of the Generator is to be able to generate realistic looking images and the Discriminator to get progressively better at detecting generated fake images from real ones.

The generative adversarial network requires calculating the loss of the generator (G) and the discriminator (D) during training, and the objective function is shown in Equation:

$$\begin{aligned} \min_{G} \max_{D} V(D,G) = E_{x\ P_{data(x)}}[log_a D(x)] \\ + E_{x\ P_{noise(z)}}[log_a(1 - D(G(z)))] \end{aligned} \tag{6}$$

The GAN has already become a popular topic in image denoising field. Over 170 papers in recent years related to GAN in image denoising are discussed in details in the following.

Some papers focused on developed the GAN for general purpose denoise, including denoising, dehazing, derain, deblur, detarget, light revising, image enhancement, image super-resolution and image restoration.

1) Denoising: Different kinds of GAN were designed for denoising [32], [305]–[326]. Some focused more on the outside noise. For example, the proposed GAN in [305] had a new generator network to produce denoised images with noisy images as input, and the entire network was trained using a new loss to represent the distance between the data distribution of clean images and denoised images. Asynchronous interactive generative adversarial network (AI-GAN) for denoising was proposed in [308], which decomposed the degraded signal into original and interfering parts progressively through a double branch structure. A novel boosting generative adversarial network (BoostNet) that not only combined all advantages of a generative adversarial sub-network and a deep convolutional neural network was shown in [310], which also successfully avoided the serious problems caused by the corruption and instability of training. Some focused more on the noise attack from the adversarial network. For example, a detector network was constructed in [306], which served as the dual network for the target classifier to be defended, being able to detect patterns of attack noise. The generative cleaning network and detector network were jointly trained using adversarial learning, fighting against each other to minimize both perceptual loss and adversarial loss.

2) Dehazing: Various kinds of GAN were also designed for dehazing [327]–[345]. Most of them focused on single image dehazing. For example, conditional adversarial networks based dehazing of hazy images (CANDY) was used in [327], which was a fully end-to-end model which directly generated a clean haze-free image from a hazy input image. Some focused on hyperspectral scenario. For example, the SkyGAN proposed in [328] was used for haze removal in aerial images, which consisted of a domain-aware hazy-to-hyperspectral (H2H) module, and a conditional GAN (cGAN) based multi-cue image-to-image translation module for dehazing.

3) Derain: There were also GAN applied for derain [580-584]. Author in [346]–[349] proposed to remove raindrops and improve image quality in the spatio-temporal domain by leveraging the inherent robustness of adopting motion cues and the restorative capabilities of conditional generative adversarial networks. A competitive single-image baseline that was capable of estimating the raindrop locations in a self-supervised manner, which was used later to bootstrap the novel spatio-temporal architecture.

4) Deblur: The GAN was also investigated in the deblur task [350]–[352]. A deep pyramid generative adversarial network with local and non-local similarity features, called LNL-PGAN, for natural motion image deblurring in [350] was proved to have superior performance against state-of-the-art methods on natural motion image deblurring in terms of visual quality and objective index.

5) Detarget: Some papers used the GAN for removal of specific target [353]–[355]. A composition GAN for removing snowflakes from a single image in [353], which comprised clean background module and a snow mask estimate module. The new background edge estimation algorithm based on the wasserstein generative adversarial network (WGAN) was proposed in [354] to distinguish the edges of the background image from the reflection. The proposed GAN in [355] eliminated hair from dermoscopic images by inducing a reconstructed distribution of images with hair to resemble a hairless distribution.

6) Light Revising: GAN was also used for denosing the image captured in the low-light environments [356], [357], [357]–[359]. For example, an mixed-attention guided generative adversarial network (MAGAN) was presented in [358] for low-light image enhancement in a fully unsupervised fashion. A mixed-attention module layer was introduced, which could model the relationship between each pixel and feature of the image.

7) Image Enhancement: GAN could be used for image enhancement. An unpaired two-way GAN learning method for image enhancement was applied in [360]. Given a set of photographs with the desired characteristics, the proposed method learned a photo enhancer which transforms an input image into an enhanced image with those characteristics.

8) Image Restoration: As for image restoration [361]–[367], GAN was also useful, which focused more on recovering the low-quality image to original high-quality image. Inspired by the recent success of image-to-image translation, the unsupervised Cycle-consistent based framework presented in [361] consisted of improved GAN. Since GAN-based methods tended to produce various artifacts with different models, model average could realize a smoother control of balancing artifacts and fidelity.

9) Image Super-resolution: GAN could be used for image super-resolution [368]–[379]. For example, a denoised high resolution generative adversarial network (DHRGAN) was presented in [368], which was capable of handling noise removal from given sample images while trying to super-resolve it to the desired magnification. As per knowledge, this was the first GAN framework equipped to remove noise while simultaneously trying to magnify images.

Considering from the denoising object, the GAN has also been widely applied in different image denoising scenario, including the medical image, synthetic aperture radar (SAR) image [239], [380]–[384], seismic image [253], [385]–[390], stellar image [391], [392], microscopy image [393]–[396], underwater image [397]–[402] and some others [121], [403]–[405]. Specially, as for medical image, the GAN could be used for CT [406]–[434], MRI [435], OCT [436]–[445], PET [446]–[451], X-ray [452], [453], ultrasound [454]–[457]. Some specific medical image processing problems could be well solved by GAN . For example, the novel joint framework proposed in [452] was for accurate COVID-19 identification by integrating an enhanced super-resolution GAN with a noise reduction filter bank of wavelet transform CNN on both Chest X-ray and chest tomography images for COVID-19 identification.

Considering from the denoising application, the GAN has also been utilized in some other special practical application. For example, the GAN was useful in investigation on factory production [458]–[465]. A method for detecting defects in rubber gloves based on normal samples (no defects) was proposed in [461], where a noise-reducing convolutional autoencoder was built in the network model as a generation network, and the least square loss is introduced for the model of confrontation training. Also, the GAN was useful in recovering the damaged documents [466]–[468]. And it also was utilized in facial image propblems [469]–[471] such as emotion enhancement, face recovering, face recognition. The GAN has also been used for dealing with dynamic video image [472], [473], such as automatic license plate recognition (ALPR) of moving vehicle and anomaly detection in surveillance systems.

The GAN-based image denoising method fits the data distribution through an adversarial learning strategy between the generator and the discriminator. The generative adversarial network has four advantages compared with other generative models:

1). Based on the actual results, GAN is able to produce better samples with sharper and clearer images than other models.

2). A generative adversarial network framework can be used to train any kinds of generator networks. Different from most of other generation frameworks requiring to have specific functional forms, such as Gaussian output layer, GAN has fewer limitations. It is also important that all other generator frameworks require non-zero mass while for GAN, points can be generated only on the thin manifold which is close to the data.

3). GAN does not need to design models following any kind of factorization. It can be functioned with any generator network or discriminator.

4). GAN does not need to repeatedly sample using Markov chains or inference during learning, avoiding the problem of approximating the intractable probability.

Comparing with PixelRNN, GAN can create a sample with less runtime. GAN produces one sample at a time, while PixelRNN needs to produce one pixel at a time. As for VAE, GAN has no lower limit of change. If the discriminator network fits perfectly, then it can recover the training distribution perfectly. Various adversarial generation networks will gradually agree towards asymptotically consistent, while the VAE turning bias. Comparing with Boltzmann and GSN, there is neither a lower bound nor a tricky partition function for GAN. The samples can be generated at one time, rather than repeated utilizing the Markov Chain operator. Referring to NICE and Real NVE, there is no limitation on the size of the latent code for GAN.

Currently the main problems of GAN can be summarized as following:

1). The distribution of the generated model has no dominant expression and shows poor interpretability.

2). Generators and discriminators need to update the parameters synchronously, while it is difficult to generate discrete data.

3). The non-convergence problem is hard to solve for GAN.

4). The Nash equilibrium is impossible to realize. All theories suggest that the GAN should perform well on a Nash equilibrium, but the equilibrium can only be guaranteed with gradient descent in the case of a convex function. Thus, the solution of Nash equilibrium has not been found. When both sides of the game are represented by neural networks, the strategy will never reach stable without an equilibrium.

5). The collapse problem will always exist. The GAN model is defined as a min-max problem without loss function, and it is difficult to distinguish progress during training. In the learning process, GAN may encounter the crash problem (collapse problem), where the generator begins to degenerate and always generates the same sample points. When the generative model collapses, the discriminant model will also point in similar directions to similar sample points, and the training cannot continue.

6). GAN does not require prior modeling leading to over freedom problem that is uncontrollable. In contrast to other generative models, GAN no longer requires a hypothetical data distribution and sampling on the distribution directly approximating ground truth data. However, this unpremodelling method will stuck in over freedom situation. For large image with more pixels, the GAN based approach is sometimes uncontrollable for training.

G. Graph Neural Network: GNN

GNNs are neural models that capture the dependence of graphs via message passing between the nodes of graphs. In recent years, variants of GNNs such as graph convolutional network (GCN), graph attention network (GAT), graph recurrent network (GRN) have demonstrated ground-breaking performances on many deep learning tasks.

CNNs can only operate on regular Euclidean data like images (2-D grids) and texts (1-D sequences) while these data structures can be regarded as instances of graphs. Therefore, it is straightforward to generalize CNNs on graphs. Based on CNNs and graph embedding, variants of GNNs are proposed to collectively aggregate information from graph structure. Thus they can model input and/or output consisting of elements and their dependency.

The general design pipeline of a GNN model for a specific task depends on a specific graph type. Generally, the pipeline contains four steps.

1). Find graph structure: At first, the graph structure needs to be figured out in the application. There are usually two scenarios: structural scenarios and non-structural scenarios. In structural scenarios, the graph structure is explicit in the applications. In non-structural scenarios, graphs are implicit so that graph is required to be built from the task. The later design process attempts to find an optimal GNN model on this specific graph.

2). Specify graph type and scale: After finding graph structure, the graph type and its scale needs to be decided. Graphs with complex types could provide more information on nodes and their connections. Graphs are usually categorized as:

- Directed/Undirected Graphs: Edges in directed graphs are all directed from one node to another, which provide more information than undirected graphs. Each edge in undirected graphs can also be regarded as two directed edges.
- Homogeneous/Heterogeneous Graphs: Nodes and edges in homogeneous graphs have same types, while nodes and edges have different types in heterogeneous graphs. Types for nodes and edges play important roles in heterogeneous graphs and should be further considered.
- Static/Dynamic Graphs: When input features or the topology of the graph vary with time, the graph is regarded as a dynamic graph. The time information should be carefully considered in dynamic graphs.

3). Design loss function: In this step, the loss function should be designed based on task type and the training setting. For graph learning tasks, there are usually three kinds of tasks:

- Node-level: Tasks focus on nodes, which include node classification, node regression, node clustering, etc. Node classification tries to categorize nodes into several classes, and node regression predicts a continuous value for each node. Node clustering aims to partition the nodes into several disjoint groups, where similar nodes should be in the same group.
- Edge-level: Tasks are edge classification and link prediction, which require the model to classify edge types or predict whether there is an edge existing between two given nodes.
- Graph-level: Tasks include graph classification, graph regression, and graph matching, all of which need the model to learn graph representations. From the perspective of supervision, the graph learning tasks can be categorized into three different training settings: supervised setting, semi-supervised setting, transductive setting, unsupervised setting.

4). Build model using computational modules: Finally, the model can be built using the computational modules. Some commonly used computational modules are: propagation module, sampling module, pooling module. With these computation modules, a typical GNN model is usually built by combining them.

Since GNN has become a popular topic in image denoising, some papers developed the GNN structure. Cross-Patch Net (CPNet), which was the first deep- learning-based real image denoising method for high resolution (HR) input was presented in [474]. The graph convolutional network (GCN) was used to capture the crosspatch contextual dependency and optimize the training loss to exploit the properties of the noise level map. The robustness merit of model-based approaches and the learning power of data-driven approaches for real image denoising were combined in [475]. Specifically, by integrating graph Laplacian regularization as a trainable module into a deep learning frame work, the framework was less susceptible to overfitting than pure CNN based approaches, achieving higher robustness to small datasets and cross-domain denoising. A novel end-to-end trainable neural network architecture was proposed in [476]. The employing layers was based on graph convolution operations, thereby creating neurons with non-local receptive fields. The graph convolution operation generalized the classic convolution to arbitrary graphs. A dual-mode iterative denoiser was used in [477] to tackle the weak label challenge for anomaly detection. The graph convolution neural network (GCN) was applied to explore the temporal correlation and the feature similarity between video clips within different rough labels, where the classifier could be constantly updated in the label denoising process. GNN using GraphBio was constructed in [478] as graph filter. Unlike convolutional filters in previous GNNs, the employed GraphBio was analytically defined and required no training, and optimized the end-to-end system only via learning of appropriate graph topology at each layer. GNN that employed grap convolutional layers in order to exploit both local and non-local similarities was presented in [479]. The graph convolutional layers dynamically constructed neighborhoods in the feature space to detect latent correlations in the feature maps produced by the hidden layers. A new image denoising method using multiple-minimum cuts based on the maximum-flow neural network (MF-NN) was used in [480]. The classical graph signal filtering was combined with deep feature learning in [481] into a competitive hybrid design, that utilized interpretable analytical low-pass graph filters.

GNN has also been widely applied in different image denoising scenario. Two graphs were specially designed in [482] to extract representations from new dimensions. The first graph models the global spatial relationship between pixels in the feature, while the second graph models the interrelationship across the channels. Motivated by the property of GCN, in [483], an encoder-decoder-based graph convolutional network (ED-GCN) was invented for CT image denoising. Using two cascaded graph convolutional networks, FaceGraph performsed global-to-local discrimination in [484] to select useful data in a noisy environment. A deep learning method that could simultaneously denoise a point cloud and remove outliers in a single Model was applied in [485], whose core was a GCN that was able to efficiently deal with the irregular domain and the permutation invariance problem.

As for denoising using GNN networked topology methods, limitations are reflected in the fact that the unstable dynamic topology reducing the expression ability of features which will negatively affect the denoising performance. The graph network cannot not extract local and global features as CNN, and the utilization of local information in the neighborhood will be directly affected by the topological instability.

H. Deep Learning Conclusion

In recent years, a series of improved approaches combining multi-scale feature fusion, transfer learning, and dual tasks based on the CNN, Res Net, and GAN networks continuously emerge.

1) Denoising approach combined with multi-scale features fusion: The model trained by a single network structure is only able to extract limited features, and the feature fusion between different scales is conducive to improving the expression power of the noise. In the feature fusion, the prior information can be considered contributing to accurately grasp the target objects. There are various ways for realizing multis-cale fusion. Jia et al. [486] enhances the long-term memory of the network during forward propagation and back propagation by solving the fractional optimal control problem (FOC) and performing an explicit discrete construction of fractional Differential equations (FODE). Liu et al. [487] designs densely connected encoders to connect features of different scales, making full use of context information. And the dense connection deepens the network and reduces the problem of gradient vanishing. Wang et al. [488] introduced the self-attention module (Self-Attention) to obtain the spatial and interchannel dependencies without increasing the number of parameters nor reducing the channel dimension, enhancing the adaptation of feature fusion to each channel. In addition, the pyramidal mode denoising network [489] can realize the information fusion of different scales through downsampling operations.

2) Duel-task image denoising method: Image denoising requires the balancing of two mutually exclusive targets, namely noise removal and preserving true details. Wang et al. [490] proposed dual-task denoising network combining GAN with CNN, where GAN was used to remove the noise, and CNN was used to recover the original image details. Two subnets were trained alternately to retain more details and remove noise through adaptive regulatory parameters. Unlike the above method, Tian et al. [491] adopted the reconstruction idea to design a Dude Net consisting of 4 modules, including feature extraction, enhancement, compression, and reconstruction. Data enhancement improves feature expression power, and data compression is conducive to reducing redundant information, reducing computational cost and memory consumption. The significant advantage of such dual-task image denoising is its ability to find equilibrium points between mutually exclusive targets, providing great help in solving problems such as smoothing, blurring, and artifacts.

3) Migration learning of the image denoising method: For the image denoising problem, on the one hand, due to the small number and single type of real image datasets, it is insufficient to train CNN which is prone to overfitting problem. On the other hand, the CNN trained by Gaussian noise cannot apply well for the real Gaussian-containing images ,because of overfitting. On the contrary, transfer learning denoising methods not only converge faster and achieve well denoising performance. It can also save a lot of memory by adaptive adjusting parameters. As described in Kim et al [492], AINDNet learns general invariant information from synthetic noise images and domain-specific information about real images from the continuous wavelet domain. AINDNet thus transfers the denoising task from synthetic noise to real noise, promoting the performance of denoising.

These improved image denoising methods achieve great performance on synthetic noise and real noise, but still have some limitations, such as insufficient accuracy when fitting real noise, difficulty in realizing dense distributed noise remove, uncontrollable relationship between denoising and details keeping in the process of convolutional feature extraction, misidentified noise resulting in noise residue and poor denoising effect.

In conclusion, image denoising algorithms designed based on different network architectures have different priorities in dealing with denoising problems. Those image denoising methods based on CNN and ResNet focuses on the calculation of long-distance correlations by maximizing information flow, improving the utilization of high and low frequency information and the expression ability of noise. The GAN-based image denoising methods focus on expanding the image dataset and improving the network denoising performance by increasing the number of training samples. GNN is mainly used to process unstructured data. Due to the complex real noise distribution, diverse types and difficult to parameterize, the traditional convolutional feature extraction method is difficult to meet the needs of practical applications, promoting the development of GNN. However, the training effect of graph network is unstable due to the complex topology and size are unstable. Therefore, when studying the image denoising task, it is necessary to select the basic network according to the problems existing in the current image denoising field and the problems to be solved.

IV. Thermal Image Dataset Based Denoising Experiment

Since most of the deep learning based denoising methods are tested based on the RGB datasets, this overview also performs these denoising methods on the thermal datasets for comparison. Two kinds of experiment, simulation test and real test, have been implemented to exam the denoising performance of these deep learning based methods on thermal image. Simulation test uses the simulated thermal image transferred from the RGB image. Real test uses the thermal image directly from the infrared data set.

A. Brief Introduction of Deep Learning Based Denoising on Thermal Image

In section 3, we have discussed different kinds of deep learning based denoising algorithms and corresponding application. Specially, papers related to thermal image denoising have been included. As one of the typical multi-modal denoising task, deep learning based thermal image denoising has been demonstrated in detail. To further introduce deep learning based thermal image denoising, we will give a brief and pertinent review on the topic again before we display our experiment results.

There are many paper considering how to remove noise from infrared image using deep CNN. For example, a infrared image denoising network was investigated in [493], whose structure composed of convolutional subnet and deconvoluted subnet. The convolution subnet extracted the features of the image, and the deconvolution subnet reconstructed the original image through the feature map. In [494], a deep CNN was used for single infrared image stripe noise removal. Similarly, a new deep network architecture for removing a stripe noise from a single meteorological satellite infrared cloud image was presented in [495]. In the proposed framework, a residual learning was utilized to directly reduce the mapping range from input to output, which speeded up the training process as well as boosts the destriping performance. Apart from focusing on the strip noise removal, non-uniformity correction problems such as loss of image details and blurred edge of image in infrared image was also investigated. An improved non-uniformity correction method of infrared images based on convolution neural network using long-short connections (LSC-CNN) was proposed in [496].

Some other papers focused on the super-resolution of thermal image. A modified architecture inspired by SRGAN was used for thermal image super-resolution in [497]. In order to make the model faster to train while having less training parameters, the number of residual blocks was reduced to 5. The batch normalization layers were excluded from the residual blocks of both the generator and discriminator networks to remove the redundancy. Before each convolution layer, reflective padding is utilized at the edges to preserve the size of the feature maps. Similarly, a channel splitting-based convolutional neural network (ChasNet) was introduced in [498] for thermal image SR eliminating the redundant features in the network. The use of channel splitting extracted the versatile features from low-resolution (LR) thermal image, helping to preserve high-frequency details in the SR images. A deep learning-based thermal image restoration method that simultaneously performed super-resolution reconstruction and deblurring was investigated in [499]. A deblur-SRRGAN was proposed for thermal image reconstruction and a light-weighted Mask R-CNN was used for object detection in the reconstructed thermal image.

Some papers were more interested in the super-resolution of thermal video. For example, a new method was introduced in [500] to achieve high dynamic range infrared image compression. In the proposed framework, the Laplace differential and Histogram projection were respectively used to sharpen and compress the raw image. Another paper presented a comparative analysis of super resolution (SR) techniques based on deep neural networks (DNN) that were applied on thermal video dataset in [501]. SRCNN, EDSR, auto-encoder, and SRGAN were also discussed and investigated. Further the results on benchmark thermal datasets including FLIR, OSU thermal pedestrian database and OSU color thermal database were evaluated and analyzed.

B. Deep Learning Based Simulation Test

Training Data Set:

The transformation training datasets are divided into two categories: gray-noisy and color-noisy images. The gray RGB image will be transfer to simulated thermal in gray scale and the color RGB image will be transferred to simulated thermal with color channel. And the relative noisy image will be formed by adding additive Gaussian noise on the original image. The gray-noise group includes the BSD400 dataset and Waterloo Exploration Database. Specially, the BSD400 dataset is composed of 400 images in .png format, and is cropped into a size of 180 $\times$ 180 for training a denoising model. The Waterloo Exploration Database consisted of 4744 nature images with a .png format. Color-noisy images in cludes the BSD432, Waterloo Exploration Database and polyU-Real-World-Noisy-Images datasets. Specifically, the polyUReal-World-Noisy-Images consisted of 100 real noisy images with sizes of 2784 $\times$ 1856 obtained by five cameras: a Nikon D800, Canon 5D Mark II, Sony A7 II, Canon 80D and Canon 600D.

Testing Data Set:

The test datasets includes gray-noisy and color-noisy image datasets. The gray-noisy image dataset was composed of Set12 and BSD68. The Set12 contained 12 scenes. The BSD68 contained 68 nature images. The color-noisy image dataset included CBSD68, Kodak24, McMaster, cc, DND, NC1, SIDD and Nam. The Kodak24 and McMaster contained 24 and 18 color noisy images, respectively. The cc contained 15 real noisy images of different ISO, i.e., 1600, 3200 and 6400. The DND contained 50 real noisy images and the clean images were captured by low-ISO images. The NC12 contained 12 noisy images and did not have ground-truth clean images. The SIDD contained real noisy images from smart phones, and consisted of 320 image pairs of noisy and ground-truth images. The Nam included 11 scenes, which were saved in JPGE format.

Experiment Results:

To verify the denoising performance of methods mentioned in the above Section, some experiments are conducted on the BSD68, CBSD68, Kodak24, McMaster datasets in terms of quantitative and qualitative evaluations. The quantitative evaluation is shown in the table, which mainly used peak-signalto-noise-ratio (PSNR) values of different denoisers to test the denoising effects. The qualitative evaluation used visual figures to show the recovered clean images in Fig. 12.

Table IV and Table V show the comparison of PSNR values of the simulation results of the gray-noisy and color-noisy group set. It can be seen from the experimental data that each network effectively improves the PSNR of the images under different noise levels indicating the denoising effectiveness. Specifically, the denoising performance of these methods are similar with similar PSNR values at the same noise level. Moreover, at the same noise level, the difference of PSNR between the traditional comparison method BM3D and deep

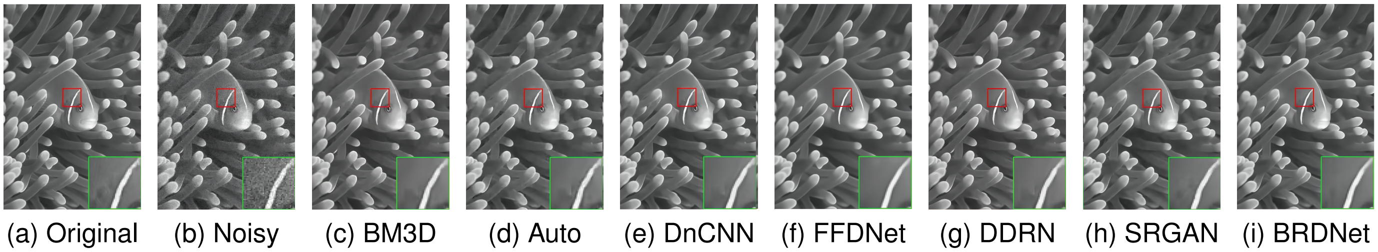

Fig. 12. Denoising results of different methods on gray-noisy group one image from the BSD68 with $\sigma = 15$: (a) original image, (b) noisy image/24.62dB, (c) BM3D/35.29dB, (d) AutoEncoder/34.98dB, (e) DnCNN/36.20dB, (f) FFDNet/36.75dB, (g) DDRN/35.94dB, (h) SRGAN/36.03dB, and (i) BRDNet/36.59dB.

learning is relatively high, indicating improvement in infrared image denoising. Comparing under the same method, the results of PSNR at different noise levels tends to decrease with the increasing of noise level, which shows that the effect of denoising begins to weaken with rising noise level.

TABLE IV
AVERAGE PSNR VALUES ON THE GRAY-NOISE GROUP UNDER ADDITIVE WHITE NOISY WITH VARIOUS NOISE LEVELS.

Dataset	Methods	$\sigma = 15$	$\sigma = 25$	$\sigma = 50$
BSD68	BM3D	31.91	29.45	26.13
	AutoEncoder	32.17	29.64	26.45
	DDRN	32.19	29.48	27.07
	DnCNN	32.04	30.11	27.10
	FFDNet	32.55	30.28	27.21
	SRGAN	32.80	30.34	27.44
CBSD68	BM3D	34.93	33.22	30.33
	DDRN	33.93	31.24	27.86
	DnCNN	34.17	32.56	29.48
	FFDNet	34.89	33.06	30.07
Kodak24	BM3D	33.25	30.85	27.40
	DnCNN	33.49	31.04	27.51
	FFDNet	33.21	30.98	27.67
McMaster	BM3D	32.17	29.80	26.05
	DnCNN	31.99	29.46	25.70
	FFDNet	32.29	29.57	25.84

C. Deep Learning Based Real Test

Training and Testing Data Set

Both of the training and testing data for real test come from the real thermal image data set such as FLIR, OSU thermal pedestrian database and OSU color thermal database which are all benchmark thermal datasets. The video frames are recorded at a rate of 30fps while the image sequences are sampled at 1fps or 2 fps. With more than 14,000 total images, it includes numerous classes like person, car, bicycle, dog etc. OSU thermal pedestrian database is captured using Raytheon 300D thermal sensor core at sampling rate less than 30Hz. Total 284 frames are contained inside the dataset. OSU

TABLE V
AVERAGE PSNR VALUES ON THE COLOR-NOISE GROUP UNDER ADDITIVE WHITE NOISY AT VARIOUS NOISE LEVELS.

Dataset	Methods	$\sigma = 15$	$\sigma = 25$	$\sigma = 50$
BSD68	BM3D	31.05	28.57	25.62
	AutoEncoder	35.51	35.63	35.19
	DDRN	34.72	35.87	34.78
	DnCNN	36.22	36.71	35.74
	FFDNet	33.01	35.73	35.35
	SRGAN	35.22	36.34	35.43
CBSD68	BM3D	33.52	30.71	27.38
	DDRN	33.93	31.24	27.86
	DnCNN	33.98	31.24	27.86
	FFDNet	33.76	31.18	27.48
Kodak24	BM3D	34.28	31.68	28.46
	DnCNN	34.73	32.23	29.02
	FFDNet	34.55	32.11	28.99
McMaster	BM3D	34.06	31.66	28.51
	DnCNN	34.08	32.47	29.21
	FFDNet	34.47	32.25	29.14

color thermal database is a mix blend of thermal and color imagery. Acquired using 25 mm Raytheon Palm IR 250 D thermal sensor, sampling rate is nearly 30Hz with total of 17089 images (colored as well as non-colored).

Experiment Set Up

The training and testing processes for the proposed algorithms are conducted on Google Colab which provide frees GPU and TPU access to accelerated. Furthermore, the algorithms were implemented in Python (version 3.7). As for the deep learning library, Keras application programming interface (API) (version 2.1.6-tf) with Tensorflflow backend engine (version 1.9.0) are used. The image processing part was implemented using the OpenCV library (version 4.3.0).

Experiment Results

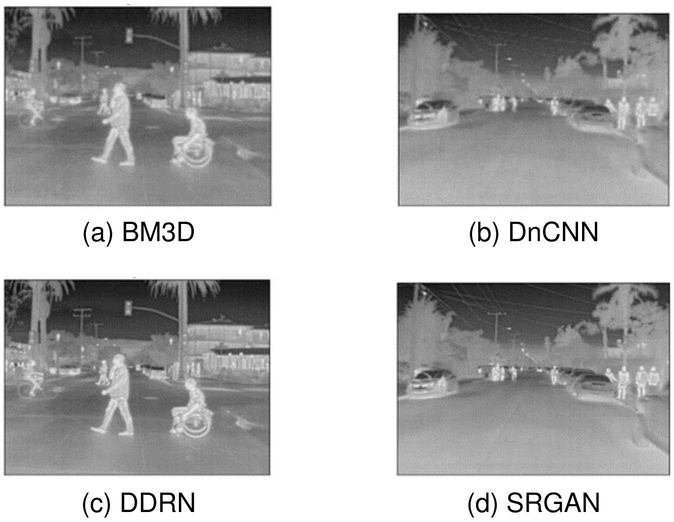

Fig. 13. Denoising results of different methods on color-noisy group one image with $\sigma = 25$: (a) BM3D/31.68dB, (b) DnCNN/29.08dB, (c) DDRN/30.03dB, (d) SRGAN/30.87dB.

The PSNR and SSIM values of the real test of the gray-noisy and color-noisy group under additive Gaussian noise condition where $\sigma = 25$ are shown in the Table VI. It can be figured out that deep learning network can help with the noisy thermal image, improving the view quality. However, campared with the simulation test results denoising with simulated thermal image, the denoising performance on the real thermal image is worse under same noise level. The average PSNR and SSIM values are relative low in the case of real thermal image.

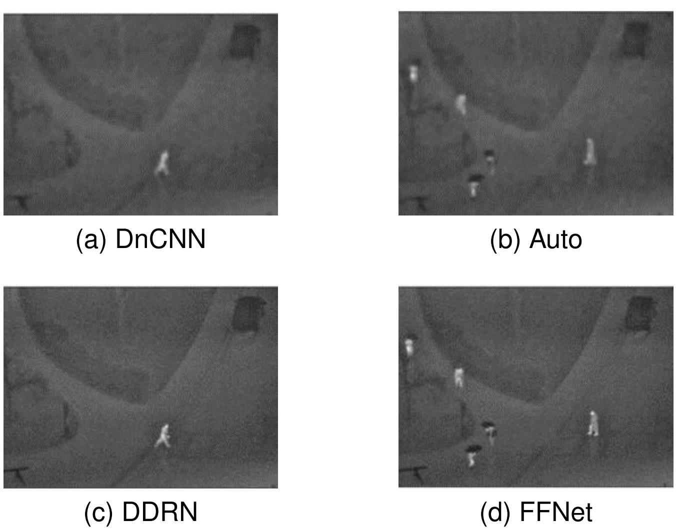

Fig. 14. Denoising results of different methods on gray-noisy group one image with $\sigma = 25$: (a) DnCNN/28.36dB, (b) AutoEncoder/34.78dB, (c) DDRN/26.03dB, (d) FFDNet/28.92dB.

The qualitative evaluation of the real test has been shown in the following, which display the recovering results of gray-noisy group in Fig.13 and Fig.14, and the recovering results of the color-noisy group in Fig.15 and Fig.16. Specially, the PSNR values for different methods have been noted in the figures. It can be roughly concluded that most of the deep learning technology perform efficiently in thermal image denoising as the networks reconstruct the fine-texture details and maintains the high-frequency component of the frame. As a result, the frames appear to be less blurry by resembling more like the original one. However, sometimes these methods often suffer from non-convergence and diminished gradient problem and are difficult to train.

TABLE VI
AVERAGE PSNR AND SSIM VALUES ON BOTH COLOR-NOISY AND GRAY-NOISY GROUPS UNDER ADDITIVE WHITE NOISY AT $\sigma = 25$.

Dataset	Methods	Channel	PSNR	SSIM
OSU	BM3D	color	28.14	0.895
		gray	31.68	0.903
	AutoEncoder	color	29.06	0.913
		gray	34.78	0.916
	DDRN	color	30.37	0.908
		gray	26.03	0.869
	DnCNN	color	30.01	0.882
		gray	28.36	0.907
	FFNet	color	31.03	0.908
		gray	28.92	0.914
	SRGAN	color	35.44	0.918
		gray	30.87	0.912
FLIR	BM3D	color	28.62	0.899
		gray	29.54	0.894
	AutoEncoder	color	30.11	0.881
		gray	28.19	0.898
	DDRN	color	29.12	0.901
		gray	30.03	0.903
	DnCNN	color	29.01	0.889
		gray	29.08	0.875
	FFNet	color	30.08	0.901
		gray	31.44	0.918
	SRGAN	color	29.63	0.819
		gray	29.62	0.915

V. CONCLUSION

Image denoising based on visible and infrared images (RGB-infrared) has attracted considerable attention and made significant progress in the past few years. In this paper, we comprehensively review existing RGB-infrared deep learning based denoising methods in the literature. These approaches can be generally divided into five categories: MLP, CNN, ResNet, GAN, GNN. Each category is introduced and summarized according to core idea and representative methods. The experimental performance of each method is also demonstrated on public (RGB) data set. For each category, we summarize and analyze main results on public large-scale datasets to potentially provide an objective performance reference for researchers in the field of RGB-infrared denoising. Specially, since most of the denoising methods are tested based on the RGB datasets, in the last experiment section, these models are also trained, tested and evaluated respectively with thermal image. We observe that the deep learning based methods give the leading performance and thus providing the most promising research direction in RGB-infrared denoising. This paper provides interested readers with an organized overview of the RGB-infrared based denoising and can serve as a starting point for researchers who are interested in this field.

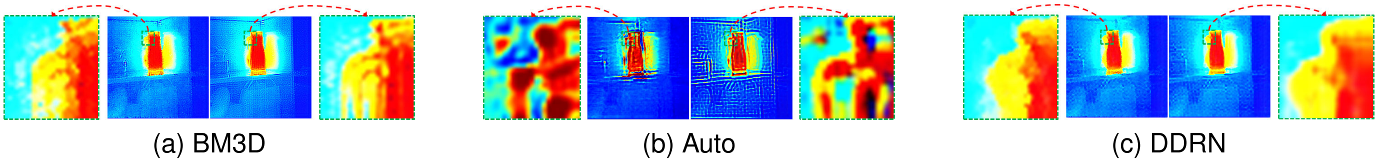

Fig. 15. Denoising results of different methods on color-noisy group one image with $\sigma = 25$: (a) BM3D/28.14dB, (b) AutoEncoder/29.06dB, (c) DDRN/30.37dB.

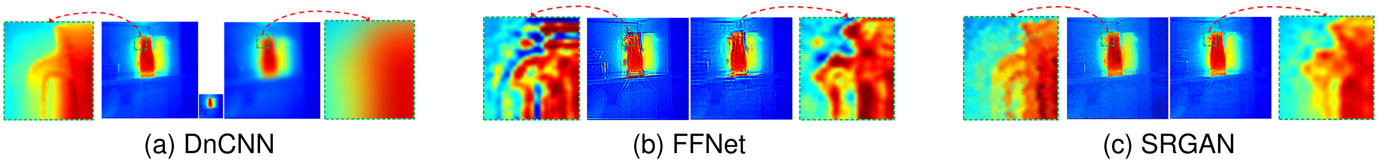

Fig. 16. Denoising results of different methods on color-noisy group one image with $\sigma = 25$: (a) DnCNN/30.014dB, (b) FFNet/31.03dB, (c) SRGAN/35.44dB.

REFERENCES

[1] H. Dai Duong and D. T. Tinh, "An efficient method for vision-based fire detection using svm classification," in *2013 International Conference on Soft Computing and Pattern Recognition (SoCPaR)*. IEEE, 2013, pp. 190–195.

[2] M. C. Motwani, M. C. Gadiya, R. C. Motwani, and F. C. Harris, "Survey of image denoising techniques," in *Proceedings of GSPX*, vol. 27, 2004, pp. 27–30.

[3] C. Tian, L. Fei, W. Zheng, Y. Xu, W. Zuo, and C.-W. Lin, "Deep learning on image denoising: An overview," *Neural Networks*, vol. 131, pp. 251–275, 2020.

[4] K. Fukushima and S. Miyake, "Neocognitron: A self-organizing neural network model for a mechanism of visual pattern recognition," in *Competition and cooperation in neural nets*. Springer, 1982, pp. 267–285.

[5] Y.-W. Chiang and B. Sullivan, "Multi-frame image restoration using a neural network," in *Proceedings of the 32nd Midwest Symposium on Circuits and Systems,*. IEEE, 1989, pp. 744–747.

[6] Y. Zhou, R. Chellappa, and B. Jenkins, "A novel approach to image restoration based on a neural network," in *Proceedings of the International Conference on Neural Networks, San Diego, California*, 1987.

[7] D. Greenhill and E. Davies, "Relative effectiveness of neural networks for image noise suppression," in *Machine Intelligence and Pattern Recognition*. Elsevier, 1994, vol. 16, pp. 367–378.

[8] D. de Ridder, R. P. Duin, P. W. Verbeek, and L. Van Vliet, "The applicability of neural networks to non-linear image processing," *Pattern Analysis & Applications*, vol. 2, no. 2, pp. 111–128, 1999.

[9] L. Bedini and A. Tonazzini, "Image restoration preserving discontinuities: the bayesian approach and neural networks," *Image and Vision Computing*, vol. 10, no. 2, pp. 108–118, 1992.

[10] E. Gardner, D. Wallace, and N. Stroud, "Training with noise and the storage of correlated patterns in a neural network model," *Journal of Physics A: Mathematical and General*, vol. 22, no. 12, p. 2019, 1989.

[11] L. Bedini and A. Tonazzini, "Neural network use in maximum entropy image restoration," *Image and Vision Computing*, vol. 8, no. 2, pp. 108–114, 1990.

[12] J. K. Paik and A. K. Katsaggelos, "Image restoration using a modified hopfield network," *IEEE Transactions on image processing*, vol. 1, no. 1, pp. 49–63, 1992.

[13] J. Nossek and T. Roska, "Special issue on cellular neural networks-introduction," pp. 145–146, 1993.

[14] K. Sivakumar and U. B. Desai, "Image restoration using a multilayer perceptron with a multilevel sigmoidal function," *IEEE transactions on signal processing*, vol. 41, no. 5, pp. 2018–2022, 1993.

[15] C.-C. Lee and J. P. de Gyvez, "Color image processing in a cellular neural-network environment," *IEEE Transactions on neural networks*, vol. 7, no. 5, pp. 1086–1098, 1996.

[16] M. Zamparelli, "Genetically trained cellular neural networks," *Neural networks*, vol. 10, no. 6, pp. 1143–1151, 1997.

[17] S.-C. Lo, S.-L. Lou, J.-S. Lin, M. T. Freedman, M. V. Chien, and S. K. Mun, "Artificial convolution neural network techniques and applications for lung nodule detection," *IEEE transactions on medical imaging*, vol. 14, no. 4, pp. 711–718, 1995.

[18] W. Ren, S. Liu, H. Zhang, J. Pan, X. Cao, and M.-H. Yang, "Single image dehazing via multi-scale convolutional neural networks," in *European conference on computer vision*. Springer, 2016, pp. 154–169.

[19] J. Liang and R. Liu, "Stacked denoising autoencoder and dropout together to prevent overfitting in deep neural network," in *2015 8th international congress on image and signal processing (CISP)*. IEEE, 2015, pp. 697–701.

[20] K. He, X. Zhang, S. Ren, and J. Sun, "Delving deep into rectifiers: Surpassing human-level performance on imagenet classification," in *Proceedings of the IEEE international conference on computer vision*, 2015, pp. 1026–1034.

[21] Z. Zhang, L. Wang, A. Kai, T. Yamada, W. Li, and M. Iwahashi, "Deep neural network-based bottleneck feature and denoising autoencoder-based dereverberation for distant-talking speaker identification," *EURASIP Journal on Audio, Speech, and Music Processing*, vol. 2015, no. 1, pp. 1–13, 2015.

[22] D. Yuan, N. Fan, and Z. He, "Learning target-focusing convolutional regression model for visual object tracking," *Knowledge-Based Systems*, vol. 194, p. 105526, 2020.

[23] D. Ren, W. Shang, P. Zhu, Q. Hu, D. Meng, and W. Zuo, "Single image deraining using bilateral recurrent network," *IEEE Transactions on Image Processing*, vol. 29, pp. 6852–6863, 2020.

[24] C. Tian, Y. Xu, W. Zuo, B. Zhang, L. Fei, and C.-W. Lin, "Coarse-to-fine cnn for image super-resolution," *IEEE Transactions on Multimedia*, vol. 23, pp. 1489–1502, 2020.

[25] X. Mao, C. Shen, and Y.-B. Yang, "Image restoration using very deep convolutional encoder-decoder networks with symmetric skip connections," *Advances in neural information processing systems*, vol. 29, 2016.

[26] K. Zhang, W. Zuo, Y. Chen, D. Meng, and L. Zhang, "Beyond a gaussian denoiser: Residual learning of deep cnn for image denoising," *IEEE transactions on image processing*, vol. 26, no. 7, pp. 3142–3155, 2017.

[27] S. Ioffe and C. Szegedy, "Batch normalization: Accelerating deep network training by reducing internal covariate shift," in *International conference on machine learning*. PMLR, 2015, pp. 448–456.

[28] V. Nair and G. E. Hinton, "Rectified linear units improve restricted boltzmann machines," in *Icml*, 2010.

[29] K. He, X. Zhang, S. Ren, and J. Sun, "Deep residual learning for image recognition," in *Proceedings of the IEEE conference on computer vision and pattern recognition*, 2016, pp. 770–778.

[30] S. Lefkimmiatis, "Non-local color image denoising with convolutional neural networks," in *Proceedings of the IEEE conference on computer vision and pattern recognition*, 2017, pp. 3587–3596.

[31] K. Zhang, W. Zuo, and L. Zhang, "Ffdnet: Toward a fast and flexible solution for cnn-based image denoising," *IEEE Transactions on Image Processing*, vol. 27, no. 9, pp. 4608–4622, 2018.

[32] J. Chen, J. Chen, H. Chao, and M. Yang, "Image blind denoising with generative adversarial network based noise modeling," in *Proceedings of the IEEE conference on computer vision and pattern recognition*, 2018, pp. 3155–3164.

[33] S. Guo, Z. Yan, K. Zhang, W. Zuo, and L. Zhang, "Toward convolutional blind denoising of real photographs," in *Proceedings of the IEEE/CVF conference on computer vision and pattern recognition*, 2019, pp. 1712–1722.

[34] K. Zhang, W. Zuo, S. Gu, and L. Zhang, "Learning deep cnn denoiser prior for image restoration," in *Proceedings of the IEEE conference on computer vision and pattern recognition*, 2017, pp. 3929–3938.

[35] J. Schmidhuber, "Deep learning in neural networks: An overview," *Neural networks*, vol. 61, pp. 85–117, 2015.

[36] B. Karlik and A. V. Olgac, "Performance analysis of various activation functions in generalized mlp architectures of neural networks," *International Journal of Artificial Intelligence and Expert Systems*, vol. 1, no. 4, pp. 111–122, 2011.

[37] A. C. Marreiros, J. Daunizeau, S. J. Kiebel, and K. J. Friston, "Population dynamics: variance and the sigmoid activation function," *Neuroimage*, vol. 42, no. 1, pp. 147–157, 2008.

[38] E. Fan, "Extended tanh-function method and its applications to nonlinear equations," *Physics Letters A*, vol. 277, no. 4-5, pp. 212–218, 2000.

[39] K. Jarrett, K. Kavukcuoglu, M. Ranzato, and Y. LeCun, "What is the best multi-stage architecture for object recognition?" in *2009 IEEE 12th international conference on computer vision*. IEEE, 2009, pp. 2146–2153.

[40] H. C. Burger, C. J. Schuler, and S. Harmeling, "Image denoising: Can plain neural networks compete with bm3d?" in *2012 IEEE conference on computer vision and pattern recognition*. IEEE, 2012, pp. 2392–2399.

[41] P. K. Sethy, L. Panda, and S. K. Behera, "Ann based image restoration in approach of multilayer perceptron," in *2016 International Conference on Inventive Computation Technologies (ICICT)*, vol. 2. IEEE, 2016, pp. 1–4.

[42] Y.-Q. Wang and J.-M. Morel, "Can a single image denoising neural network handle all levels of gaussian noise?" *IEEE Signal Processing Letters*, vol. 21, no. 9, pp. 1150–1153, 2014.

[43] D. Zhang, L. Zhao, D. Xu, and D. Lu, "Comparing and combining mlps and cnns for image denoising," in *2018 IEEE 4th International Conference on Computer and Communications (ICCC)*. IEEE, 2018, pp. 1680–1684.

[44] M. F. M. Jimenez, O. DeGuchy, and R. F. Marcia, "Deep convolutional autoencoders for deblurring and denoising low-resolution images," in *2020 International Symposium on Information Theory and Its Applications (ISITA)*. IEEE, 2020, pp. 549–553.

[45] A. Rubel, O. Rubel, V. Abramova, G. Proskura, and V. Lukin, "Improved noisy image quality assessment using multilayer neural networks," in *2019 IEEE 2nd Ukraine Conference on Electrical and Computer Engineering (UKRCON)*. IEEE, 2019, pp. 1046–1051.

[46] O. Keohane and I. Aizenberg, "Impulse noise filtering using mlmvn," in *2020 International Joint Conference on Neural Networks (IJCNN)*. IEEE, 2020, pp. 1–8.

[47] I. Aizenberg, O. Keohane, and A. Lara, "Mlmvn in speckle noise filtering," in *2020 IEEE Third International Conference on Data Stream Mining & Processing (DSMP)*. IEEE, 2020, pp. 78–83.

[48] Q. Xing and C. Chen, "Path tracing denoising based on sure adaptive sampling and neural network," *IEEE Access*, vol. 8, pp. 116 336–116 349, 2020.

[49] O. Rubel, A. Rubel, V. Lukin, and K. Egiazarian, "Blind dct-based prediction of image denoising efficiency using neural networks," in *2018 7th European Workshop on Visual Information Processing (EUVIP)*. IEEE, 2018, pp. 1–6.

[50] K. Youssef, N. N. Jarenwattananon, and L.-S. Bouchard, "Feature-preserving noise removal," *IEEE Transactions on Medical Imaging*, vol. 34, no. 9, pp. 1822–1829, 2015.

[51] Y. Yang, L. Cao, Q. Liu, and P. Yang, "A stacked multi-granularity convolution denoising auto-encoder," *IEEE Access*, vol. 7, pp. 83 888–83 899, 2019.

[52] X. Liu, S. Mei, Z. Zhang, Y. Zhang, J. Ji, and Q. Du, "Decs-net: Convolutional self-encoding network for hyperspectral image denoising," in *IGARSS 2019-2019 IEEE International Geoscience and Remote Sensing Symposium*. IEEE, 2019, pp. 1951–1954.

[53] M. Sharma, S. Chaudhury, and B. Lall, "Deep learning based frameworks for image super-resolution and noise-resilient super-resolution," in *2017 International Joint Conference on Neural Networks (IJCNN)*. IEEE, 2017, pp. 744–751.

[54] B. Gokulnath *et al.*, "Elastic sdae: An adaptive noise selection for stacked denoising auto encoder," in *2020 International Conference on Emerging Trends in Information Technology and Engineering (ic-ETITE)*. IEEE, 2020, pp. 1–5.

[55] Q. Xiang and X. Pang, "Improved denoising auto-encoders for image denoising," in *2018 11th International Congress on Image and Signal Processing, BioMedical Engineering and Informatics (CISP-BMEI)*. IEEE, 2018, pp. 1–9.

[56] H. Bhojwani, V. Bhavsar, R. Gajjar, and M. Patel, "Image resolution enhancement using convolutional autoencoders with skip connections," in *2021 2nd International Conference on Range Technology (ICORT)*. IEEE, 2021, pp. 1–5.

[57] S. Kuanar, V. Athitsos, D. Mahapatra, K. Rao, Z. Akhtar, and D. Dasgupta, "Low dose abdominal ct image reconstruction: An unsupervised learning based approach," in *2019 IEEE International Conference on Image Processing (ICIP)*. IEEE, 2019, pp. 1351–1355.

[58] H. Chen, Y. Zhang, M. K. Kalra, F. Lin, Y. Chen, P. Liao, J. Zhou, and G. Wang, "Low-dose ct with a residual encoder-decoder convolutional neural network," *IEEE transactions on medical imaging*, vol. 36, no. 12, pp. 2524–2535, 2017.

[59] S. Nasrin, M. Z. Alom, R. Burada, T. M. Taha, and V. K. Asari, "Medical image denoising with recurrent residual u-net (r2u-net) base auto-encoder," in *2019 IEEE National Aerospace and Electronics Conference (NAECON)*. IEEE, 2019, pp. 345–350.

[60] R. Wang and D. Tao, "Non-local auto-encoder with collaborative stabilization for image restoration," *IEEE Transactions on Image Processing*, vol. 25, no. 5, pp. 2117–2129, 2016.

[61] D. Zhao, B. Guo, J. Wu, W. Ning, and Y. Yan, "Robust feature learning by improved auto-encoder from non-gaussian noised images," in *2015 IEEE International Conference on Imaging Systems and Techniques (IST)*. IEEE, 2015, pp. 1–5.

[62] Y. Suzuki, K. Kawaji, A. R. Patel, S. Tamura, and S. Hayamizu, "Toward effective noise reduction for sub-nyquist high-frame-rate mri techniques with deep learning," in *2017 Asia-Pacific Signal and Information Processing Association Annual Summit and Conference (APSIPA ASC)*. IEEE, 2017, pp. 1136–1139.

[63] M. Sharma, K. K. Sarma, and N. Mastorakis, "Ae and sae based aircraft image denoising," in *2018 5th International Conference on Mathematics and Computers in Sciences and Industry (MCSI)*. IEEE, 2018, pp. 81–85.

[64] A. Saranya and K. Kottilingam, "An efficient combined approach for denoising fibrous dysplasia images," in *2021 International Conference on System, Computation, Automation and Networking (ICSCAN)*. IEEE, 2021, pp. 1–6.

[65] A. S. Ahmed, W. H. El-Behaidy, and A. A. Youssif, "Automatic enhancement of two-dimensional gel electrophoresis images using denoising autoencoder," in *2019 14th International Conference on Computer Engineering and Systems (ICCES)*. IEEE, 2019, pp. 357–361.

[66] M. Tajmirriahi, R. Kafieh, Z. Amini, and H. Rabbani, "A lightweight mimic convolutional auto-encoder for denoising retinal optical coherence tomography images," *IEEE Transactions on Instrumentation and Measurement*, vol. 70, pp. 1–8, 2021.

[67] C. Liu, X. Li, L. Zhuo, J. Li, and Q. Zhou, "A novel speckle noise reduction algorithm for old movies recovery," in *2018 11th International Congress on Image and Signal Processing, BioMedical Engineering and Informatics (CISP-BMEI)*. IEEE, 2018, pp. 1–6.

[68] N. S. Rani, B. N. BJ, S. Karthik, and A. Srinidhi, "Binarization of degraded photographed document images-a variational denoising auto encoder," in *2021 Third International Conference on Inventive Research in Computing Applications (ICIRCA)*. IEEE, 2021, pp. 119–124.

[69] T. G. Kamod, P. P. Rege, and S. Kulkarni, "Denoise auto-encoder based speckle reduction for risat-1 sar imagery," in *2021 8th International Conference on Signal Processing and Integrated Networks (SPIN)*. IEEE, 2021, pp. 216–221.

[70] J. Kim, S. Song, and S.-C. Yu, "Denoising auto-encoder based image enhancement for high resolution sonar image," in *2017 IEEE underwater technology (UT)*. IEEE, 2017, pp. 1–5.

[71] Y. Zhong, S. Jia, and Y. Hu, "Denoising auto-encoder network combined classfication module for brain tumors detection," in *2022 3rd International Conference on Electronic Communication and Artificial Intelligence (IWECAI)*. IEEE, 2022, pp. 540–543.

[72] Y. Gao, Y. Lu, H. Li, B. Liu, Y. Li, M. Chen, G. Wang, and Y. Lian, "Eit-cdae: A 2-d electrical impedance tomography image reconstruction method based on auto encoder technique," in *2019 IEEE Biomedical Circuits and Systems Conference (BioCAS)*. IEEE, 2019, pp. 1–4.

[73] S. Jadhav and P. Kulkarni, "Image denoising using deep auto-encoder network for production monitoring in real-time," in *2021 International Conference on Advances in Electrical, Computing, Communication and Sustainable Technologies (ICAECT)*. IEEE, 2021, pp. 1–7.

[74] D. Aspandi, O. Martinez, F. Sukno, and X. Binefa, "Robust facial alignment with internal denoising auto-encoder," in *2019 16th Conference on Computer and Robot Vision (CRV)*. IEEE, 2019, pp. 143–150.

[75] C. S. N. Pathirage, L. Li, W. Liu, and M. Zhang, "Stacked face denoising auto encoders for expression-robust face recognition," in *2015 International Conference on Digital Image Computing: Techniques and Applications (DICTA)*. IEEE, 2015, pp. 1–8.

[76] H. V. Nguyen, M. O. Ulfarsson, and J. R. Sveinsson, "Hyperspectral image denoising using sure-based unsupervised convolutional neural networks," *IEEE Transactions on Geoscience and Remote Sensing*, vol. 59, no. 4, pp. 3369–3382, 2020.

[77] W. Fang, L. Fu, and H. Li, "Unsupervised cnn based on self-similarity for seismic data denoising," *IEEE Geoscience and Remote Sensing Letters*, vol. 19, pp. 1–5, 2021.

[78] B. Liu, J. Yue, Z. Zuo, X. Xu, C. Fu, S. Yang, and P. Jiang, "Unsupervised deep learning for random noise attenuation of seismic data," *IEEE Geoscience and Remote Sensing Letters*, vol. 19, pp. 1–5, 2021.

[79] M. Zhang, Y. Liu, and Y. Chen, "Unsupervised seismic random noise attenuation based on deep convolutional neural network," *IEEE Access*, vol. 7, pp. 179 810–179 822, 2019.

[80] J. Lehtinen, J. Munkberg, J. Hasselgren, S. Laine, T. Karras, M. Aittala, and T. Aila, "Noise2noise: Learning image restoration without clean data," *arXiv preprint arXiv:1803.04189*, 2018.

[81] A. F. Calvarons, "Improved noise2noise denoising with limited data," in *Proceedings of the IEEE/CVF Conference on Computer Vision and Pattern Recognition*, 2021, pp. 796–805.

[82] N. Moran, D. Schmidt, Y. Zhong, and P. Coady, "Noisier2noise: Learning to denoise from unpaired noisy data," in *Proceedings of the IEEE/CVF Conference on Computer Vision and Pattern Recognition*, 2020, pp. 12 064–12 072.

[83] W. Fang, D. Wu, K. Kim, R. Singh, M. K. Kalra, L. Li, and Q. Li, "Direct dual energy ct material decomposition using noise2noise prior," in *2020 IEEE Nuclear Science Symposium and Medical Imaging Conference (NSS/MIC)*. IEEE, pp. 1–3.

[84] A. M. Hasan, M. R. Mohebbian, K. A. Wahid, and P. Babyn, "Hybrid-collaborative noise2noise denoiser for low-dose ct images," *IEEE Transactions on Radiation and Plasma Medical Sciences*, vol. 5, no. 2, pp. 235–244, 2020.

[85] C. Chan, J. Zhou, L. Yang, W. Qi, and E. Asma, "Noise to noise ensemble learning for pet image denoising," in *2019 IEEE Nuclear Science Symposium and Medical Imaging Conference (NSS/MIC)*. IEEE, 2019, pp. 1–3.

[86] D. Shao, Y. Zhao, Y. Li, and T. Li, "Noisy2noisy: Denoise pre-stack seismic data without paired training data with labels," *IEEE Geoscience and Remote Sensing Letters*, vol. 19, pp. 1–5, 2022.

[87] J. Lefebvre, A. Javer, M. Dmitrieva, J. Rittscher, B. Lewków, E. Allgeyer, G. Sirinakis, and D. S. Johnston, "Single-molecule localization microscopy reconstruction using noise2noise for super-resolution imaging of actin filaments," in *2020 IEEE 17th International Symposium on Biomedical Imaging (ISBI)*. IEEE, 2020, pp. 1596–1599.

[88] S. Tan, X. Zhang, H. Wang, L. Yu, Y. Du, J. Yin, and B. Wu, "A cnn-based self-supervised synthetic aperture radar image denoising approach," *IEEE Transactions on Geoscience and Remote Sensing*, 2021.

[89] A. Krull, T.-O. Buchholz, and F. Jug, "Noise2void-learning denoising from single noisy images," in *Proceedings of the IEEE/CVF Conference on Computer Vision and Pattern Recognition*, 2019, pp. 2129–2137.

[90] A. Krull, T. Vičar, M. Prakash, M. Lalit, and F. Jug, "Probabilistic noise2void: Unsupervised content-aware denoising," *Frontiers in Computer Science*, vol. 2, p. 5, 2020.

[91] M. Prakash, M. Lalit, P. Tomancak, A. Krul, and F. Jug, "Fully unsupervised probabilistic noise2void," in *2020 IEEE 17th International Symposium on Biomedical Imaging (ISBI)*. IEEE, 2020, pp. 154–158.

[92] H. S. Park, J. Baek, S. K. You, J. K. Choi, and J. K. Seo, "Unpaired image denoising using a generative adversarial network in x-ray ct," *IEEE Access*, vol. 7, pp. 110 414–110 425, 2019.

[93] C. Broaddus, A. Krull, M. Weigert, U. Schmidt, and G. Myers, "Removing structured noise with self-supervised blind-spot networks," in *2020 IEEE 17th International Symposium on Biomedical Imaging (ISBI)*. IEEE, 2020, pp. 159–163.

[94] T.-A. Song and J. Dutta, "Noise2void denoising of pet images," in *2020 IEEE Nuclear Science Symposium and Medical Imaging Conference (NSS/MIC)*. IEEE, pp. 1–2.

[95] M. Prakash, T.-O. Buchholz, M. Lalit, P. Tomancak, F. Jug, and A. Krull, "Leveraging self-supervised denoising for image segmentation," in *2020 IEEE 17th International Symposium on Biomedical Imaging (ISBI)*. IEEE, 2020, pp. 428–432.

[96] J. Batson and L. Royer, "Noise2self: Blind denoising by self-supervision," in *International Conference on Machine Learning*. PMLR, 2019, pp. 524–533.

[97] Y. Quan, M. Chen, T. Pang, and H. Ji, "Self2self with dropout: Learning self-supervised denoising from single image," in *Proceedings of the IEEE/CVF conference on computer vision and pattern recognition*, 2020, pp. 1890–1898.

[98] K. Lee and W.-K. Jeong, "Iscl: Interdependent self-cooperative learning for unpaired image denoising," *IEEE Transactions on Medical Imaging*, vol. 40, no. 11, pp. 3238–3248, 2021.

[99] T. Huang, S. Li, X. Jia, H. Lu, and J. Liu, "Neighbor2neighbor: Self-supervised denoising from single noisy images," in *Proceedings of the IEEE/CVF Conference on Computer Vision and Pattern Recognition*, 2021, pp. 14 781–14 790.

[100] A. A. Hendriksen, D. M. Pelt, and K. J. Batenburg, "Noise2inverse: Self-supervised deep convolutional denoising for tomography," *IEEE Transactions on Computational Imaging*, vol. 6, pp. 1320–1335, 2020.

[101] J. Xu, Y. Huang, M.-M. Cheng, L. Liu, F. Zhu, Z. Xu, and L. Shao, "Noisy-as-clean: Learning self-supervised denoising from corrupted image," *IEEE Transactions on Image Processing*, vol. 29, pp. 9316–9329, 2020.

[102] G. Lee, S. Hong, and D. Cho, "Self-supervised feature enhancement networks for small object detection in noisy images," *IEEE Signal Processing Letters*, vol. 28, pp. 1026–1030, 2021.

[103] H. Liu, X. Liu, J. Lu, and S. Tan, "Self-supervised image prior learning with gmm from a single noisy image," in *Proceedings of the IEEE/CVF International Conference on Computer Vision*, 2021, pp. 2845–2854.

[104] W. Khademi, S. Rao, C. Minnerath, G. Hagen, and J. Ventura, "Self-supervised poisson-gaussian denoising," in *Proceedings of the IEEE/CVF Winter Conference on Applications of Computer Vision*, 2021, pp. 2131–2139.

[105] A. B. Molini, D. Valsesia, G. Fracastoro, and E. Magli, "Speckle2void: Deep self-supervised sar despeckling with blind-spot convolutional neural networks," *IEEE Transactions on Geoscience and Remote Sensing*, vol. 60, pp. 1–17, 2021.

[106] R. Ke and C.-B. Schonlieb, "Unsupervised image restoration using partially linear denoisers," *IEEE Transactions on Pattern Analysis and Machine Intelligence*, 2021.

[107] Y. Gao, H. Wang, X. Liu, N. Huang, G. Wang, and S. Zhang, "A denoising self-supervised approach for covid-19 pneumonia lesion segmentation with limited annotated ct images," in *2021 43rd Annual International Conference of the IEEE Engineering in Medicine & Biology Society (EMBC)*. IEEE, 2021, pp. 3705–3708.

[108] K. Liang, L. Zhang, Y. Yang, H. Yang, and Y. Xing, "A self-supervised deep learning network for low-dose ct reconstruction," in *2018 IEEE Nuclear Science Symposium and Medical Imaging Conference Proceedings (NSS/MIC)*. IEEE, 2018, pp. 1–4.

[109] D. A. Oliveira, D. G. Semin, and S. Zaytsev, "Self-supervised ground-roll noise attenuation using self-labeling and paired data synthesis," *IEEE Transactions on Geoscience and Remote Sensing*, vol. 59, no. 8, pp. 7147–7159, 2020.

[110] F. Meng, Q. Fan, and Y. Li, "Self-supervised learning for seismic data reconstruction and denoising," *IEEE Geoscience and Remote Sensing Letters*, vol. 19, pp. 1–5, 2021.

[111] V. Sterzentsenko, L. Saroglou, A. Chatzitofis, S. Thermos, N. Zioulis, A. Doumanoglou, D. Zarpalas, and P. Daras, "Self-supervised deep depth denoising," in *Proceedings of the IEEE/CVF International Conference on Computer Vision*, 2019, pp. 1242–1251.

[112] A. Shabanov, I. Krotov, N. Chinaev, V. Poletaev, S. Kozlukov, I. Pasechnik, B. Yakupov, A. Sanakoyeu, V. Lebedev, and D. Ulyanov, "Self-supervised depth denoising using lower-and higher-quality rgb-d sensors," in *2020 International Conference on 3D Vision (3DV)*. IEEE, 2020, pp. 743–752.

[113] T. T. T. Phung, T. H. T. Ma, D. Q. Vu *et al.*, "Self-supervised learning for action recognition by video denoising," in *2021 RIVF International Conference on Computing and Communication Technologies (RIVF)*. IEEE, 2021, pp. 1–6.

[114] V. Dewil, J. Anger, A. Davy, T. Ehret, G. Facciolo, and P. Arias, "Self-supervised training for blind multi-frame video denoising," in *Proceedings of the IEEE/CVF Winter Conference on Applications of Computer Vision*, 2021, pp. 2724–2734.

[115] U. Schmidt and S. Roth, "Shrinkage fields for effective image restoration," in *Proceedings of the IEEE conference on computer vision and pattern recognition*, 2014, pp. 2774–2781.

[116] K. Dabov, A. Foi, V. Katkovnik, and K. Egiazarian, "Image denoising by sparse 3-d transform-domain collaborative filtering," *IEEE Transactions on image processing*, vol. 16, no. 8, pp. 2080–2095, 2007.
[117] S. Gu, L. Zhang, W. Zuo, and X. Feng, "Weighted nuclear norm minimization with application to image denoising," in *Proceedings of the IEEE conference on computer vision and pattern recognition*, 2014, pp. 2862–2869.
[118] D. Zoran and Y. Weiss, "From learning models of natural image patches to whole image restoration," in *2011 International Conference on Computer Vision*. IEEE, 2011, pp. 479–486.
[119] Y. Chen and T. Pock, "Trainable nonlinear reaction diffusion: A flexible framework for fast and effective image restoration," *IEEE transactions on pattern analysis and machine intelligence*, vol. 39, no. 6, pp. 1256–1272, 2016.
[120] J. Chen, G. Zhang, S. Xu, and H. Yu, "A blind cnn denoising model for random-valued impulse noise," *IEEE Access*, vol. 7, pp. 124 647–124 661, 2019.
[121] S. Lin, X. Han, Y. Wang, Z. Lu, Y. Zhang, and T. Jia, "A convolutional neural network for small sample's ring structured light denoising," in *2021 33rd Chinese Control and Decision Conference (CCDC)*. IEEE, 2021, pp. 1063–1068.
[122] W. Li, H. Liu, and J. Wang, "A deep learning method for denoising based on a fast and flexible convolutional neural network," *IEEE Transactions on Geoscience and Remote Sensing*, vol. 60, pp. 1–13, 2021.
[123] X. Duan, R. Xie, and J. Han, "An energy-efficient image denoising accelerator with depth-wise separable convolution and fused-layer architecture," in *2021 IEEE 14th International Conference on ASIC (ASICON)*. IEEE, 2021, pp. 1–4.
[124] H. Zhang and F. Meng, "An image denoising algorithm based on image quality assessment," in *2020 International Conference on Culture-oriented Science & Technology (ICCST)*. IEEE, 2020, pp. 587–591.
[125] Q. Bin, Q. Mengyue, Z. Pan, and Y. Miao, "Data noise reduction based on adaptive butterworth filtering and dncnn," in *2021 IEEE 21st International Conference on Communication Technology (ICCT)*. IEEE, 2021, pp. 1491–1495.
[126] M. Jaszewski and S. Parameswaran, "Exploring efficient and tunable convolutional blind image denoising networks," in *2019 IEEE Applied Imagery Pattern Recognition Workshop (AIPR)*. IEEE, 2019, pp. 1–9.
[127] R. Alaguselvi and K. Murugan, "Image enhancement using convolutional neural networks," in *2019 IEEE International Conference on Clean Energy and Energy Efficient Electronics Circuit for Sustainable Development (INCCES)*. IEEE, 2019, pp. 1–5.
[128] L. Fan and Z. Long, "Optimization of nadam algorithm for image denoising based on convolutional neural network," in *2020 7th International Conference on Information Science and Control Engineering (ICISCE)*. IEEE, 2020, pp. 957–961.
[129] L.-Y. Hsu and H.-T. Hu, "Qdct-based blind color image watermarking with aid of gwo and dncnn for performance improvement," *IEEE Access*, vol. 9, pp. 155 138–155 152, 2021.
[130] Y. Zhao, H. Ren, B. Zhang, and X. Lu, "Ship image denoising algorithm research based on deep learning," in *2020 IEEE 11th International Conference on Software Engineering and Service Science (ICSESS)*. IEEE, 2020, pp. 321–325.
[131] A. Kuchida and T. Goto, "Image quality improvement of surveillance camera images by noise removal using learning method," in *2021 IEEE 10th Global Conference on Consumer Electronics (GCCE)*. IEEE, 2021, pp. 569–570.
[132] H. Xu, L. Zhang, M. J. Er, and Q. Yang, "Underwater sonar image segmentation based on deep learning of receptive field block and search attention mechanism," in *2021 4th International Conference on Intelligent Autonomous Systems (ICoIAS)*. IEEE, 2021, pp. 44–48.
[133] W. Cheng, J. Lu, X. Zhu, J. Hong, X. Liu, M. Li, and P. Li, "Dilated residual learning with skip connections for real-time denoising of laser speckle imaging of blood flow in a log-transformed domain," *IEEE Transactions on Medical Imaging*, vol. 39, no. 5, pp. 1582–1593, 2019.
[134] S. Li, H. Xu, S. Gao, W. Liu, C. Li, and A. Liu, "An interferometric phase noise reduction method based on modified denoising convolutional neural network," *IEEE Journal of Selected Topics in Applied Earth Observations and Remote Sensing*, vol. 13, pp. 4947–4959, 2020.
[135] S. Li, H. Xu, S. Gao, and C. Li, "Non-fuzzy interferometric phase estimation method based on deep learning," in *IGARSS 2019-2019 IEEE International Geoscience and Remote Sensing Symposium*. IEEE, 2019, pp. 194–197.
[136] Q. Zhao, S. Wu, Z. Zhang, Y. Sun, Y. Fu, and H. Wang, "Sar image noise reduction based on wavelet transform and dncnn," in *2021 2nd China International SAR Symposium (CISS)*. IEEE, 2021, pp. 1–4.
[137] X. Yang, T. Pan, W. Yang, and H.-C. Li, "Polsar image despeckling using trained models on single channel sar images," in *2019 6th Asia-Pacific Conference on Synthetic Aperture Radar (APSAR)*. IEEE, 2019, pp. 1–4.
[138] X. Liu, X. Pu, Y. Shi, and J. Song, "A novel method to denoise ceus image combining bidirectional convlstm with 3d dncnn," in *2021 IEEE International Conference on Bioinformatics and Biomedicine (BIBM)*. IEEE, 2021, pp. 1590–1594.
[139] M. Geng, X. Meng, J. Yu, L. Zhu, L. Jin, Z. Jiang, B. Qiu, H. Li, H. Kong, J. Yuan *et al.*, "Content-noise complementary learning for medical image denoising," *IEEE Transactions on Medical Imaging*, 2021.
[140] Q. Wang, H. Zhang, R. Zhang, X. Li, J. Wang, and X. Duan, "Eit image reconstruction method based on dncnn," in *2021 IEEE International Instrumentation and Measurement Technology Conference (I2MTC)*. IEEE, 2021, pp. 1–5.
[141] K. Kim, D. Wu, K. Gong, J. H. Kim, Y. D. Son, H. K. Kim, G. El Fakhria, and Q. Li, "Penalized pet reconstruction using cnn prior," in *2017 IEEE Nuclear Science Symposium and Medical Imaging Conference (NSS/MIC)*. IEEE, 2017, pp. 1–4.
[142] K. Kim, D. Wu, K. Gong, J. Dutta, J. H. Kim, Y. D. Son, H. K. Kim, G. El Fakhri, and Q. Li, "Penalized pet reconstruction using deep learning prior and local linear fitting," *IEEE transactions on medical imaging*, vol. 37, no. 6, pp. 1478–1487, 2018.
[143] H. Ma, Y. Wang, Y. Li, and Y. Zhao, "Desert seismic low-frequency noise attenuation using low-rank decomposition-based denoising convolutional neural network," *IEEE Transactions on Geoscience and Remote Sensing*, vol. 60, pp. 1–9, 2021.
[144] T. Zhong, M. Cheng, X. Dong, and N. Wu, "Seismic random noise attenuation by applying multiscale denoising convolutional neural network," *IEEE transactions on geoscience and remote sensing*, vol. 60, pp. 1–13, 2021.
[145] L. Guo, R. Luo, X. Li, Y. Zhou, T. Juanjuan, and C. Lei, "Seismic random noise removal based on a multiscale convolution and densely connected network for noise level evaluation," *IEEE Access*, vol. 10, pp. 13 911–13 925, 2022.
[146] Y. Zhao, Y. Li, X. Dong, and B. Yang, "Low-frequency noise suppression method based on improved dncnn in desert seismic data," *IEEE Geoscience and Remote Sensing Letters*, vol. 16, no. 5, pp. 811–815, 2018.
[147] D. Liu, W. Wang, X. Wang, C. Wang, J. Pei, and W. Chen, "Poststack seismic data denoising based on 3-d convolutional neural network," *IEEE Transactions on Geoscience and Remote Sensing*, vol. 58, no. 3, pp. 1598–1629, 2019.
[148] Y. Tan, K. Liao, X. Bai, C. Deng, Z. Zhao, and B. Zhao, "Denoising convolutional neural networks based dust accumulation status evaluation of photovoltaic panel," in *2019 IEEE International Conference on Energy Internet (ICEI)*. IEEE, 2019, pp. 560–566.
[149] Y. Liu, S. Xu, and Z. Lin, "An improved combination of image denoisers using spatial local fusion strategy," *IEEE Access*, vol. 8, pp. 150 407–150 421, 2020.
[150] H. Duan, X. Dong, S. You, and S. Han, "A deep learning denoising framework based on ffdnet for sar image change detection," in *2021 IEEE 11th International Conference on Electronics Information and Emergency Communication (ICEIEC) 2021 IEEE 11th International Conference on Electronics Information and Emergency Communication (ICEIEC)*. IEEE, 2021, pp. 1–4.
[151] X. Yang, Y. Mei, X. Hu, R. Luo, and K. Liu, "Compressed sensing mri by integrating deep denoiser and weighted schatten p-norm minimization," *IEEE Signal Processing Letters*, 2021.
[152] A. Wahyudiono, A. Herawan, M. R. Fakhlevi, M. Soediarwo, and P. R. Hakim, "Denoising lapan a3 high-resolution digital camera images: A comparative study," in *2021 IEEE International Conference on Aerospace Electronics and Remote Sensing Technology (ICARES)*. IEEE, 2021, pp. 1–5.
[153] H. Qiu, Y. Wang, and D. Meng, "Effective snapshot compressive-spectral imaging via deep denoising and total variation priors," in *Proceedings of the IEEE/CVF Conference on Computer Vision and Pattern Recognition*, 2021, pp. 9127–9136.
[154] W. Dong, L. Zhang, G. Shi, and X. Li, "Nonlocally centralized sparse representation for image restoration," *IEEE transactions on Image Processing*, vol. 22, no. 4, pp. 1620–1630, 2012.
[155] Q. Zhao, D. Meng, Z. Xu, W. Zuo, and L. Zhang, "Robust principal component analysis with complex noise," in *International conference on machine learning*. PMLR, 2014, pp. 55–63.
[156] K. Zhang, W. Zuo, Y. Chen, D. Meng, and L. Zhang, "Beyond a gaussian denoiser: Residual learning of deep cnn for image denoising,"

IEEE Transactions on Image Processing, vol. 26, no. 7, pp. 3142–3155, Jul. 2017.

[157] M. F. I. Amal, H. P. Alim Wicaksono, and H. Prasetyo, "Deep residual networks for impulsive noise suppression," in *2020 27th International Conference on Telecommunications (ICT)*. Bali, Indonesia: IEEE, Oct. 2020, pp. 1–5.

[158] T. S. Borkar and L. J. Karam, "Deepcorrect: Correcting dnn models against image distortions," *IEEE Transactions on Image Processing*, vol. 28, no. 12, pp. 6022–6034, Dec. 2019.

[159] Y. I. Jang and N. I. Cho, "Dual path denoising network for real photographic noise," *IEEE SIGNAL PROCESSING LETTERS*, vol. 27, p. 5, 2020.

[160] H. Zou, R. Lan, Y. Zhong, Z. Liu, and X. Luo, "Edcnn: A novel network for image denoising," p. 5.

[161] Y. Guo, A. Davy, G. Facciolo, J.-M. Morel, and Q. Jin, "Fast, nonlocal and neural: A lightweight high quality solution to image denoising," *IEEE Signal Processing Letters*, vol. 28, pp. 1515–1519, 2021.

[162] P. H. Thanh Binh, C. Cruz, and K. Egiazarian, "Flashlight cnn image denoising," in *2020 28th European Signal Processing Conference (EUSIPCO)*. Amsterdam, Netherlands: IEEE, Jan. 2021, pp. 670–674.

[163] S. Anwar, C. P. Huynh, and F. Porikli, "Identity enhanced residual image denoising," p. 10.

[164] M. Khamassi, M. Kaaniche, and A. Benazza-Benyahia, "Joint denoising of stereo images using 3d cnn," in *2020 10th International Symposium on Signal, Image, Video and Communications (ISIVC)*. Saint-Etienne, France: IEEE, Apr. 2021, pp. 1–6.

[165] T. Huang, F. F. Wu, W. Dong, G. Shi, and X. Li, "Lightweight deep residue learning for joint color image demosaicking and denoising," in *2018 24th International Conference on Pattern Recognition (ICPR)*. Beijing: IEEE, Aug. 2018, pp. 127–132.

[166] S.-F. Wang, W.-K. Yu, and Y.-X. Li, "Multi-wavelet residual dense convolutional neural network for image denoising," *IEEE Access*, vol. 8, pp. 214 413–214 424, 2020.

[167] L. Fan and Z. Long, "Optimization of nadam algorithm for image denoising based on convolutional neural network," in *2020 7th International Conference on Information Science and Control Engineering (ICISCE)*. Changsha, China: IEEE, Dec. 2020, pp. 957–961.

[168] S. Anwar and N. Barnes, "Real image denoising with feature attention," in *2019 IEEE/CVF International Conference on Computer Vision (ICCV)*. Seoul, Korea (South): IEEE, Oct. 2019, pp. 3155–3164.

[169] A. Roy, P. Anju, L. Tomy, and M. Rajeswari, "Recent study on image denoising using deep cnn techniques," in *2021 7th International Conference on Advanced Computing and Communication Systems (ICACCS)*. Coimbatore, India: IEEE, Mar. 2021, pp. 1838–1843.

[170] S. Sadrizadeh, H. Otroshi-Shahreza, and F. Marvasti, "Removing impulsive noise from color images via a residual deep neural network enhanced by post-processing," in *2021 29th European Signal Processing Conference (EUSIPCO)*. Dublin, Ireland: IEEE, Aug. 2021, pp. 656–660.

[171] L. Yu, Y. Zhang, H. Han, L. Zhang, and F. Wu, "Robust median filtering forensics by cnn-based multiple residuals learning," *IEEE Access*, vol. 7, pp. 120 594–120 602, 2019.

[172] W. Shan, Y. Yi, J. Qiu, and A. Yin, "Robust median filtering forensics using image deblocking and filtered residual fusion," *IEEE Access*, vol. 7, pp. 17 174–17 183, 2019.

[173] K. Zhang and K. Chen, "Semi-supervised learning-based image denoising for big data," *IEEE Access*, vol. 8, pp. 172 678–172 691, 2020.

[174] Y. Zhao, H. Ren, B. Zhang, and X. Lu, "Ship image denoising algorithm research based on deep learning," in *2020 IEEE 11th International Conference on Software Engineering and Service Science (ICSESS)*. Beijing, China: IEEE, Oct. 2020, pp. 321–325.

[175] D. Li and W. Yu, "A lightweight and effective deep learning model for gaussian noise removal," p. 6.

[176] K. B, M. Mounika, S. B. Pravallika, and K. Mahitha, "Deep cnn with residual learning and dilated convolution for image denoising," in *2021 Second International Conference on Electronics and Sustainable Communication Systems (ICESC)*. Coimbatore, India: IEEE, Aug. 2021, pp. 1327–1333.

[177] T. Wang, M. Sun, and K. Hu, "Dilated deep residual network for image denoising," in *2017 IEEE 29th International Conference on Tools with Artificial Intelligence (ICTAI)*. Boston, MA: IEEE, Nov. 2017, pp. 1272–1279.

[178] J. Zhang, Y. Zhu, W. Li, W. Fu, and L. Cao, "Drnet: A deep neural network with multi-layer residual blocks improves image denoising," *IEEE Access*, vol. 9, pp. 79 936–79 946, 2021.

[179] G. Chen, Z. Gao, P. Zhu, and Z. Chen, "Learning a multi-scale deep residual network of dilated-convolution for image denoising," in *2020 IEEE 5th International Conference on Cloud Computing and Big Data Analytics (ICCCBDA)*. Chengdu, China: IEEE, Apr. 2020, pp. 348–353.

[180] J. Ma, C. Peng, X. Tian, and J. Jiang, "Dbdnet: A deep boosting strategy for image denoising," *IEEE Transactions on Multimedia*, pp. 1–1, 2021.

[181] R. G. Pires, D. F. S. Santos, C. F. Santos, M. C. Santana, and J. P. Papa, "Image denoising using attention-residual convolutional neural networks," in *2020 33rd SIBGRAPI Conference on Graphics, Patterns and Images (SIBGRAPI)*. Recife/Porto de Galinhas, Brazil: IEEE, Nov. 2020, pp. 101–107.

[182] R. Ma, B. Zhang, Y. Zhou, Z. Li, and F. Lei, "Pid controller-guided attention neural network learning for fast and effective real photographs denoising," *IEEE Transactions on Neural Networks and Learning Systems*, pp. 1–14, 2021.

[183] G. Hou, Y. Yang, and J.-H. Xue, "Residual dilated network with attention for image blind denoising," in *2019 IEEE International Conference on Multimedia and Expo (ICME)*. Shanghai, China: IEEE, Jul. 2019, pp. 248–253.

[184] J. Gurrola-Ramos, O. Dalmau, and T. E. Alarcon, "A residual dense u-net neural network for image denoising," *IEEE Access*, vol. 9, pp. 31 742–31 754, 2021.

[185] L. Bao, Z. Yang, S. Wang, D. Bai, and J. Lee, "Real image denoising based on multi-scale residual dense block and cascaded u-net with block-connection," in *2020 IEEE/CVF Conference on Computer Vision and Pattern Recognition Workshops (CVPRW)*. Seattle, WA, USA: IEEE, Jun. 2020, pp. 1823–1831.

[186] D.-W. Kim, J. R. Chung, and S.-W. Jung, "Grdn:grouped residual dense network for real image denoising and gan-based real-world noise modeling," in *2019 IEEE/CVF Conference on Computer Vision and Pattern Recognition Workshops (CVPRW)*. Long Beach, CA, USA: IEEE, Jun. 2019, pp. 2086–2094.

[187] Q. Wang, H. Liu, G. Xie, and Y. Zhang, "Image denoising using an improved generative adversarial network with wasserstein distance," in *2021 40th Chinese Control Conference (CCC)*. Shanghai, China: IEEE, Jul. 2021, pp. 7027–7032.

[188] Y. Song, C. Chen, X. Hu, H. Yu, and F. Qu, "Denoising in monte carlo rendering based on clustered-residual block network," in *2020 International Conference on Virtual Reality and Visualization (ICVRV)*. Recife, Brazil: IEEE, Nov. 2020, pp. 10–14.

[189] H. Zhu, D. Zhang, and Y. Kou, "Dual attention fusion network for single image dehazing," in *2021 13th International Conference on Wireless Communications and Signal Processing (WCSP)*. Changsha, China: IEEE, Oct. 2021, pp. 1–5.

[190] A. Dang, T. H. Vu, and J.-C. Wang, "Encoder-recurrent decoder network for single image dehazing," in *ICASSP 2020 - 2020 IEEE International Conference on Acoustics, Speech and Signal Processing (ICASSP)*. Barcelona, Spain: IEEE, May 2020, pp. 4432–4436.

[191] T. Feng, Z. Li, C. Wang, X. Chen, and J. Wu, "Image dehazing network based on dilated convolution feature extraction," in *2019 12th International Congress on Image and Signal Processing, BioMedical Engineering and Informatics (CISP-BMEI)*. Suzhou, China: IEEE, Oct. 2019, pp. 1–5.

[192] J. Li, G. Li, and H. Fan, "Image dehazing using residual-based deep cnn," *IEEE Access*, vol. 6, pp. 26 831–26 842, 2018.

[193] J. Shen, Z. Li, L. Yu, G.-S. Xia, and W. Yang, "Implicit euler ode networks for single-image dehazing," in *2020 IEEE/CVF Conference on Computer Vision and Pattern Recognition Workshops (CVPRW)*. Seattle, WA, USA: IEEE, Jun. 2020, pp. 877–886.

[194] Z. Yang, D. Pan, and P. Shi, "Joint image dehazing and super-resolution: Closed shared source residual attention fusion network," *IEEE Access*, vol. 9, pp. 105 477–105 492, 2021.

[195] J. Yan, C. Li, S. Xu, and X. Yan, "Mmp-net: A multi-scale feature multiple parallel fusion network for single image haze removal," vol. 8, p. 11, 2020.

[196] J. Zhou, C. T. Leong, and C. Li, "Multi-scale and attention residual network for single image dehazing," in *2021 6th International Conference on Intelligent Computing and Signal Processing (ICSP)*. Xi'an, China: IEEE, Apr. 2021, pp. 483–487.

[197] H. Zhang, V. Sindagi, and V. M. Patel, "Multi-scale single image dehazing using perceptual pyramid deep network," in *2018 IEEE/CVF Conference on Computer Vision and Pattern Recognition Workshops (CVPRW)*. Salt Lake City, UT, USA: IEEE, Jun. 2018, pp. 1015–101 509.

[198] D. Zhao, L. Xu, L. Ma, J. Li, and Y. Yan, "Pyramid global context network for image dehazing," *IEEE Transactions on Circuits and Systems for Video Technology*, vol. 31, no. 8, pp. 3037–3050, Aug. 2021.

[199] Y. Du and X. Li, "Recursive deep residual learning for single image dehazing," in *2018 IEEE/CVF Conference on Computer Vision and Pattern Recognition Workshops (CVPRW)*. Salt Lake City, UT, USA: IEEE, Jun. 2018, pp. 843–8437.

[200] ——, "Recursive image dehazing via perceptually optimized generative adversarial network (pogan)," in *2019 IEEE/CVF Conference on Computer Vision and Pattern Recognition Workshops (CVPRW)*. Long Beach, CA, USA: IEEE, Jun. 2019, pp. 1824–1832.

[201] S. Song, R. Zhang, Z. Qiu, J. Jin, and S. Yu, "Res-attention net: An image dehazing network," in *2021 IEEE International Conference on Computer Science, Artificial Intelligence and Electronic Engineering (CSAIEE)*. SC, USA: IEEE, Aug. 2021, pp. 200–205.

[202] A. Dudhane, H. S. Aulakh, and S. Murala, "Ri-gan: An end-to-end network for single image haze removal," in *2019 IEEE/CVF Conference on Computer Vision and Pattern Recognition Workshops (CVPRW)*. Long Beach, CA, USA: IEEE, Jun. 2019, pp. 2014–2023.

[203] K. Zhao, T. Lu, Y. Wang, Y. Wang, and X. Nie, "Single image dehazing based on enhanced generative adversarial network," in *2020 5th International Conference on Control, Robotics and Cybernetics (CRC)*. Wuhan, China: IEEE, Oct. 2020, pp. 129–133.

[204] Y. Huang, Y. Wang, and Z. Su, "Single image dehazing via a joint deep modeling," in *2018 25th IEEE International Conference on Image Processing (ICIP)*. Athens: IEEE, Oct. 2018, pp. 2840–2844.

[205] X. Yang, H. Li, Y.-L. Fan, and R. Chen, "Single image haze removal via region detection network," *IEEE Transactions on Multimedia*, vol. 21, no. 10, pp. 2545–2560, Oct. 2019.

[206] J. Xiao, L. Luo, E. liu, J. Lei, and R. Klette, "Single-image dehazing algorithm based on convolutional neural networks," in *2018 24th International Conference on Pattern Recognition (ICPR)*. Beijing: IEEE, Aug. 2018, pp. 1259–1264.

[207] Y. Que, S. Li, and H. J. Lee, "Attentive composite residual network for robust rain removal from single images," *IEEE Transactions on Multimedia*, vol. 23, pp. 3059–3072, 2021.

[208] S. Deng, M. Wei, J. Wang, Y. Feng, L. Liang, H. Xie, F. L. Wang, and M. Wang, "Detail-recovery image deraining via context aggregation networks," in *2020 IEEE/CVF Conference on Computer Vision and Pattern Recognition (CVPR)*. Seattle, WA, USA: IEEE, Jun. 2020, pp. 14 548–14 557.

[209] Y. Ding, X. Xue, Z. Wang, Z. Jiang, X. Fan, and Z. Luo, "Domain knowledge driven deep unrolling for rain removal from single image," in *2018 7th International Conference on Digital Home (ICDH)*. Guilin, China: IEEE, Nov. 2018, pp. 14–19.

[210] R. Yasarla and V. M. Patel, "Uncertainty guided multi-scale residual learning-using a cycle spinning cnn for single image de-raining," in *2019 IEEE/CVF Conference on Computer Vision and Pattern Recognition (CVPR)*. Long Beach, CA, USA: IEEE, Jun. 2019, pp. 8397–8406.

[211] W. Xu, M. Lee, Y. Zhang, J. You, S. Suk, and J.-Y. Choi, "Deep residual convolutional network for natural image denoising and brightness enhancement," p. 6.

[212] P. Maharjan, L. Li, Z. Li, N. Xu, C. Ma, and Y. Li, "Improving extreme low-light image denoising via residual learning," in *2019 IEEE International Conference on Multimedia and Expo (ICME)*. Shanghai, China: IEEE, Jul. 2019, pp. 916–921.

[213] F. Kokkinos and S. Lefkimmiatis, "Iterative residual cnns for burst photography applications," p. 10.

[214] Y. Liu, Z. Wang, Y. Zeng, H. Zeng, and D. Zhao, "Pd-gan: Perceptual-details gan for extremely noisy low light image enhancement," p. 5.

[215] X. Wei, X. Zhang, and Y. Li, "Sarn: A lightweight stacked attention residual network for low-light image enhancement," p. 5.

[216] S. Chen, S. Li, and C. Zhu, "Advanced generative adversarial network based on dense connection for single image super resolution," in *2019 IEEE THE 2nd INTERNATIONAL CONFERENCE ON MICRO/NANO SENSORS for AI, HEALTHCARE, AND ROBOTICS (NSENS)*. Shenzhen, China: IEEE, Oct. 2019, pp. 68–71.

[217] J. Lee and J. Kim, "Edge profile super resolution," vol. 9, p. 11, 2021.

[218] D. Park, K. Kim, and S. Y. Chun, "Efficient module based single image super resolution for multiple problems," in *2018 IEEE/CVF Conference on Computer Vision and Pattern Recognition Workshops (CVPRW)*. Salt Lake City, UT, USA: IEEE, Jun. 2018, pp. 995–9958.

[219] F. Li, H. Bai, and Y. Zhao, "Filternet: Adaptive information filtering network for accurate and fast image super-resolution," *IEEE TRANSACTIONS ON CIRCUITS AND SYSTEMS FOR VIDEO TECHNOLOGY*, vol. 30, no. 6, p. 13, 2020.

[220] D. F. Noor, Y. Li, Z. Li, S. Bhattacharyya, and G. York, "Gradient image super-resolution for low-resolution image recognition," in *ICASSP 2019 - 2019 IEEE International Conference on Acoustics, Speech and Signal Processing (ICASSP)*. Brighton, United Kingdom: IEEE, May 2019, pp. 2332–2336.

[221] Z. Hou and S.-Y. Kung, "Hierarchically aggregated residual transformation for single image super resolution," in *2020 25th International Conference on Pattern Recognition (ICPR)*. Milan, Italy: IEEE, Jan. 2021, pp. 2248–2255.

[222] D. F. Noor, L. Li, Z. Li, and S. Bhattacharyya, "Multi-frame super resolution with deep residual learning on flow registered non-integer pixel images," in *2019 IEEE International Conference on Image Processing (ICIP)*. Taipei, Taiwan: IEEE, Sep. 2019, pp. 2164–2168.

[223] Y. Zuo, Q. Wu, Y. Fang, P. An, L. Huang, and Z. Chen, "Multi-scale frequency reconstruction for guided depth map super-resolution via deep residual network," *IEEE Transactions on Circuits and Systems for Video Technology*, vol. 30, no. 2, pp. 297–306, Feb. 2020.

[224] R. Chen, Y. Qu, K. Zeng, J. Guo, C. Li, and Y. Xie, "Persistent memory residual network for single image super resolution," in *2018 IEEE/CVF Conference on Computer Vision and Pattern Recognition Workshops (CVPRW)*. Salt Lake City, UT: IEEE, Jun. 2018, pp. 922–9227.

[225] Z. Jin, M. Z. Iqbal, D. Bobkov, W. Zou, X. Li, and E. Steinbach, "A flexible deep cnn framework for image restoration," *IEEE Transactions on Multimedia*, vol. 22, no. 4, pp. 1055–1068, Apr. 2020.

[226] J. F. P. J. Abascal, S. Bussod, N. Ducros, S. Si-Mohamed, P. Douek, C. Chappard, and F. Peyrin, "A residual u-net network with image prior for 3d image denoising," in *2020 28th European Signal Processing Conference (EUSIPCO)*. Amsterdam, Netherlands: IEEE, Jan. 2021, pp. 1264–1268.

[227] S. Anwar, N. Barnes, and L. Petersson, "Attention-based real image restoration," *IEEE Transactions on Neural Networks and Learning Systems*, pp. 1–11, 2021.

[228] J. Wang, "Image restoration on residual aggregation network in poor weather condition," in *2020 International Conference on Computing, Electronics & Communications Engineering (iCCECE)*. Southend, United Kingdom: IEEE, Aug. 2020, pp. 137–142.

[229] Y. Zhang, Y. Tian, Y. Kong, B. Zhong, and Y. Fu, "Residual dense network for image restoration," *IEEE Transactions on Pattern Analysis and Machine Intelligence*, vol. 43, no. 7, pp. 2480–2495, Jul. 2021.

[230] H. M. Jung, B. H. Kim, and M. Y. Kim, "Residual forward-subtracted u-shaped network for dynamic and static image restoration," *IEEE Access*, vol. 8, pp. 145 401–145 412, 2020.

[231] J. Liang, J. Cao, G. Sun, K. Zhang, L. Van Gool, and R. Timofte, "Swinir: Image restoration using swin transformer," in *2021 IEEE/CVF International Conference on Computer Vision Workshops (ICCVW)*. Montreal, BC, Canada: IEEE, Oct. 2021, pp. 1833–1844.

[232] Y. Chen, L. Bruzzone, L. Jiang, and Q. Sun, "Aru-net: Reduction of atmospheric phase screen in sar interferometry using attention-based deep residual u-net," *IEEE Transactions on Geoscience and Remote Sensing*, vol. 59, no. 7, pp. 5780–5793, Jul. 2021.

[233] D. Gleich and D. Sipos, "Deep despeckling of sar images," in *IGARSS 2019 - 2019 IEEE International Geoscience and Remote Sensing Symposium*. Yokohama, Japan: IEEE, Jul. 2019, pp. 1907–1910.

[234] M. Qin, F. Xie, W. Li, Z. Shi, and H. Zhang, "Dehazing for multispectral remote sensing images based on a convolutional neural network with the residual architecture," *IEEE Journal of Selected Topics in Applied Earth Observations and Remote Sensing*, vol. 11, no. 5, pp. 1645–1655, May 2018.

[235] T. Davis, V. Jain, A. Ley, O. D'Hondt, S. Valade, and O. Hellwich, "Reference-free despeckling of synthetic-aperture radar images using a deep convolutional network," in *IGARSS 2020 - 2020 IEEE International Geoscience and Remote Sensing Symposium*. Waikoloa, HI, USA: IEEE, Sep. 2020, pp. 3908–3911.

[236] F. Gu, H. Zhang, C. Wang, and B. Zhang, "Residual encoder-decoder network introduced for multisource sar image despeckling," in *2017 SAR in Big Data Era: Models, Methods and Applications (BIGSARDATA)*. Beijing: IEEE, Nov. 2017, pp. 1–5.

[237] H. Shen, C. Zhou, J. Li, and Q. Yuan, "Sar image despeckling employing a recursive deep cnn prior," *IEEE Transactions on Geoscience and Remote Sensing*, vol. 59, no. 1, pp. 273–286, Jan. 2021.

[238] P. Wang, H. Zhang, and V. M. Patel, "Sar image despeckling using a convolutional neural network," *IEEE Signal Processing Letters*, vol. 24, no. 12, pp. 1763–1767, Dec. 2017.

[239] M. Newey and P. Sharma, "Self-supervised speckle reduction gan for synthetic aperture radar," in *2021 IEEE Radar Conference (RadarConf21)*. Atlanta, GA, USA: IEEE, May 2021, pp. 1–6.

[240] F. Sica, G. Gobbi, P. Rizzoli, and L. Bruzzone, "Φ-net: Deep residual learning for insar parameters estimation," *IEEE Transactions on Geoscience and Remote Sensing*, vol. 59, no. 5, pp. 3917–3941, May 2021.

[241] Y. Yuan, H. Ma, and G. Liu, "A new multiscale residual learning network for hsi inconsistent noise removal," *IEEE Geoscience and Remote Sensing Letters*, vol. 19, pp. 1–5, 2022.

[242] Y. Zhao, D. Zhai, J. Jiang, and X. Liu, "Adrn: Attention-based deep residual network for hyperspectral image denoising," in *ICASSP 2020 - 2020 IEEE International Conference on Acoustics, Speech and Signal Processing (ICASSP)*. Barcelona, Spain: IEEE, May 2020, pp. 2668–2672.

[243] Q. Yuan, Q. Zhang, J. Li, H. Shen, and L. Zhang, "Hyperspectral image denoising employing a spatial–spectral deep residual convolutional neural network," *IEEE Transactions on Geoscience and Remote Sensing*, vol. 57, no. 2, pp. 1205–1218, Feb. 2019.

[244] A. Othman, N. Iqbal, S. M. Hanafy, and U. B. Waheed, "Automated event detection and denoising method for passive seismic data using residual deep convolutional neural networks," *IEEE Transactions on Geoscience and Remote Sensing*, vol. 60, pp. 1–11, 2022.

[245] L. Yang, W. Chen, H. Wang, and Y. Chen, "Deep learning seismic random noise attenuation via improved residual convolutional neural network," *IEEE Transactions on Geoscience and Remote Sensing*, vol. 59, no. 9, pp. 7968–7981, Sep. 2021.

[246] H. Ma, H. Yao, Y. Li, and H. Wang, "Deep residual encoder–decoder networks for desert seismic noise suppression," *IEEE Geoscience and Remote Sensing Letters*, vol. 17, no. 3, pp. 529–533, Mar. 2020.

[247] H. Yao, H. Ma, Y. Li, and Q. Feng, "Dnresnext network for desert seismic data denoising," *IEEE Geoscience and Remote Sensing Letters*, vol. 19, pp. 1–5, 2022.

[248] Q. Wang and H. Li, "Multi-scale residual network for seismic data denoising and reconstruction," in *2020 15th IEEE International Conference on Signal Processing (ICSP)*. Beijing, China: IEEE, Dec. 2020, pp. 333–336.

[249] D. Liu, W. Wang, X. Wang, C. Wang, J. Pei, and W. Chen, "Poststack seismic data denoising based on 3-d convolutional neural network," *IEEE Transactions on Geoscience and Remote Sensing*, vol. 58, no. 3, pp. 1598–1629, Mar. 2020.

[250] C. Yang, Y. Zhou, H. He, J. He, and Y. Chi, "Pyramid residual neural network with attention for seismic data denoising," in *2021 International Conference on Computer Engineering and Artificial Intelligence (ICCEAI)*. IEEE, 2021, pp. 387–390.

[251] L. Yang, W. Chen, W. Liu, B. Zha, and L. Zhu, "Random noise attenuation based on residual convolutional neural network in seismic datasets," *IEEE Access*, vol. 8, pp. 30 271–30 286, 2020.

[252] T. Zhong, M. Cheng, S. Lu, X. Dong, and Y. Li, "Rcen: A deep-learning-based background noise suppression method for das-vsp records," *IEEE Geoscience and Remote Sensing Letters*, vol. 19, pp. 1–5, 2022.

[253] W. Li and J. Wang, "Residual learning of cycle-gan for seismic data denoising," *IEEE Access*, vol. 9, pp. 11 585–11 597, 2021.

[254] F. Wang and S. Chen, "Residual learning of deep convolutional neural network for seismic random noise attenuation," *IEEE Geoscience and Remote Sensing Letters*, vol. 16, no. 8, pp. 1314–1318, Aug. 2019.

[255] Y. Yu, X. Yang, J. Chen, B. Huang, and J. Wu, "Deep learning based in-loop filter for video coding," in *2019 IEEE Visual Communications and Image Processing (VCIP)*. Sydney, Australia: IEEE, Dec. 2019, pp. 1–4.

[256] M. C. El Rai, H. Al Ahmad, O. Gouda, D. Jamal, M. A. Talib, and Q. Nasir, "Fighting deepfake by residual noise using convolutional neural networks," in *2020 3rd International Conference on Signal Processing and Information Security (ICSPIS)*. DUBAI, United Arab Emirates: IEEE, Nov. 2020, pp. 1–4.

[257] C. Herrmann, D. Willersinn, and J. Beyerer, "Low-quality video face recognition with deep networks and polygonal chain distance," in *2016 International Conference on Digital Image Computing: Techniques and Applications (DICTA)*. Gold Coast, QLD, Australia: IEEE, Nov. 2016, pp. 1–7.

[258] L. Yu, L. Shen, H. Yang, L. Wang, and P. An, "Quality enhancement network via multi-reconstruction recursive residual learning for video coding," *IEEE Signal Processing Letters*, vol. 26, no. 4, pp. 557–561, Apr. 2019.

[259] H. Zhang, Y. Lan, T. Dai, R. Qiao, Y. Xu, Y. Yao, and S.-T. Xia, "Residual frame for noisy video classification according to perceptual quality in convolutional neural networks," in *2019 IEEE International Conference on Multimedia and Expo (ICME)*. Shanghai, China: IEEE, Jul. 2019, pp. 242–247.

[260] Z. Han, H. Shangguan, X. Zhang, P. Zhang, X. Cui, and H. Ren, "A dual-encoder-single-decoder based low-dose ct denoising network," *IEEE Journal of Biomedical and Health Informatics*, pp. 1–1, 2022.

[261] J. Shen and H. Chen, "Ct denoising by multi-feature concat residual network with cross-domain attention blcok," in *2021 2nd International Symposium on Computer Engineering and Intelligent Communications (ISCEIC)*. Nanjing, China: IEEE, Aug. 2021, pp. 112–116.

[262] C. You, W. Cong, M. W. Vannier, P. K. Saha, E. A. Hoffman, G. Wang, G. Li, Y. Zhang, X. Zhang, H. Shan, M. Li, S. Ju, Z. Zhao, and Z. Zhang, "Ct super-resolution gan constrained by the identical, residual, and cycle learning ensemble (gan-circle)," *IEEE Transactions on Medical Imaging*, vol. 39, no. 1, pp. 188–203, Jan. 2020.

[263] E. Kang, W. Chang, J. Yoo, and J. C. Ye, "Deep convolutional framelet denosing for low-dose ct via wavelet residual network," *IEEE Transactions on Medical Imaging*, vol. 37, no. 6, pp. 1358–1369, Jun. 2018.

[264] J. Liu, Z. Xia, Y. Kang, and J. Qiang, "Deep residual convolutional sparse coding networks for low dose ct imaging," in *2021 14th International Congress on Image and Signal Processing, BioMedical Engineering and Informatics (CISP-BMEI)*. Shanghai, China: IEEE, Oct. 2021, pp. 1–6.

[265] Y. Zhang, J. Chi, C. Wu, and X. Yu, "Deep residual network based medical image reconstruction," in *2019 Chinese Control Conference (CCC)*. Guangzhou, China: IEEE, Jul. 2019, pp. 8550–8555.

[266] N. Thanh Trung, D.-H. Trinh, N. Linh Trung, T. Thi Thuy Quynh, and M.-H. Luu, "Dilated residual convolutional neural networks for low-dose ct image denoising," in *2020 IEEE Asia Pacific Conference on Circuits and Systems (APCCAS)*. Ha Long, Vietnam: IEEE, Dec. 2020, pp. 189–192.

[267] X. Yin, J.-L. Coatrieux, Q. Zhao, J. Liu, W. Yang, J. Yang, G. Quan, Y. Chen, H. Shu, and L. Luo, "Domain progressive 3d residual convolution network to improve low-dose ct imaging," *IEEE Transactions on Medical Imaging*, vol. 38, no. 12, pp. 2903–2913, Dec. 2019.

[268] X. Lv, X. Ren, P. He, M. Zhou, Z. Long, X. Guo, C. Fan, B. Wei, and P. Feng, "Image denoising and ring artifacts removal for spectral ct via deep neural network," *IEEE Access*, vol. 8, pp. 225 594–225 601, 2020.

[269] A. Panda, R. Naskar, S. Rajbans, and S. Pal, "A 3d wide residual network with perceptual loss for brain mri image denoising," in *2019 10th International Conference on Computing, Communication and Networking Technologies (ICCCNT)*. Kanpur, India: IEEE, Jul. 2019, pp. 1–7.

[270] G. Suryanarayana, K. Chandran, O. I. Khalaf, Y. Alotaibi, A. Alsufyani, and S. A. Alghamdi, "Accurate magnetic resonance image super-resolution using deep networks and gaussian filtering in the stationary wavelet domain," *IEEE Access*, vol. 9, pp. 71 406–71 417, 2021.

[271] Q. Xiangxiang, Z. Yu, and Z. Bingbing, "Automated segmentation based on residual u-net model for mr prostate images," in *2018 11th International Congress on Image and Signal Processing, BioMedical Engineering and Informatics (CISP-BMEI)*. Beijing, China: IEEE, Oct. 2018, pp. 1–6.

[272] R. Hou, F. Li, and G. Zhang, "Truncated residual based plug-and-play admm algorithm for mri reconstruction," *IEEE Transactions on Computational Imaging*, vol. 8, pp. 96–108, 2022.

[273] Y. Luo, S. Majoe, J. Kui, H. Qi, K. Pushparajah, and K. Rhode, "Ultra-dense denoising network: Application to cardiac catheter-based x-ray procedures," *IEEE Transactions on Biomedical Engineering*, vol. 68, no. 9, pp. 2626–2636, Sep. 2021.

[274] X. Wei, X. Liu, A. Yu, T. Fu, and D. Liu, "Clustering-oriented multiple convolutional neural networks for optical coherence tomography image denoising," p. 5.

[275] C.-H. Lin, W.-M. Liao, J.-W. Liang, P.-H. Chen, C.-E. Ko, C.-H. Yang, and C.-K. Lu, "Denoising performance evaluation of automated age-related macular degeneration detection on optical coherence tomography images," *IEEE Sensors Journal*, vol. 21, no. 1, pp. 790–801, Jan. 2021.

[276] G. Corda-D'Incan, J. A. Schnabel, and A. J. Reader, "Iteration-dependent networks and losses for unrolled deep learned fbsem pet image reconstruction," in *2020 IEEE Nuclear Science Symposium and Medical Imaging Conference (NSS/MIC)*. Boston, MA, USA: IEEE, Oct. 2020, pp. 1–4.

[277] K. Gong, J. Guan, K. Kim, X. Zhang, J. Yang, Y. Seo, G. El Fakhri, J. Qi, and Q. Li, "Iterative pet image reconstruction using convolu-

tional neural network representation," *IEEE Transactions on Medical Imaging*, vol. 38, no. 3, pp. 675–685, Mar. 2019.
[278] A. Mehranian and A. J. Reader, "Model-based deep learning pet image reconstruction using forward–backward splitting expectation–maximization," *IEEE Transactions on Radiation and Plasma Medical Sciences*, vol. 5, no. 1, pp. 54–64, Jan. 2021.
[279] C. Chan, J. Zhou, L. Yang, W. Qi, J. Kolthammer, and E. Asma, "Noise adaptive deep convolutional neural network for whole-body pet denoising," in *2018 IEEE Nuclear Science Symposium and Medical Imaging Conference Proceedings (NSS/MIC)*. Sydney, Australia: IEEE, Nov. 2018, pp. 1–4.
[280] W. Cheng, J. Lu, X. Zhu, J. Hong, X. Liu, M. Li, and P. Li, "Dilated residual learning with skip connections for real-time denoising of laser speckle imaging of blood flow in a log-transformed domain," *IEEE Transactions on Medical Imaging*, vol. 39, no. 5, pp. 1582–1593, May 2020.
[281] G. Cai, J. Wang, and Z. Chi, "An improved convolutional neural network for 3d unsupervised medical image registration," in *2020 IEEE 6th International Conference on Computer and Communications (ICCC)*. Chengdu, China: IEEE, Dec. 2020, pp. 1908–1914.
[282] C. Song, Y. Yang, M. N. Wernick, P. H. Pretorius, and M. A. King, "Approximate 4d reconstruction of cardiac-gated spect images using a residual convolutional neural network," p. 5.
[283] H. Arabi and H. Zaidi, "Three-dimensional shape completion using deep convolutional neural networks: Application to truncation compensation and metal artifact reduction in pet/mri attenuation correction," p. 3.
[284] B. Nair B J and A. S. Nair, "Ancient horoscopic palm leaf binarization using a deep binarization model - resnet," in *2021 5th International Conference on Computing Methodologies and Communication (ICCMC)*. Erode, India: IEEE, Apr. 2021, pp. 1524–1529.
[285] F. H. Gil Zuluaga, F. Bardozzo, J. I. Rios Patino, and R. Tagliaferri, "Blind microscopy image denoising with a deep residual and multiscale encoder/decoder network," in *2021 43rd Annual International Conference of the IEEE Engineering in Medicine & Biology Society (EMBC)*. Mexico: IEEE, Nov. 2021, pp. 3483–3486.
[286] M. Sung, H. Joe, J. Kim, and S.-C. Yu, "Convolutional neural network based resolution enhancement of underwater sonar image without losing working range of sonar sensors," in *2018 OCEANS - MTS/IEEE Kobe Techno-Oceans (OTO)*. Kobe: IEEE, May 2018, pp. 1–6.
[287] A. Gungor, B. Askin, D. A. Soydan, C. Baris Top, and T. Cukur, "Deep learned super resolution of system matrices for magnetic particle imaging," in *2021 43rd Annual International Conference of the IEEE Engineering in Medicine & Biology Society (EMBC)*. Mexico: IEEE, Nov. 2021, pp. 3749–3752.
[288] Y. Zuo, Y. Fang, Y. Yang, X. Shang, and Q. Wu, "Depth map enhancement by revisiting multi-scale intensity guidance within coarse-to-fine stages," *IEEE Transactions on Circuits and Systems for Video Technology*, vol. 30, no. 12, pp. 4676–4687, Dec. 2020.
[289] G. Song, K. Song, and Y. Yan, "Edrnet: Encoder–decoder residual network for salient object detection of strip steel surface defects," *IEEE Transactions on Instrumentation and Measurement*, vol. 69, no. 12, pp. 9709–9719, Dec. 2020.
[290] Z. Yang, Y. Xu, and G. Lu, "Efficient method for high-resolution fingerprint image enhancement using deep residual network," in *2020 IEEE Symposium Series on Computational Intelligence (SSCI)*. Canberra, ACT, Australia: IEEE, Dec. 2020, pp. 1725–1730.
[291] H. Noprisson, E. Ermatita, A. Abdiansah, V. Ayumi, M. Purba, and M. Utami, "Hand-woven fabric motif recognition methods: A systematic literature review," in *2021 International Conference on Informatics, Multimedia, Cyber and Information System (ICIMCIS*. Jakarta, Indonesia: IEEE, Oct. 2021, pp. 90–95.
[292] Y. Zhang and W. Wei, "Improving the image quality of machine vision thread detection," in *2021 14th International Congress on Image and Signal Processing, BioMedical Engineering and Informatics (CISP-BMEI)*. Shanghai, China: IEEE, Oct. 2021, pp. 1–6.
[293] Z. Roslan, Z. A. Long, and R. Ismail, "Individual tree crown detection using gan and retinanet on tropical forest," in *2021 15th International Conference on Ubiquitous Information Management and Communication (IMCOM)*. Seoul, Korea (South): IEEE, Jan. 2021, pp. 1–7.
[294] W. Fang and L. Li, "Non-uniformity correction for photon-counting detectors using neural network," in *2018 IEEE Nuclear Science Symposium and Medical Imaging Conference Proceedings (NSS/MIC)*. Sydney, Australia: IEEE, Nov. 2018, pp. 1–3.
[295] J. Yu and X. Zhou, "One-dimensional residual convolutional autoencoder based feature learning for gearbox fault diagnosis," *IEEE Transactions on Industrial Informatics*, vol. 16, no. 10, pp. 6347–6358, Oct. 2020.
[296] W. Wu, Q. Wang, S. Yu, Q. Luo, S. Lin, Z. Han, and Y. Tang, "Outside box and contactless palm vein recognition based on a wavelet denoising resnet," *IEEE Access*, vol. 9, pp. 82 471–82 484, 2021.
[297] R. Kallel, A. Ben Salem, and H. Ben Ghezala, "Residual convolutional neural networks model for image denoising on real time," in *2020 International Conference on Control, Automation and Diagnosis (ICCAD)*. Paris, France: IEEE, Oct. 2020, pp. 1–4.
[298] X. Mou, X. Chen, J. Guan, Y. Dong, and N. Liu, "Sea clutter suppression for radar ppi images based on scs-gan," *IEEE Geoscience and Remote Sensing Letters*, vol. 18, no. 11, pp. 1886–1890, Nov. 2021.
[299] C. Wu, B. Ju, Y. Wu, and N. Xiong, "Slimrgbd: A geographic information photography noise reduction system for aerial remote sensing," *IEEE Access*, vol. 8, pp. 15 144–15 158, 2020.
[300] D. Mishra, S. Chaudhury, M. Sarkar, and A. S. Soin, "Ultrasound image enhancement using structure oriented adversarial network," *IEEE Signal Processing Letters*, vol. 25, no. 9, pp. 1349–1353, Sep. 2018.
[301] Y. Guo, H. Li, and P. Zhuang, "Underwater image enhancement using a multiscale dense generative adversarial network," *IEEE Journal of Oceanic Engineering*, vol. 45, no. 3, pp. 862–870, Jul. 2020.
[302] Z. Zhong, C. Zhang, Y. Liu, and Y. Wu, "Viaseg: Visual information assisted lightweight point cloud segmentation," in *2019 IEEE International Conference on Image Processing (ICIP)*. Taipei, Taiwan: IEEE, Sep. 2019, pp. 1500–1504.
[303] H. Zhang, S. Liu, Z. Ge, and P. Li, "Yarn-dyed shirt cut pieces defect detection using attention vector quantized-variational autoencoder," in *2021 IEEE 10th Data Driven Control and Learning Systems Conference (DDCLS)*. Suzhou, China: IEEE, May 2021, pp. 1356–1361.
[304] I. Goodfellow, J. Pouget-Abadie, M. Mirza, B. Xu, D. Warde-Farley, S. Ozair, A. Courville, and Y. Bengio, "Generative adversarial nets," *Advances in neural information processing systems*, vol. 27, 2014.
[305] Q. ZhiPing, Z. YuanQi, S. Yi, and L. XiangBo, "A new generative adversarial network for texture preserving image denoising," in *2018 Eighth International Conference on Image Processing Theory, Tools and Applications (IPTA)*. IEEE, 2018, pp. 1–5.
[306] Y. Zhang, K. Li, K. Li, G. Sun, Y. Kong, and Y. Fu, "Accurate and fast image denoising via attention guided scaling," *IEEE Transactions on Image Processing*, vol. 30, pp. 6255–6265, 2021.
[307] J. Yuan and Z. He, "Adversarial dual network learning with randomized image transform for restoring attacked images," *IEEE Access*, vol. 8, pp. 22 617–22 624, 2020.
[308] Z. Zou, T. Shi, Z. Shi, and J. Ye, "Adversarial training for solving inverse problems in image processing," *IEEE Transactions on Image Processing*, vol. 30, pp. 2513–2525, 2021.
[309] X. Jin, Z. Chen, J. Lin, W. Zhou, J. Chen, and C. Shan, "Ai-gan: Signal de-interference via asynchronous interactive generative adversarial network," in *2019 IEEE International Conference on Multimedia & Expo Workshops (ICMEW)*. IEEE, 2019, pp. 228–233.
[310] M. Yi, W. Li, A. Elibol, and N.-Y. Chong, "Attention-model guided image enhancement for robotic vision applications," in *2020 17th International Conference on Ubiquitous Robots (UR)*. IEEE, 2020, pp. 514–519.
[311] D. M. Vo, T. P. Le, D. M. Nguyen, and S.-W. Lee, "Boostnet: A boosted convolutional neural network for image blind denoising," *IEEE Access*, vol. 9, pp. 115 145–115 164, 2021.
[312] H. Zhang and K. Sakurai, "Conditional generative adversarial network-based image denoising for defending against adversarial attack," *IEEE Access*, vol. 9, pp. 169 031–169 043, 2021.
[313] K. Wu and C. Zhang, "Deep generative adversarial networks for the sparse signal denoising," in *2018 24th International Conference on Pattern Recognition (ICPR)*. Beijing: IEEE, Aug. 2018, pp. 1127–1132.
[314] L. Yanchun and X. Nanfeng, "Generative adversarial networks based on denoising and reconstruction regularization," in *2019 IEEE 21st International Conference on High Performance Computing and Communications; IEEE 17th International Conference on Smart City; IEEE 5th International Conference on Data Science and Systems (HPCC/SmartCity/DSS)*. Zhangjiajie, China: IEEE, Aug. 2019, pp. 2162–2168.
[315] D.-W. Kim, J. Ryun Chung, and S.-W. Jung, "Grdn: Grouped residual dense network for real image denoising and gan-based real-world noise modeling," in *Proceedings of the IEEE/CVF Conference on Computer Vision and Pattern Recognition Workshops*, 2019, pp. 0–0.
[316] F. Chiaroni, M.-C. Rahal, N. Hueber, and F. Dufaux, "Hallucinating a cleanly labeled augmented dataset from a noisy labeled dataset using

gan," in *2019 IEEE International Conference on Image Processing (ICIP)*. IEEE, 2019, pp. 3616–3620.

[317] G. Ohayon, T. Adrai, G. Vaksman, M. Elad, and P. Milanfar, "High perceptual quality image denoising with a posterior sampling cgan," in *Proceedings of the IEEE/CVF International Conference on Computer Vision*, 2021, pp. 1805–1813.

[318] W. Guo, F. Chen, and H. Cheng, "Image denoising and colorization based on plug and play framework," in *2021 IEEE 6th International Conference on Signal and Image Processing (ICSIP)*. IEEE, 2021, pp. 472–477.

[319] A. Alsaiari, R. Rustagi, M. M. Thomas, A. G. Forbes *et al.*, "Image denoising using a generative adversarial network," in *2019 IEEE 2nd International Conference on Information and Computer Technologies (ICICT)*. IEEE, 2019, pp. 126–132.

[320] Q. Wang, H. Liu, G. Xie, and Y. Zhang, "Image denoising using an improved generative adversarial network with wasserstein distance," in *2021 40th Chinese Control Conference (CCC)*. IEEE, 2021, pp. 7027–7032.

[321] P. Wang, "Image denoising using deep cgan with bi-skip connections," in *Proceedings of the IEEE/CVF Conference on Computer Vision and Pattern Recognition Workshops*, 2019, pp. 0–0.

[322] U. Maheshwari, V. P. K. Turlapati, and U. Kiruthika, "Lucid-gan: An adversarial network for enhanced image inpainting," in *2021 IEEE International Conference on Computational Intelligence and Virtual Environments for Measurement Systems and Applications (CIVEMSA)*. Hong Kong, China: IEEE, Jun. 2021, pp. 1–6.

[323] V. Nuthna, K. Chachadi, and L. S. Joshi, "Modeling and performance evaluation of generative adversarial network for image denoising," in *2018 International Conference on Computational Techniques, Electronics and Mechanical Systems (CTEMS)*. IEEE, 2018, pp. 7–11.

[324] X. Di and P. Yu, "Multiplicative noise channel in generative adversarial networks," in *Proceedings of the IEEE International Conference on Computer Vision Workshops*, 2017, pp. 1165–1172.

[325] G. Liu, Y. Jiang, and S. Yang, "Noise reduction algorithm for communication based on improved generative adversarial network," in *2020 IEEE 9th Joint International Information Technology and Artificial Intelligence Conference (ITAIC)*, vol. 9. IEEE, 2020, pp. 1130–1136.

[326] M. Shirasaki, K. Moriwaki, T. Oogi, N. Yoshida, S. Ikeda, and T. Nishimichi, "Noise reduction for weak lensing mass mapping: an application of generative adversarial networks to subaru hyper suprime-cam first-year data," *Monthly Notices of the Royal Astronomical Society*, vol. 504, no. 2, pp. 1825–1839, 2021.

[327] K. Swami and S. K. Das, "Candy: Conditional adversarial networks based end-to-end system for single image haze removal," in *2018 24th International Conference on Pattern Recognition (ICPR)*. IEEE, 2018, pp. 3061–3067.

[328] A. Mehta, H. Sinha, M. Mandal, and P. Narang, "Domain-aware unsupervised hyperspectral reconstruction for aerial image dehazing," in *Proceedings of the IEEE/CVF Winter Conference on Applications of Computer Vision*, 2021, pp. 413–422.

[329] M. Fu, H. Liu, Y. Yu, J. Chen, and K. Wang, "Dw-gan: A discrete wavelet transform gan for nonhomogeneous dehazing," in *Proceedings of the IEEE/CVF Conference on Computer Vision and Pattern Recognition*, 2021, pp. 203–212.

[330] S. Ki, H. Sim, J.-S. Choi, S. Kim, and M. Kim, "Fully end-to-end learning based conditional boundary equilibrium gan with receptive field sizes enlarged for single ultra-high resolution image dehazing," in *Proceedings of the IEEE Conference on Computer Vision and Pattern Recognition Workshops*, 2018, pp. 817–824.

[331] X. Jiang, L. Lu, M. Zhu, Z. Hao, and W. Gao, "Haze relevant feature attention network for single image dehazing," *IEEE Access*, vol. 9, pp. 106 476–106 488, 2021.

[332] A. Mehta, H. Sinha, P. Narang, and M. Mandal, "Hidegan: A hyperspectral-guided image dehazing gan," in *Proceedings of the IEEE/CVF Conference on Computer Vision and Pattern Recognition Workshops*, 2020, pp. 212–213.

[333] H. Sim, S. Ki, J.-S. Choi, S. Seo, S. Kim, and M. Kim, "High-resolution image dehazing with respect to training losses and receptive field sizes," in *Proceedings of the IEEE Conference on Computer Vision and Pattern Recognition Workshops*, 2018, pp. 912–919.

[334] J. Xiao, J. Zhou, J. Lei, C. Xu, and H. Sui, "Image hazing algorithm based on generative adversarial networks," *IEEE Access*, vol. 8, pp. 15 883–15 894, 2019.

[335] Y. Guo, J. Chen, X. Ren, A. Wang, and W. Wang, "Joint raindrop and haze removal from a single image," *IEEE Transactions on Image Processing*, vol. 29, pp. 9508–9519, 2020.

[336] K. Gan, J. Zhao, and H. Chen, "Multilevel image dehazing algorithm using conditional generative adversarial networks," *IEEE Access*, vol. 8, pp. 55 221–55 229, 2020.

[337] Q. Jia and Z. Ma, "Patch-based generative adversarial network for single image haze removal," in *2020 International Conference on Computer Engineering and Application (ICCEA)*. IEEE, 2020, pp. 882–886.

[338] G. Long, W. Lu, L. Zha, and H. Zhang, "Phc-gan: Physical constraint generative adversarial network for single image dehazing," in *2020 IEEE 32nd International Conference on Tools with Artificial Intelligence (ICTAI)*. IEEE, 2020, pp. 545–549.

[339] Y. Du and X. Li, "Recursive image dehazing via perceptually optimized generative adversarial network (pogan)," in *2019 IEEE/CVF Conference on Computer Vision and Pattern Recognition Workshops (CVPRW)*. IEEE, 2019, pp. 1824–1832.

[340] A. Dudhane, H. Singh Aulakh, and S. Murala, "Ri-gan: An end-to-end network for single image haze removal," in *Proceedings of the IEEE/CVF Conference on Computer Vision and Pattern Recognition Workshops*, 2019, pp. 0–0.

[341] P. Wei, X. Wang, L. Wang, and J. Xiang, "Sidgan: Single image dehazing without paired supervision," in *2020 25th International Conference on Pattern Recognition (ICPR)*. Milan, Italy: IEEE, Jan. 2021, pp. 2958–2965.

[342] K. Zhao, T. Lu, Y. Wang, Y. Wang, and X. Nie, "Single image dehazing based on enhanced generative adversarial network," in *2020 5th International Conference on Control, Robotics and Cybernetics (CRC)*. IEEE, 2020, pp. 129–133.

[343] H. Zhu, Y. Cheng, X. Peng, J. T. Zhou, Z. Kang, S. Lu, Z. Fang, L. Li, and J.-H. Lim, "Single-image dehazing via compositional adversarial network," *IEEE Transactions on Cybernetics*, vol. 51, no. 2, pp. 829–838, 2019.

[344] Y. Jin, G. Gao, Q. Liu, and Y. Wang, "Unsupervised conditional disentangle network for image dehazing," in *2020 IEEE International Conference on Image Processing (ICIP)*. IEEE, 2020, pp. 963–967.

[345] Y. Pang, J. Xie, and X. Li, "Visual haze removal by a unified generative adversarial network," *IEEE Transactions on Circuits and Systems for Video Technology*, vol. 29, no. 11, pp. 3211–3221, Nov. 2019.

[346] S. Alletto, C. Carlin, L. Rigazio, Y. Ishii, and S. Tsukizawa, "Adherent raindrop removal with self-supervised attention maps and spatio-temporal generative adversarial networks," in *Proceedings of the IEEE/CVF International Conference on Computer Vision Workshops*, 2019, pp. 0–0.

[347] P. K. Sharma, P. Jain, and A. Sur, "Dual-domain single image de-raining using conditional generative adversarial network," in *2019 IEEE International conference on image processing (ICIP)*. IEEE, 2019, pp. 2796–2800.

[348] T. Matsui and M. Ikehara, "Gan-based rain noise removal from single-image considering rain composite models," *IEEE Access*, vol. 8, pp. 40 892–40 900, 2020.

[349] S. Li, Y. Hou, H. Yue, and Z. Guo, "Single image de-raining via generative adversarial nets," in *2019 IEEE International Conference on Multimedia and Expo (ICME)*. IEEE, 2019, pp. 1192–1197.

[350] B. Zhao, W. Li, and W. Gong, "Deep pyramid generative adversarial network with local and nonlocal similarity features for natural motion image deblurring," *IEEE Access*, vol. 7, pp. 185 893–185 907, 2019.

[351] H. Tomosada, T. Kudo, T. Fujisawa, and M. Ikehara, "Gan-based image deblurring using dct discriminator," in *2020 25th International Conference on Pattern Recognition (ICPR)*. Milan, Italy: IEEE, Jan. 2021, pp. 3675–3681.

[352] ——, "Gan-based image deblurring using dct loss with customized datasets," *IEEE Access*, vol. 9, pp. 135 224–135 233, 2021.

[353] Z. Li, J. Zhang, Z. Fang, B. Huang, X. Jiang, Y. Gao, and J.-N. Hwang, "Single image snow removal via composition generative adversarial networks," *IEEE Access*, vol. 7, pp. 25 016–25 025, 2019.

[354] X. Wang, Y. Pan, and D. P. Lun, "Stereoscopic image reflection removal based on wasserstein generative adversarial network," in *2020 IEEE International Conference on Visual Communications and Image Processing (VCIP)*. IEEE, 2020, pp. 148–151.

[355] D. Kim and B.-W. Hong, "Unsupervised feature elimination via generative adversarial networks: Application to hair removal in melanoma classification," *IEEE Access*, vol. 9, pp. 42 610–42 620, 2021.

[356] H. Zhou, J. Sun, Y. Yacoob, and D. W. Jacobs, "Label denoising adversarial network (ldan) for inverse lighting of faces," in *Proceedings of the IEEE Conference on Computer Vision and Pattern Recognition*, 2018, pp. 6238–6247.

[357] A. Chopra, A. Maan, and A. Kesharwani, "Low light gan-based photo enhancement," in *2021 Second International Conference on Electronics*

and Sustainable Communication Systems (ICESC). Coimbatore, India: IEEE, Aug. 2021, pp. 103–110.

[358] R. Wang, B. Jiang, C. Yang, Q. Li, and B. Zhang, "Magan: Unsupervised low-light image enhancement guided by mixed-attention," *Big Data Mining and Analytics*, vol. 5, no. 2, pp. 110–119, Jun. 2022.

[359] Y. Liu, Z. Wang, Y. Zeng, H. Zeng, and D. Zhao, "Pd-gan: Perceptual-details gan for extremely noisy low light image enhancement," in *ICASSP 2021-2021 IEEE International Conference on Acoustics, Speech and Signal Processing (ICASSP)*. IEEE, 2021, pp. 1840–1844.

[360] Y.-S. Chen, Y.-C. Wang, M.-H. Kao, and Y.-Y. Chuang, "Deep photo enhancer: Unpaired learning for image enhancement from photographs with gans," in *Proceedings of the IEEE Conference on Computer Vision and Pattern Recognition*, 2018, pp. 6306–6314.

[361] S. Wu, C. Dong, and Y. Qiao, "Blind image restoration based on cycle-consistent network," *IEEE Transactions on Multimedia*, 2022.

[362] V. Kandarpa, A. Bousse, D. Benoit, and D. Visvikis, "Dug-recon: a framework for direct image reconstruction using convolutional generative networks," *IEEE Transactions on Radiation and Plasma Medical Sciences*, vol. 5, no. 1, pp. 44–53, 2020.

[363] L.-H. Chen, C. G. Bampis, Z. Li, and A. C. Bovik, "Learning to distort images using generative adversarial networks," *IEEE Signal Processing Letters*, vol. 27, pp. 2144–2148, 2020.

[364] A. Lahiri, S. Bairagya, S. Bera, S. Haldar, and P. K. Biswas, "Lightweight modules for efficient deep learning based image restoration," *IEEE Transactions on Circuits and Systems for Video Technology*, vol. 31, no. 4, pp. 1395–1410, 2020.

[365] F. Luo and X. Wu, "Maximum a posteriori on a submanifold: A general image restoration method with gan," in *2020 International Joint Conference on Neural Networks (IJCNN)*. Glasgow, United Kingdom: IEEE, Jul. 2020, pp. 1–7.

[366] C. Zhu, Y. Chen, Y. Zhang, S. Liu, and G. Li, "Resgan: A low-level image processing network to restore original quality of jpeg compressed images," in *2019 Data Compression Conference (DCC)*. IEEE, 2019, pp. 616–616.

[367] V. Abeykoon, Z. Liu, R. Kettimuthu, G. Fox, and I. Foster, "Scientific image restoration anywhere," in *2019 IEEE/ACM 1st Annual Workshop on Large-scale Experiment-in-the-Loop Computing (XLOOP)*. IEEE, 2019, pp. 8–13.

[368] R. Kumar and S. Kumar Maji, "A novel framework for denoised high resolution generative adversarial network – dhrgan," in *2020 7th International Conference on Signal Processing and Integrated Networks (SPIN)*. Noida, India: IEEE, Feb. 2020, pp. 1033–1038.

[369] S. Chen, S. Li, and C. Zhu, "Advanced generative adversarial network based on dense connection for single image super resolution," in *2019 IEEE THE 2nd INTERNATIONAL CONFERENCE ON MICRO/NANO SENSORS for AI, HEALTHCARE, AND ROBOTICS (NSENS)*. IEEE, pp. 68–71.

[370] Y. Guo, Q. Chen, J. Chen, Q. Wu, Q. Shi, and M. Tan, "Auto-embedding generative adversarial networks for high resolution image synthesis," *IEEE Transactions on Multimedia*, vol. 21, no. 11, pp. 2726–2737, 2019.

[371] F. Shahidi, "Breast cancer histopathology image super-resolution using wide-attention gan with improved wasserstein gradient penalty and perceptual loss," *IEEE Access*, vol. 9, pp. 32 795–32 809, 2021.

[372] C.-C. Hsu and K.-Y. Huang, "Coupled adversarial learning for single image super-resolution," in *2020 IEEE 11th Sensor Array and Multichannel Signal Processing Workshop (SAM)*. IEEE, 2020, pp. 1–5.

[373] A. Rana, P. Singh, G. Valenzise, F. Dufaux, N. Komodakis, and A. Smolic, "Deep tone mapping operator for high dynamic range images," *IEEE Transactions on Image Processing*, vol. 29, pp. 1285–1298, 2019.

[374] L. Chen, W. Dan, L. Cao, C. Wang, and J. Li, "Joint denoising and super-resolution via generative adversarial training," in *2018 24th International Conference on Pattern Recognition (ICPR)*. Beijing: IEEE, Aug. 2018, pp. 2753–2758.

[375] M. Adil, S. Mamoon, A. Zakir, M. A. Manzoor, and Z. Lian, "Multi scale-adaptive super-resolution person re-identification using gan," *IEEE Access*, vol. 8, pp. 177 351–177 362, 2020.

[376] K. Ning, Z. Zhang, K. Han, S. Han, and X. Zhang, "Multi-frame super-resolution algorithm based on a wgan," *IEEE Access*, vol. 9, pp. 85 839–85 851, 2021.

[377] X. Yang, X. Wang, N. Wang, and X. Gao, "Srdn: A unified super-resolution and motion deblurring network for space image restoration," *IEEE Transactions on Geoscience and Remote Sensing*, 2021.

[378] J. Shao, L. Chen, and Y. Wu, "Srwgantv: Image super-resolution through wasserstein generative adversarial networks with total variational regularization," in *2021 IEEE 13th International Conference on Computer Research and Development (ICCRD)*. IEEE, 2021, pp. 21–26.

[379] Y. Yuan, S. Liu, J. Zhang, Y. Zhang, C. Dong, and L. Lin, "Unsupervised image super-resolution using cycle-in-cycle generative adversarial networks," in *Proceedings of the IEEE Conference on Computer Vision and Pattern Recognition Workshops*, 2018, pp. 701–710.

[380] F. Gu, H. Zhang, and C. Wang, "A gan-based method for sar image despeckling," in *2019 SAR in Big Data Era (BIGSARDATA)*. IEEE, 2019, pp. 1–5.

[381] P. Wang, H. Zhang, and V. M. Patel, "Generative adversarial network-based restoration of speckled sar images," in *2017 IEEE 7th international workshop on computational advances in multi-sensor adaptive processing (CAMSAP)*. IEEE, 2017, pp. 1–5.

[382] R. Liu, Y. Li, and L. Jiao, "Sar image specle reduction based on a generative adversarial network," in *2020 International Joint Conference on Neural Networks (IJCNN)*. IEEE, 2020, pp. 1–6.

[383] F. Gu, H. Zhang, C. Wang, and F. Wu, "Sar image super-resolution based on noise-free generative adversarial network," in *IGARSS 2019-2019 IEEE International Geoscience and Remote Sensing Symposium*. IEEE, 2019, pp. 2575–2578.

[384] X. Mou, X. Chen, J. Guan, Y. Dong, and N. Liu, "Sea clutter suppression for radar ppi images based on scs-gan," *IEEE Geoscience and Remote Sensing Letters*, vol. 18, no. 11, pp. 1886–1890, 2020.

[385] S. Wang, Y. Li, N. Wu, Y. Zhao, and H. Yao, "Attribute-based double constraint denoising network for seismic data," *IEEE Transactions on Geoscience and Remote Sensing*, vol. 59, no. 6, pp. 5304–5316, Jun. 2021.

[386] X. Dong and Y. Li, "Denoising the optical fiber seismic data by using convolutional adversarial network based on loss balance," *IEEE Transactions on Geoscience and Remote Sensing*, vol. 59, no. 12, pp. 10 544–10 554, 2020.

[387] H. Wang, Y. Li, and X. Dong, "Generative adversarial network for desert seismic data denoising," *IEEE Transactions on Geoscience and Remote Sensing*, vol. 59, no. 8, pp. 7062–7075, 2020.

[388] H. Ma, Y. Sun, N. Wu, and Y. Li, "Relative attributes-based generative adversarial network for desert seismic noise suppression," *IEEE Geoscience and Remote Sensing Letters*, vol. 19, pp. 1–5, 2021.

[389] Y. Li, X. Luo, N. Wu, and X. Dong, "The application of semisupervised attentional generative adversarial networks in desert seismic data denoising," *IEEE Geoscience and Remote Sensing Letters*, vol. 19, pp. 1–5, 2021.

[390] Y. Li, H. Wang, and X. Dong, "The denoising of desert seismic data based on cycle-gan with unpaired data training," *IEEE Geoscience and Remote Sensing Letters*, vol. 18, no. 11, pp. 2016–2020, 2020.

[391] Y. Chen, F. Wu, and J. Zhao, "Motion deblurring via using generative adversarial networks for space-based imaging," in *2018 IEEE 16th International Conference on Software Engineering Research, Management and Applications (SERA)*. IEEE, 2018, pp. 37–41.

[392] M. Wu, Y. Bu, J. Pan, Z. Yi, and X. Kong, "Spectra-gans: A new automated denoising method for low-s/n stellar spectra," *IEEE Access*, vol. 8, pp. 107 912–107 926, 2020.

[393] L. Zhong, G. Liu, and G. Yang, "Blind denoising of fluorescence microscopy images using gan-based global noise modeling," in *2021 IEEE 18th International Symposium on Biomedical Imaging (ISBI)*. IEEE, 2021, pp. 863–867.

[394] S. Chen, D. Shi, M. Sadiq, and X. Cheng, "Image denoising with generative adversarial networks and its application to cell image enhancement," *IEEE Access*, vol. 8, pp. 82 819–82 831, 2020.

[395] S. Lee, S. Han, P. Salama, K. W. Dunn, and E. J. Delp, "Three dimensional blind image deconvolution for fluorescence microscopy using generative adversarial networks," in *2019 IEEE 16th International Symposium on Biomedical Imaging (ISBI 2019)*. IEEE, 2019, pp. 538–542.

[396] T. B. Issa, C. Vinegoni, A. Shaw, P. F. Feruglio, R. Weissleder, and D. Uminsky, "Video-rate acquisition fluorescence microscopy via generative adversarial networks," in *2020 IEEE 20th International Conference on Bioinformatics and Bioengineering (BIBE)*. IEEE, 2020, pp. 569–576.

[397] M. Siddiqua, N. Akhter, and J. Khurshid, "Comparative study of image to image translation models for underwater image enhancement," in *2021 International Conference on Robotics and Automation in Industry (ICRAI)*. IEEE, 2021, pp. 1–4.

[398] C. Fabbri, M. J. Islam, and J. Sattar, "Enhancing underwater imagery using generative adversarial networks," in *2018 IEEE International Conference on Robotics and Automation (ICRA)*. IEEE, 2018, pp. 7159–7165.

[399] X. Chen, J. Yu, S. Kong, Z. Wu, X. Fang, and L. Wen, "Towards real-time advancement of underwater visual quality with gan," *IEEE Transactions on Industrial Electronics*, vol. 66, no. 12, pp. 9350–9359, 2019.

[400] H. Ashraf, Y. Jeong, and C. H. Lee, "Underwater ambient-noise removing gan based on magnitude and phase spectra," *IEEE Access*, vol. 9, pp. 24 513–24 530, 2021.

[401] R. Han, Y. Guan, Z. Yu, P. Liu, and H. Zheng, "Underwater image enhancement based on a spiral generative adversarial framework," *IEEE Access*, vol. 8, pp. 218 838–218 852, 2020.

[402] Y. Guo, H. Li, and P. Zhuang, "Underwater image enhancement using a multiscale dense generative adversarial network," *IEEE Journal of Oceanic Engineering*, vol. 45, no. 3, pp. 862–870, 2019.

[403] H. Lu, H. Han, and S. K. Zhou, "Dual-gan: Joint bvp and noise modeling for remote physiological measurement," in *Proceedings of the IEEE/CVF Conference on Computer Vision and Pattern Recognition*, 2021, pp. 12 404–12 413.

[404] G. Ye, L. Ding, and Y. Zhu, "Gan-based monochromatic full-focus thz imaging," in *2019 IEEE International Conference on Signal, Information and Data Processing (ICSIDP)*. IEEE, 2019, pp. 1–5.

[405] C. Zhao, C. Li, S. Feng, and N. Su, "Hyperspectral anomaly detection using bilateral-filtered generative adversarial networks," in *2021 IEEE International Geoscience and Remote Sensing Symposium IGARSS*. IEEE, 2021, pp. 4408–4411.

[406] H. Shan, Y. Zhang, Q. Yang, U. Kruger, M. K. Kalra, L. Sun, W. Cong, and G. Wang, "3-d convolutional encoder-decoder network for low-dose ct via transfer learning from a 2-d trained network," *IEEE transactions on medical imaging*, vol. 37, no. 6, pp. 1522–1534, 2018.

[407] J. Zhang, D. Li, Q. Hua, X. Qi, Z. Wen *et al.*, "3d remote healthcare for noisy ct images in the internet of things using edge computing," *IEEE Access*, vol. 9, pp. 15 170–15 180, 2021.

[408] Z. Han, H. Shangguan, X. Zhang, P. Zhang, X. Cui, and H. Ren, "A dual-encoder-single-decoder based low-dose ct denoising network," *IEEE Journal of Biomedical and Health Informatics*, 2022.

[409] X. Zhang, Z. Han, H. Shangguan, X. Han, X. Cui, and A. Wang, "Artifact and detail attention generative adversarial networks for low-dose ct denoising," *IEEE Transactions on Medical Imaging*, vol. 40, no. 12, pp. 3901–3918, 2021.

[410] Z. Huang, Z. Chen, Q. Zhang, G. Quan, M. Ji, C. Zhang, Y. Yang, X. Liu, D. Liang, H. Zheng *et al.*, "Cagan: A cycle-consistent generative adversarial network with attention for low-dose ct imaging," *IEEE Transactions on Computational Imaging*, vol. 6, pp. 1203–1218, 2020.

[411] S. Ataei, P. Babyn, A. Ahmadian, and J. Alirezaie, "Cascaded learning with generative adversarial networks for low dose ct denoising," in *2021 43rd Annual International Conference of the IEEE Engineering in Medicine & Biology Society (EMBC)*. Mexico: IEEE, Nov. 2021, pp. 3053–3056.

[412] Y. Zhang, D. Hu, Q. Zhao, G. Quan, J. Liu, Q. Liu, Y. Zhang, G. Coatrieux, Y. Chen, and H. Yu, "Clear: comprehensive learning enabled adversarial reconstruction for subtle structure enhanced low-dose ct imaging," *IEEE Transactions on Medical Imaging*, vol. 40, no. 11, pp. 3089–3101, 2021.

[413] K. C. Kusters, L. A. Zavala-Mondragón, J. O. Bescós, P. Rongen, P. H. de With, and F. van der Sommen, "Conditional generative adversarial networks for low-dose ct image denoising aiming at preservation of critical image content," in *2021 43rd Annual International Conference of the IEEE Engineering in Medicine & Biology Society (EMBC)*. IEEE, 2021, pp. 2682–2687.

[414] C. You, G. Li, Y. Zhang, X. Zhang, H. Shan, M. Li, S. Ju, Z. Zhao, Z. Zhang, W. Cong *et al.*, "Ct super-resolution gan constrained by the identical, residual, and cycle learning ensemble (gan-circle)," *IEEE transactions on medical imaging*, vol. 39, no. 1, pp. 188–203, 2019.

[415] B. V. Gajera, S. R. Kapil, D. Ziaei, J. Mangalagiri, E. Siegel, and D. Chapman, "Ct-scan denoising using a charbonnier loss generative adversarial network," vol. 9, p. 17, 2021.

[416] Z. Huang, J. Zhang, Y. Zhang, and H. Shan, "Du-gan: Generative adversarial networks with dual-domain u-net-based discriminators for low-dose ct denoising," *IEEE Transactions on Instrumentation and Measurement*, vol. 71, pp. 1–12, 2022.

[417] C. Yan, H. Chen, and Z. Yang, "End-to-end medical image denoising via cycle-consistent generative adversarial network," in *2021 International Conference on Information Science, Parallel and Distributed Systems (ISPDS)*. IEEE, 2021, pp. 30–33.

[418] W. Su, Y. Qu, C. Deng, Y. Wang, F. Zheng, and Z. Chen, "Enhance generative adversarial networks by wavelet transform to denoise low-dose ct images," in *2020 IEEE International Conference on Image Processing (ICIP)*. IEEE, 2020, pp. 350–354.

[419] L. Yang, H. Shangguan, X. Zhang, A. Wang, and Z. Han, "High-frequency sensitive generative adversarial network for low-dose ct image denoising," *IEEE Access*, vol. 8, pp. 930–943, 2020.

[420] Z. Li, S. Zhou, J. Huang, L. Yu, and M. Jin, "Investigation of low-dose ct image denoising using unpaired deep learning methods," *IEEE Transactions on Radiation and Plasma Medical Sciences*, vol. 5, no. 2, pp. 224–234, 2020.

[421] M. Eslami, S. Tabarestani, and M. Adjouadi, "Joint low dose ct denoising and kidney segmentation," in *2020 IEEE 17th International Symposium on Biomedical Imaging Workshops (ISBI Workshops)*. Iowa City, IA, USA: IEEE, Apr. 2020, pp. 1–4.

[422] L. Marcos, J. Alirezaie, and P. Babyn, "Low dose ct image denoising using boosting attention fusion gan with perceptual loss," in *2021 43rd Annual International Conference of the IEEE Engineering in Medicine & Biology Society (EMBC)*. IEEE, 2021, pp. 3407–3410.

[423] Y. Ma, B. Wei, P. Feng, P. He, X. Guo, and G. Wang, "Low-dose ct image denoising using a generative adversarial network with a hybrid loss function for noise learning," *IEEE Access*, vol. 8, pp. 67 519–67 529, 2020.

[424] Q. Yang, P. Yan, Y. Zhang, H. Yu, Y. Shi, X. Mou, M. K. Kalra, Y. Zhang, L. Sun, and G. Wang, "Low-dose ct image denoising using a generative adversarial network with wasserstein distance and perceptual loss," *IEEE transactions on medical imaging*, vol. 37, no. 6, pp. 1348–1357, 2018.

[425] Y. Lyu, W. Jiang, Y. Lin, L. Voros, M. Zhang, B. Mueller, B. Mychalczak, and Y. Song, "Motion-blind blur removal for ct images with wasserstein generative adversarial networks," in *2018 11th International Congress on Image and Signal Processing, BioMedical Engineering and Informatics (CISP-BMEI)*. IEEE, 2018, pp. 1–5.

[426] K. Choi, M. Vania, and S. Kim, "Semi-supervised learning for low-dose ct image restoration with hierarchical deep generative adversarial network (hd-gan)," in *2019 41st Annual International Conference of the IEEE Engineering in Medicine and Biology Society (EMBC)*. IEEE, 2019, pp. 2683–2686.

[427] J. Chi, C. Wu, X. Yu, P. Ji, and H. Chu, "Single low-dose ct image denoising using a generative adversarial network with modified u-net generator and multi-level discriminator," *IEEE Access*, vol. 8, pp. 133 470–133 487, 2020.

[428] K. Choi, J. S. Lim, and S. Kim, "Statnet: statistical image restoration for low-dose ct using deep learning," *IEEE Journal of Selected Topics in Signal Processing*, vol. 14, no. 6, pp. 1137–1150, 2020.

[429] C. You, W. Cong, G. Wang, Q. Yang, H. Shan, L. Gjesteby, G. Li, S. Ju, Z. Zhang, Z. Zhao, and Y. Zhang, "Structurally-sensitive multi-scale deep neural network for low-dose ct denoising," *IEEE Access*, vol. 6, pp. 41 839–41 855, 2018.

[430] S. Zhou, L. Yu, and M. Jin, "Supervised and unsupervised deep learning methods for low-dose ct image denoising," in *2020 IEEE Nuclear Science Symposium and Medical Imaging Conference (NSS/MIC)*. IEEE, pp. 1–3.

[431] M. B. de Almeida, L. F. A. Pereira, T. I. Ren, G. D. Cavalcanti, and J. Sijbers, "The gated recurrent conditional generative adversarial network (grc-gan): application to denoising of low-dose ct images," in *2021 34th SIBGRAPI Conference on Graphics, Patterns and Images (SIBGRAPI)*. IEEE, 2021, pp. 129–135.

[432] J. Mangalagiri, D. Chapman, A. Gangopadhyay, Y. Yesha, J. Galita, S. Menon, Y. Yesha, B. Saboury, M. Morris, and P. Nguyen, "Toward generating synthetic ct volumes using a 3d-conditional generative adversarial network," in *2020 International Conference on Computational Science and Computational Intelligence (CSCI)*. IEEE, 2020, pp. 858–862.

[433] H. S. Park, J. Baek, S. K. You, J. K. Choi, and J. K. Seo, "Unpaired image denoising using a generative adversarial network in x-ray ct," *IEEE Access*, vol. 7, pp. 110 414–110 425, 2019.

[434] Z. Yang, C. Yan, and H. Chen, "Unpaired low-dose ct denoising using conditional gan with structural loss," in *2021 International Conference on Wireless Communications and Smart Grid (ICWCSG)*. Hangzhou, China: IEEE, Aug. 2021, pp. 272–275.

[435] M. Tian and K. Song, "Boosting magnetic resonance image denoising with generative adversarial networks," *IEEE Access*, vol. 9, pp. 62 266–62 275, 2021.

[436] Z. Fu, X. Yu, C. Ge, M. Z. Aziz, and L. Liu, "Adgan: An asymmetric despeckling generative adversarial network for unpaired oct image speckle noise reduction," in *2021 IEEE 6th Optoelectronics Global Conference (OGC)*. IEEE, 2021, pp. 212–216.

[437] M. J. Hasan, M. S. Alom, U. Fatema, and M. F. Wahid, "Deep learning based retinal oct image denoising using generative adversarial

network," in *2021 International Conference on Automation, Control and Mechatronics for Industry 4.0 (ACMI)*. IEEE, 2021, pp. 1–6.

[438] A. Yu, X. Liu, X. Wei, T. Fu, and D. Liu, "Generative adversarial networks with dense connection for optical coherence tomography images denoising," in *2018 11th International Congress on Image and Signal Processing, BioMedical Engineering and Informatics (CISP-BMEI)*. Beijing, China: IEEE, Oct. 2018, pp. 1–5.

[439] Y. Huang, W. Xia, Z. Lu, Y. Liu, H. Chen, J. Zhou, L. Fang, and Y. Zhang, "Noise-powered disentangled representation for unsupervised speckle reduction of optical coherence tomography images," *IEEE Transactions on Medical Imaging*, vol. 40, no. 10, pp. 2600–2614, Oct. 2021.

[440] I. A. Viedma Escalona, D. Alonso-Caneiro, S. Read, and M. Collins, "Oct retinal image-to-image translation: Analysing the use of cyclegan to improve retinal boundary semantic segmentation," *Proceedings of the 2021 Digital Image Computing: Techniques and Applications (DICTA)*, 2021.

[441] M. Wang, W. Zhu, K. Yu, Z. Chen, F. Shi, Y. Zhou, Y. Ma, Y. Peng, D. Bao, S. Feng, L. Ye, D. Xiang, and X. Chen, "Semi-supervised capsule cgan for speckle noise reduction in retinal oct images," *IEEE Transactions on Medical Imaging*, vol. 40, no. 4, pp. 1168–1183, Apr. 2021.

[442] N. A. Kande, R. Dakhane, A. Dukkipati, and P. K. Yalavarthy, "Siamesegan: A generative model for denoising of spectral domain optical coherence tomography images," *IEEE Transactions on Medical Imaging*, vol. 40, no. 1, pp. 180–192, Jan. 2021.

[443] Y. Zhou, K. Yu, M. Wang, Y. Ma, Y. Peng, Z. Chen, W. Zhu, F. Shi, and X. Chen, "Speckle noise reduction for oct images based on image style transfer and conditional gan," *IEEE Journal of Biomedical and Health Informatics*, 2021.

[444] A. Guo, L. Fang, M. Qi, and S. Li, "Unsupervised denoising of optical coherence tomography images with nonlocal-generative adversarial network," *IEEE Transactions on Instrumentation and Measurement*, vol. 70, pp. 1–12, 2020.

[445] V. Das, S. Dandapat, and P. K. Bora, "Unsupervised super-resolution of oct images using generative adversarial network for improved age-related macular degeneration diagnosis," *IEEE Sensors Journal*, vol. 20, no. 15, pp. 8746–8756, 2020.

[446] G. S. Mok, J. Sun, Q. Zhang, and Y. Du, "Comparison of projection-based and reconstruction-based low dose spect image denoising using a conditional generative adversarial network," in *2020 IEEE Nuclear Science Symposium and Medical Imaging Conference (NSS/MIC)*. IEEE, pp. 1–3.

[447] Z. Hu, H. Xue, Q. Zhang, J. Gao, N. Zhang, S. Zou, Y. Teng, X. Liu, Y. Yang, D. Liang *et al.*, "Dpir-net: Direct pet image reconstruction based on the wasserstein generative adversarial network," *IEEE Transactions on Radiation and Plasma Medical Sciences*, vol. 5, no. 1, pp. 35–43, 2020.

[448] J. Sun, Q. Zhang, D. Zhang, P. H. Pretorius, M. A. King, and G. S. Mok, "Generative adversarial network for denoising in dual gated myocardial perfusion spect using a population of phantoms and clinical data," in *2019 IEEE Nuclear Science Symposium and Medical Imaging Conference (NSS/MIC)*. IEEE, 2019, pp. 1–2.

[449] G. S. Mok, Q. Zhang, X. Cun, D. Zhang, P. H. Pretorius, and M. A. King, "Initial investigation of using a generative adversarial network for denoising in dual gating myocardial perfusion spect," in *2018 IEEE Nuclear Science Symposium and Medical Imaging Conference Proceedings (NSS/MIC)*. IEEE, 2018, pp. 1–3.

[450] Y. Gong, H. Shan, Y. Teng, N. Tu, M. Li, G. Liang, G. Wang, and S. Wang, "Parameter-transferred wasserstein generative adversarial network (pt-wgan) for low-dose pet image denoising," *IEEE Transactions on Radiation and Plasma Medical Sciences*, vol. 5, no. 2, pp. 213–223, 2020.

[451] C. Chrysostomou, "Sinogram denoise based on generative adversarial networks," in *2020 IEEE Nuclear Science Symposium and Medical Imaging Conference (NSS/MIC)*. IEEE, 2021, pp. 1–4.

[452] M. Gao, J. A. Fessler, and H.-P. Chan, "Deep convolutional neural network with adversarial training for denoising digital breast tomosynthesis images," *IEEE Transactions on Medical Imaging*, vol. 40, no. 7, pp. 1805–1816, 2021.

[453] S. Tian, M. Wang, F. Yuan, N. Dai, Y. Sun, W. Xie, and J. Qin, "Efficient computer-aided design of dental inlay restoration: A deep adversarial framework," *IEEE Transactions on Medical Imaging*, vol. 40, no. 9, pp. 2415–2427, 2021.

[454] Z. Huang, R. Zhao, F. H. Leung, K.-M. Lam, S. H. Ling, J. Lyu, S. Banerjee, T. T.-Y. Lee, D. Yang, and Y.-P. Zheng, "Da-gan: Learning structured noise removal in ultrasound volume projection imaging for enhanced spine segmentation," in *2021 IEEE 18th International Symposium on Biomedical Imaging (ISBI)*. IEEE, 2021, pp. 770–774.

[455] J. Tang, B. Zou, C. Li, S. Feng, and H. Peng, "Plane-wave image reconstruction via generative adversarial network and attention mechanism," *IEEE Transactions on Instrumentation and Measurement*, vol. 70, pp. 1–15, 2021.

[456] D. Mishra, S. Chaudhury, M. Sarkar, and A. S. Soin, "Ultrasound image enhancement using structure oriented adversarial network," *IEEE Signal Processing Letters*, vol. 25, no. 9, pp. 1349–1353, 2018.

[457] H. G. Khor, G. Ning, X. Zhang, and H. Liao, "Ultrasound speckle reduction using wavelet-based generative adversarial network," *IEEE Journal of Biomedical and Health Informatics*, pp. 1–1, 2022.

[458] K. Komoto, S. Nakatsuka, H. Aizawa, K. Kato, H. Kobayashi, and K. Banno, "A performance evaluation of defect detection by using denoising autoencoder generative adversarial networks," in *2018 international workshop on advanced image technology (IWAIT)*. IEEE, 2018, pp. 1–4.

[459] H.-P. Lu and C.-T. Su, "Cnns combined with a conditional gan for mura defect classification in tft-lcds," *IEEE Transactions on Semiconductor Manufacturing*, vol. 34, no. 1, pp. 25–33, 2021.

[460] Y. Feng, Z. Chen, D. Wang, J. Chen, and Z. Feng, "Deepwelding: A deep learning enhanced approach to gtaw using multisource sensing images," *IEEE Transactions on Industrial Informatics*, vol. 16, no. 1, pp. 465–474, 2019.

[461] N. Yu, H. Wang, Q. Xu, and J. Lin, "Defect detection of rubber gloves based on normal samples," in *2021 IEEE 6th International Conference on Cloud Computing and Big Data Analytics (ICCCBDA)*. Chengdu, China: IEEE, Apr. 2021, pp. 612–618.

[462] A. Panda, R. Naskar, and S. Pal, "Generative adversarial networks for noise removal in plain carbon steel microstructure images," *IEEE Sensors Letters*, vol. 6, no. 3, pp. 1–4, 2022.

[463] D. Li, S. Gong, S. Niu, Z. Wang, D. Zhou, and H. Lu, "Image blind denoising using a generative adversarial network for led chip visual localization," *IEEE Sensors Journal*, vol. 20, no. 12, pp. 6582–6595, Jun. 2020.

[464] H.-I. Lin and P. Menendez, "Image denoising of printed circuit boards using conditional generative adversarial network," in *2019 IEEE 10th International Conference on Mechanical and Intelligent Manufacturing Technologies (ICMIMT)*. IEEE, 2019, pp. 98–103.

[465] X. Liu, Y. Wei, Z. Zhao, W. Qian, Y. Liang, X. Li, and C. Li, "Research on denoising algorithms and corner detection of dangerous chemicals storage and stacking based on generative adversarial networks," in *2019 IEEE 6th International Conference on Cloud Computing and Intelligence Systems (CCIS)*. IEEE, 2019, pp. 200–206.

[466] H. Neji, J. Nogueras-Iso, J. Lacasta, M. B. Halima, and A. M. Alimi, "Adversarial autoencoders for denoising digitized historical documents: the use case of incunabula," in *2019 International Conference on Document Analysis and Recognition Workshops (ICDARW)*, vol. 6. IEEE, 2019, pp. 31–34.

[467] A. Ray, M. Sharma, A. Upadhyay, M. Makwana, S. Chaudhury, A. Trivedi, A. Singh, and A. Saini, "An end-to-end trainable framework for joint optimization of document enhancement and recognition," in *2019 International Conference on Document Analysis and Recognition (ICDAR)*. IEEE, 2019, pp. 59–64.

[468] L. T. Ho, S. T. Tran, and D. Dinh, "Nom document background removal using generative adversarial network," in *2021 IEEE International Conference on Signal and Image Processing Applications (ICSIPA)*. IEEE, 2021, pp. 100–104.

[469] J. Wei and C. Ying, "Aggregative adversarial network for still-to-video face recognition," in *2020 5th International Conference on Computer and Communication Systems (ICCCS)*. IEEE, 2020, pp. 266–270.

[470] J.-H. Kim and C. S. Won, "Emotion enhancement for facial images using gan," in *2020 IEEE International Conference on Consumer Electronics-Asia (ICCE-Asia)*. IEEE, 2020, pp. 1–4.

[471] M. Li and Y.-m. Cheung, "Identity-preserved complete face recovering network for partial face image," *IEEE Transactions on Emerging Topics in Computational Intelligence*, 2021.

[472] V.-G. Nguyen and D. L. Nguyen, "Joint image deblurring and binarization for license plate images using deep generative adversarial networks," in *2018 5th NAFOSTED Conference on Information and Computer Science (NICS)*. IEEE, 2018, pp. 430–435.

[473] U. Muneeb, E. Koyuncu, Y. Keshtkarjahromi, H. Seferoglu, M. F. Erden, and A. E. Cetin, "Robust and computationally-efficient anomaly detection using powers-of-two networks," in *ICASSP 2020-2020 IEEE International Conference on Acoustics, Speech and Signal Processing (ICASSP)*. IEEE, 2020, pp. 2992–2996.

[474] Y. Li, X. Fu, and Z.-J. Zha, "Cross-patch graph convolutional network for image denoising," in *Proceedings of the IEEE/CVF International Conference on Computer Vision*, 2021, pp. 4651–4660.

[475] J. Zeng, J. Pang, W. Sun, and G. Cheung, "Deep graph laplacian regularization for robust denoising of real images," in *Proceedings of the IEEE/CVF Conference on Computer Vision and Pattern Recognition Workshops*, 2019, pp. 0–0.

[476] D. Valsesia, G. Fracastoro, and E. Magli, "Deep graph-convolutional image denoising," *IEEE Transactions on Image Processing*, vol. 29, pp. 8226–8237, 2020.

[477] S. Lin and H. Yang, "Dual-mode iterative denoiser: Tackling the weak label for anomaly detection," in *2020 25th International Conference on Pattern Recognition (ICPR)*. IEEE, 2021, pp. 6742–6749.

[478] W.-t. Su, G. Cheung, R. Wildes, and C.-W. Lin, "Graph neural net using analytical graph filters and topology optimization for image denoising," in *ICASSP 2020-2020 IEEE International Conference on Acoustics, Speech and Signal Processing (ICASSP)*. IEEE, 2020, pp. 8464–8468.

[479] D. Valsesia, G. Fracastoro, and E. Magli, "Image denoising with graph-convolutional neural networks," in *2019 IEEE international conference on image processing (ICIP)*. IEEE, 2019, pp. 2399–2403.

[480] M. Sato, T. Otake, H. Aomori, and M. Tanaka, "New image denoising method using multiple-minimum cuts based on maximum-flow neural network," in *2015 European Conference on Circuit Theory and Design (ECCTD)*. IEEE, 2015, pp. 1–4.

[481] H. Vu, G. Cheung, and Y. C. Eldar, "Unrolling of deep graph total variation for image denoising," in *ICASSP 2021-2021 IEEE International Conference on Acoustics, Speech and Signal Processing (ICASSP)*. IEEE, 2021, pp. 2050–2054.

[482] X. Fu, Q. Qi, Z.-J. Zha, X. Ding, F. Wu, and J. Paisley, "Successive graph convolutional network for image de-raining," *International Journal of Computer Vision*, vol. 129, no. 5, pp. 1691–1711, 2021.

[483] Y.-J. Chen, C.-Y. Tsai, X. Xu, Y. Shi, T.-Y. Ho, M. Huang, H. Yuan, and J. Zhuang, "Ct image denoising with encoder-decoder based graph convolutional networks," in *2021 IEEE 18th International Symposium on Biomedical Imaging (ISBI)*. IEEE, 2021, pp. 400–404.

[484] Y. Zhang, W. Deng, M. Wang, J. Hu, X. Li, D. Zhao, and D. Wen, "Global-local gcn: Large-scale label noise cleansing for face recognition," in *Proceedings of the IEEE/CVF Conference on Computer Vision and Pattern Recognition*, 2020, pp. 7731–7740.

[485] F. Pistilli, G. Fracastoro, D. Valsesia, and E. Magli, "Learning robust graph-convolutional representations for point cloud denoising," *IEEE Journal of Selected Topics in Signal Processing*, vol. 15, no. 2, pp. 402–414, 2020.

[486] X. Jia, S. Liu, X. Feng, and L. Zhang, "Focnet: A fractional optimal control network for image denoising," in *Proceedings of the IEEE/CVF Conference on Computer Vision and Pattern Recognition*, 2019, pp. 6054–6063.

[487] Y. Liu, X. Zhang, S. Wang, S. Ma, and W. Gao, "Progressive multi-scale residual network for single image super-resolution," *arXiv preprint arXiv:2007.09552*, 2020.

[488] C. Wang, Y. Wu, Z. Su, and J. Chen, "Joint self-attention and scale-aggregation for self-calibrated deraining network," in *Proceedings of the 28th ACM International Conference on Multimedia*, 2020, pp. 2517–2525.

[489] Y. Zhao, Z. Jiang, A. Men, and G. Ju, "Pyramid real image denoising network," in *2019 IEEE Visual Communications and Image Processing (VCIP)*. IEEE, 2019, pp. 1–4.

[490] Z. Wang, J. Li, and G. Song, "Dtdn: Dual-task de-raining network," in *Proceedings of the 27th ACM International Conference on Multimedia*, 2019, pp. 1833–1841.

[491] C. Tian, Y. Xu, W. Zuo, B. Du, C.-W. Lin, and D. Zhang, "Designing and training of a dual cnn for image denoising," *Knowledge-Based Systems*, vol. 226, p. 106949, 2021.

[492] Y. Kim, J. W. Soh, G. Y. Park, and N. I. Cho, "Transfer learning from synthetic to real-noise denoising with adaptive instance normalization," in *Proceedings of the IEEE/CVF Conference on Computer Vision and Pattern Recognition*, 2020, pp. 3482–3492.

[493] S. Cheng, P. Mingqiang, Z. Bin, and Z. Zongjian, "Infrared image denoising based on convolutional neural network," in *2018 13th World Congress on Intelligent Control and Automation (WCICA)*. IEEE, 2018, pp. 499–502.

[494] X. Kuang, X. Sui, Y. Liu, Q. Chen, and G. Guohua, "Single infrared image optical noise removal using a deep convolutional neural network," *IEEE photonics Journal*, vol. 10, no. 2, pp. 1–15, 2017.

[495] P. Xiao, Y. Guo, and P. Zhuang, "Removing stripe noise from infrared cloud images via deep convolutional networks," *IEEE Photonics Journal*, vol. 10, no. 4, pp. 1–14, 2018.

[496] T. Li, Y. Zhao, Y. Li, and G. Zhou, "Non-uniformity correction of infrared images based on improved cnn with long-short connections," *IEEE Photonics Journal*, vol. 13, no. 3, pp. 1–13, 2021.

[497] S. Deepak, S. Sahoo, and D. Patra, "Super-resolution of thermal images using gan network," in *2021 Advanced Communication Technologies and Signal Processing (ACTS)*. IEEE, 2021, pp. 1–5.

[498] K. Prajapati, V. Chudasama, H. Patel, A. Sarvaiya, K. P. Upla, K. Raja, R. Ramachandra, and C. Busch, "Channel split convolutional neural network (chasnet) for thermal image super-resolution," in *Proceedings of the IEEE/CVF Conference on Computer Vision and Pattern Recognition*, 2021, pp. 4368–4377.

[499] G. Batchuluun, J. K. Kang, D. T. Nguyen, T. D. Pham, M. Arsalan, and K. R. Park, "Deep learning-based thermal image reconstruction and object detection," *IEEE Access*, vol. 9, pp. 5951–5971, 2020.

[500] Y. Zeng, Z. Zhang, X. Zhou, and Y. Liu, "High dynamic range infrared image compression and denoising," in *2019 International Conference on Information Technology and Computer Application (ITCA)*. IEEE, 2019, pp. 65–69.

[501] A. Gautam and S. Singh, "A comparative analysis of deep learning based super-resolution techniques for thermal videos," in *2020 Third International Conference on Smart Systems and Inventive Technology (ICSSIT)*. IEEE, 2020, pp. 919–925.